

TRANSCRIPTIONAL REGULATION OF CARDIO-PULMONARY DEVELOPMENT

APPROVED BY SUPERVISORY COMMITTEE

Mentor: DEEPAK SRIVASTAVA, M.D.\_\_\_\_\_

Committee Chairperson: CAROLE MENDELSON, PH.D.\_\_\_\_\_

Committee Member: PHILIP SHAUL, M.D.\_\_\_\_\_

Committee Member: MASASHI YANAGISAWA, M.D, PH.D.\_\_\_\_\_

**To my mother**  
**for her constant love, support, and encouragement**

TRANSCRIPTIONAL REGULATION OF CARDIO-PULMONARY DEVELOPMENT

by

APARNA R. AIYER

DISSERTATION

Presented to the Faculty of the Graduate School of Biomedical Sciences

The University of Texas Southwestern Medical Center at Dallas

In Partial Fulfillment of the Requirements

For the Degree of

DOCTOR OF PHILOSOPHY

The University of Texas Southwestern Medical Center at Dallas

Dallas, Texas

November, 2003

## Acknowledgements

There are so many whom I would like to thank for making these years in Dallas fruitful and enjoyable. First and foremost, I thank my mentor, Deepak, for his patience, his unwavering enthusiasm, for allowing me the freedom to pursue diverse scientific questions and for creating such a wonderful lab environment. To the members of the Srivastava lab, I have no words to thank you for the friendship, all the fun times and the support during the past five years. A big thank you to Stephen for teaching me so much about computers and for his continued friendship and to Ildi, my bay-mate, who is like a big sister to me.

I am grateful to both past and present members of my dissertation committee, Drs. Ivor Benjamin, Carole Mendelson, Philip Shaul, and Masashi Yanagisawa for their time and effort. Their insights have been critical in completing this body of work. A special thanks to James Richardson for help with histological analysis, and John, Chris, Jeff and David in the molecular pathology core for assistance with sectioning, radioactive *in situ* hybridizations and immunohistochemistry.

I am thankful to all my friends in Dallas for having made these years so memorable and to Hari, my fiancé, for bringing so much joy into my life.

And finally, I thank my mother; none of this would have been possible without her.

Copyright

by

Aparna R. Aiyer 2003

All Rights Reserved

# TRANSCRIPTIONAL REGULATION OF CARDIO-PULMONARY DEVELOPMENT

Publication No.

Aparna R. Aiyer, Ph.D.

The University of Texas Southwestern Medical Center at Dallas, 2003

Supervising Professor: Deepak Srivastava, M.D.

Organogenesis is a complex process, disruption of which results in developmental anomalies. In recent years, genetic dissection of the pathways involved in cardiogenesis, have shown a striking similarity in molecular mechanisms across species. One conserved protein is dHAND, a basic helix-loop-helix (bHLH) transcription factor that is required for normal development of the right ventricle, the pharyngeal arches and limb buds. Loss of dHAND leads to apoptosis in the aforementioned tissues and to embryonic lethality at E10.0. A differential display analysis was performed to identify genes dysregulated in *dHAND*<sup>-/-</sup> hearts.

Characterization of such genes could potentially shed light on the molecular mechanisms involved in the defects seen in *dHAND* mutants, while also identifying genes required for normal embryonic development. This thesis represents work on two molecules that were identified in this screen.

Bnip3, a hypoxia inducible, pro-apoptotic molecule that can induce mitochondrial damage, was upregulated in the *dHAND*<sup>-/-</sup> pharyngeal arches and heart, suggesting a role for mitochondrial damage in the observed apoptosis. I have shown that while Apaf-1, a downstream mediator of mitochondrial-induced apoptosis, is required for the apoptosis observed in *dHAND*-null pharyngeal and aortic arch mesenchyme, cardiomyocyte apoptosis in *dHAND* mutants is Apaf-1 independent. Rescue of pharyngeal arches revealed that premature closure of the pharyngeal arch arteries likely contributes to the early lethality observed in *dHAND*<sup>-/-</sup> embryos.

The mouse ortholog of Bcl-2 associated transcription factor (Btf), which was similar to thyroid hormone receptor associated protein 150 (TRAP150), was down regulated in *dHAND* mutants. TRAPs are a family of transcriptional co-activators that are required for normal cardiac and embryonic development. Mice lacking Btf showed normal cardiac development, however, the animals had hypercellular lungs and died within 24 hours after birth. Analysis of lung ultrastructure and cell specific markers showed presence of immature secretory cells in the proximal airways of the lung and aberrant proximal-distal patterning. The ectopic presence of stem cell-like proximal epithelial cells (Clara cells) in the distal epithelium may explain the hypercellularity observed in *btf*-null lungs. These results show

that Btf is required for normal maturation and patterning of the pulmonary epithelium and survival of the animal.



# Table of contents

<b>ACKNOWLEDGEMENTS .....</b>	<b>IV</b>
<b>TABLE OF CONTENTS .....</b>	<b>IX</b>
<b>PRIOR PUBLICATIONS .....</b>	<b>XI</b>
<b>LIST OF FIGURES AND TABLES .....</b>	<b>XII</b>
<b>CHAPTER ONE.....</b>	<b>1</b>
<b>INTRODUCTION.....</b>	<b>1</b>
<i>Initiation of cardiogenesis .....</i>	<i>1</i>
<i>Cardiac looping and chamber specification .....</i>	<i>2</i>
<i>Role of neural crest in cardiac development.....</i>	<i>4</i>
<i>Congenital heart defects .....</i>	<i>5</i>
REFERENCES .....	7
<b>CHAPTER TWO .....</b>	<b>9</b>
<b>GENETIC AND COMPARATIVE MAPPING OF GENES DYSREGULATED IN MOUSE HEARTS LACKING THE DHAND TRANSCRIPTION FACTOR .....</b>	<b>9</b>
BACKGROUND.....	9
METHODS .....	13
<i>Tissue collection and RNA extraction .....</i>	<i>13</i>
<i>Differential display analysis .....</i>	<i>13</i>
RT-PCR.....	14
<i>Whole mount and radioactive in situ hybridization.....</i>	<i>15</i>
<i>Characterization of EST sequences .....</i>	<i>15</i>
RACE .....	16
RH mapping.....	16
Comparative mapping .....	17
FISH analysis .....	18
RESULTS.....	19
<i>Selection of fragments from differential display analysis screen.....</i>	<i>19</i>
<i>Mapping of ESTs .....</i>	<i>24</i>
<i>Confirmation of dysregulation.....</i>	<i>26</i>
<i>DDA sequence expression and mapped phenotypes.....</i>	<i>27</i>
<i>DDA23 is the mouse ortholog of nebullette (NEBL).....</i>	<i>29</i>
DISCUSSION .....	31
REFERENCES .....	36
<b>CHAPTER THREE .....</b>	<b>43</b>
<b>LOSS OF APAF-1 LEADS TO PARTIAL RESCUE OF THE DHAND-NULL PHENOTYPE.....</b>	<b>43</b>
BACKGROUND.....	43
MATERIALS AND METHODS.....	45
<i>Differential display analysis .....</i>	<i>45</i>
<i>Generation of dHAND<sup>-/-</sup> Apaf-1<sup>-/-</sup> embryos.....</i>	<i>46</i>
Histology.....	46
<i>Whole Mount in situ Hybridization .....</i>	<i>47</i>
<i>Radioactive Section in situ Hybridization.....</i>	<i>47</i>
TUNEL Assay for Apoptosis .....	48

<i>Neonatal rat cardiomyocyte culture</i> .....	48
<i>Adenovirus treatment and induction of apoptosis</i> .....	48
RESULTS.....	49
<i>Loss of dHAND activates pro-apoptotic factors</i> .....	49
<i>Loss of Apaf-1 leads to partial rescue of the dHAND-null phenotype</i> .....	49
<i>Table 1</i> .....	53
<i>dHAND does not prevent apoptosis in differentiated cardiomyocytes in vitro</i> .....	57
DISCUSSION .....	57
REFERENCES .....	61
<b>CHAPTER FOUR.....</b>	<b>66</b>
<b>BTF: A TRANSCRIPTIONAL REGULATOR REQUIRED FOR NORMAL PROGENITOR CELL DEVELOPMENT IN THE LUNG .....</b>	<b>66</b>
BACKGROUND.....	66
MATERIALS AND METHODS.....	70
<i>Identification and cloning of mouse btf</i> .....	70
<i>Northern blot analysis</i> .....	71
<i>In situ hybridization</i> .....	71
<i>Gene targeting and genotyping</i> .....	71
<i>RT-PCR</i> .....	72
<i>Histology</i> .....	72
<i>Immunohistochemistry</i> .....	73
<i>LacZ staining</i> .....	74
<i>Electron microscopy</i> .....	74
<i>Lung morphometry</i> .....	75
<i>Measurment of body weight and blood glucose</i> .....	75
<i>Quantification of proliferation</i> .....	75
<i>TUNEL assay</i> .....	76
RESULTS.....	76
<i>Mouse Btf shows similarity to TRAP150</i> .....	76
<i>Loss of Btf in mice leads to perinatal lethality</i> .....	80
<i>Abnormal lung morphology in btf<sup>-/-</sup> animals</i> .....	83
<i>Btf is expressed in various cell types in the newborn lung but is restricted to Clara cells of the proximal         airways in the adult</i> .....	85
<i>Normal surfactant protein expression and type I and type II pneumocyte morphology in btf<sup>-/-</sup> lungs</i> .....	87
<i>Abnormal Clara cell morphology in btf<sup>-/-</sup> pups</i> .....	89
<i>Ectopic CC-10 expression in btf<sup>-/-</sup> lungs and presence of Clara-like cells in the alveolar walls</i> .....	91
DISCUSSION .....	94
REFERENCES .....	97
<b>CHAPTER 5 .....</b>	<b>104</b>
<b>CONCLUSIONS .....</b>	<b>104</b>
<i>Mechanism of apoptosis in dHAND<sup>-/-</sup> embryos</i> .....	104
<i>Role of btf in embryonic and postnatal development</i> .....	105
<b>VITAE.....</b>	<b>109</b>

## **Prior Publications**

Villanueva, M. P., **Aiyer, A. R.**, Muller, S., Pletcher, M. T., Liu, X., Emanuel, B., Srivastava, D., and Reeves, R. H. (2002). Genetic and comparative mapping of genes dysregulated in mouse hearts lacking the Hand2 transcription factor gene. *Genomics* 80, 593-600.

# List of figures and tables

<b>CHAPTER ONE</b> .....	<b>1</b>
<b>Figure 1.</b> Schematic diagram of early cardiogenesis.....	2
<b>Figure 2.</b> Cardiac morphogenesis.....	3
<b>CHAPTER TWO</b> .....	<b>9</b>
<b>Figure 1.</b> Representative sample of DDA gel electrophoresis.....	20
<b>Figure 2.</b> Mapping the <i>NEBL</i> gene by FISH.....	30
<b>Table 1:</b> List of differentially displayed fragments.....	21
<b>Table 2:</b> EST RH Mapping Results, Mouse/Human Map Positions, and Phenotypes Associated with Map Positions.....	25
<b>Table 3:</b> Transcript Alignments of DDA Sequences.....	28
<b>CHAPTER THREE</b> .....	<b>43</b>
<b>Figure 1.</b> Decrease in <i>Apaf-1</i> gene dosage leads to partial rescue of <i>dHAND</i> <sup>-/-</sup> phenotype.....	51
<b>Figure 2.</b> Cardiac defect in <i>dHAND</i> <sup>-/-</sup> <i>Apaf-1</i> <sup>-/-</sup> embryos at E9.5.....	52
<b>Figure 3.</b> Decreased apoptosis in pharyngeal arches of <i>dHAND</i> <sup>-/-</sup> <i>Apaf-1</i> <sup>-/-</sup> and <i>dHAND</i> <sup>-/-</sup> <i>Apaf-1</i> <sup>+/-</sup> embryos.....	54
<b>Figure 4.</b> Decreased apoptosis in limb buds of <i>dHAND</i> <sup>-/-</sup> <i>Apaf-1</i> <sup>-/-</sup> embryos.....	55
<b>Figure 5.</b> Histological analysis of <i>dHAND</i> <sup>-/-</sup> <i>Apaf-1</i> <sup>-/-</sup> embryos .....	56
<b>Table 1.</b> Genotype of embryos from <i>dHAND</i> <sup>+/-</sup> <i>Apaf-1</i> <sup>+/-</sup> intercrosses.....	53
<b>CHAPTER FOUR</b> .....	<b>66</b>
<b>Figure 1.</b> Sequence alignment of mBtf with hBtf and hTRAP150.....	77
<b>Figure 2.</b> <i>Btf</i> expression at postnatal day 0 (P0) and in the adult.....	78
<b>Figure 3.</b> <i>Btf</i> is specifically downregulated in the <i>dHAND</i> <sup>-/-</sup> heart .....	79
<b>Figure 4.</b> <i>Btf</i> knock-out and genotyping strategy.....	80
<b>Figure 5.</b> Animals homozygous for the mutant allele lack <i>btf</i> transcript .....	81
<b>Figure 6.</b> <i>Btf</i> <sup>-/-</sup> animals do not express <i>btf</i> transcript at postnatal day 0 (P0).....	82
<b>Figure 7.</b> Hyper-cellularity in <i>btf</i> <sup>-/-</sup> lungs.....	83
<b>Figure 8.</b> Increased proliferation in <i>btf</i> -null lungs.....	84
<b>Figure 9.</b> <i>Btf</i> is expressed in Clara cells, typeI and typeII pneumocytes at postnatal day 0 (P0).....	86
<b>Figure 10.</b> <i>Btf</i> is expressed exclusively in the proximal airway in the adult.....	87
<b>Figure 11.</b> Normal lamellar body ultrastructure in <i>btf</i> -null lungs.....	88
<b>Figure 12.</b> Loss of <i>btf</i> leads to delayed Clara cell development.....	90
<b>Figure 13.</b> Ectopic <i>CC10</i> expression in lungs of <i>btf</i> -null animals.....	92
<b>Figure 14.</b> <i>Btf</i> -null lungs have Clara-like cells in the distal epithelium.....	93
<b>Table1.</b> Genotype of pups at postnatal day 10 (P10) from <i>btf</i> <sup>+/-</sup> intercrosses.....	81

# **CHAPTER ONE**

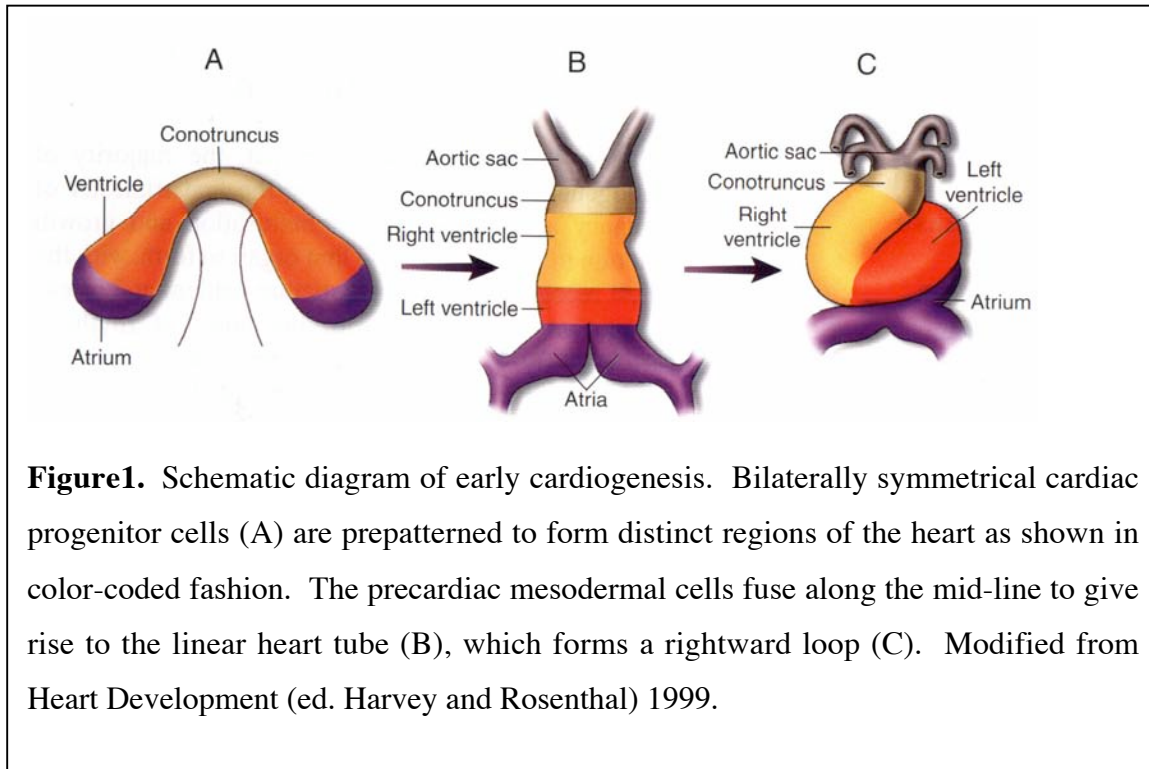
## **INTRODUCTION**

Organogenesis is an extremely complex morphogenetic process, requiring a well-orchestrated series of steps, which involve cell proliferation, migration, differentiation and cell death. In recent years the genetic dissection of cardiogenesis has revealed similarities in molecular pathways of cardiogenesis in organisms as diverse as fruitflies and mammals, allowing a better understanding of the molecular mechanisms involved in this highly complex process.

### **Initiation of cardiogenesis**

Cardiogenesis in vertebrates begins with the specification of cardiac progenitor cells in the anterior lateral plate mesoderm, which condense to form the cardiac crescent, in response to inductive signals from the adjacent endoderm. This bilaterally symmetric cardiogenic field then fuses along the mid-line to form the straight heart tube (Fig. 1). The straight heart tube, which is made up of an outer myocardium and an inner endocardium, initiates rhythmic contractions by embryonic day 8.0 (E8.0) in mice. The heart tube is regionalized, with specific segments along the antero-posterior (A/P) axis fated to form distinct regions of the mature heart (Fig. 1B). From anterior-posterior, these regions give

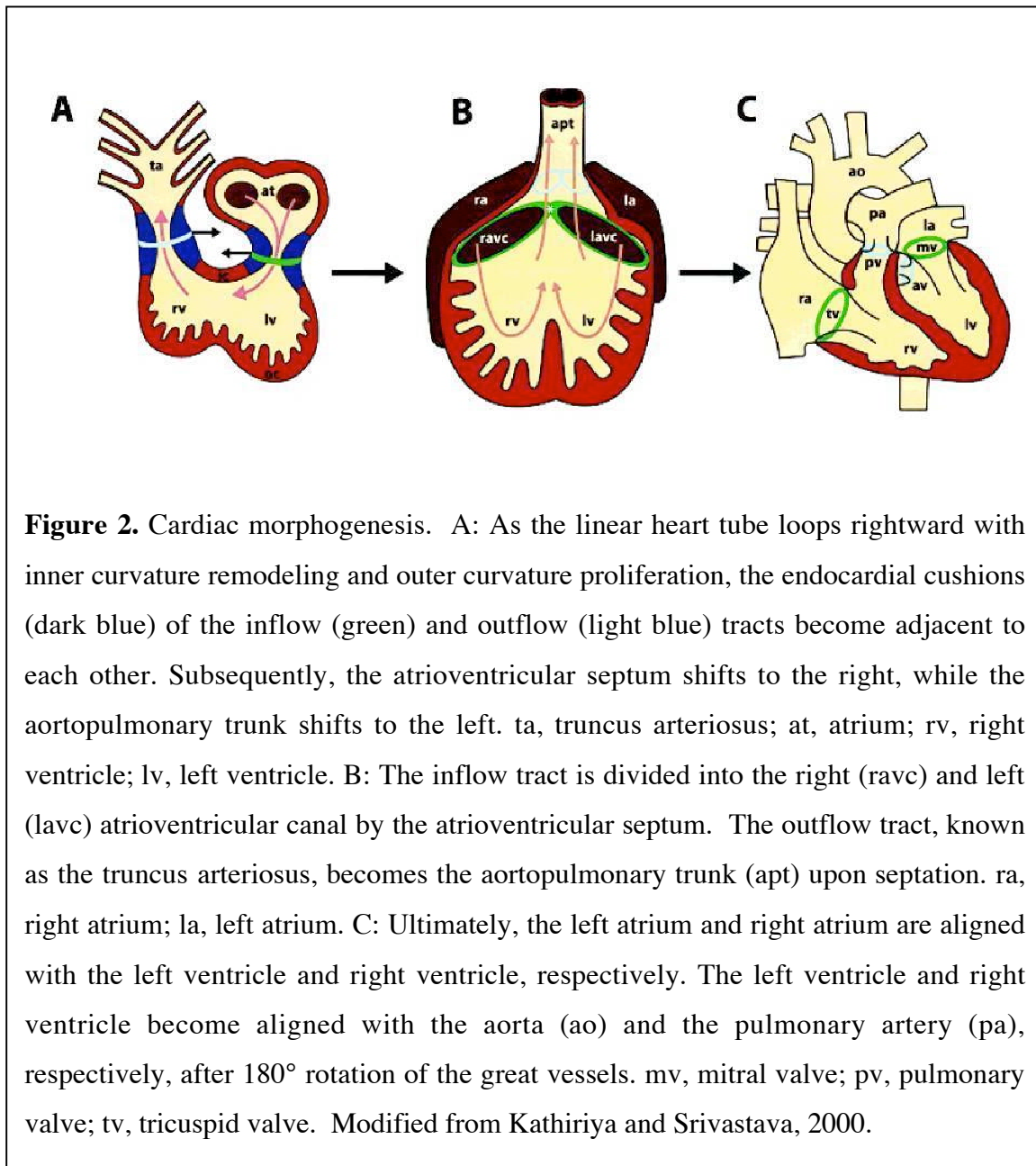
rise to the outflow tract (conotruncus), the ventricles, the atria and the inflow tract (Yutzey and Bader, 1995).



### Cardiac looping and chamber specification

In all vertebrates, the straight heart tube initiates a rightward looping, which converts the A/P patterning to a left-right (L/R) patterning (Brown and Wolpert, 1990, Levin, 1997) (Fig. 1C). The bend in the loop occurs between the future right and left ventricles and leads to positioning of the common atrium anterior to the ventricles. In addition, the endocardial cushions at the atrioventricular region fuse to form the atrioventricular septum (AVS), which divides the AV canal into the left and right inlets. Also, the cushions at the junction between the conotruncus and the right ventricle expand and fuse to form the conal septum. The

formation of the atrial, ventricular and aortopulmonary septum is also initiated at this stage. In the later stage of looping, the outflow tract shifts to overlie the ventricles and the right AV canal is positioned over the primitive right ventricle. The cushions surrounding the AV and conal septae undergo further differentiation to form the valve leaflets. Finally the septated



outflow tract, turns, to align the aorta over the left ventricle and the pulmonary artery over the right ventricle (Fig. 2) (Kathiriya and Srivastava, 2000). The outflow tract has been documented to shrink during this final step to form the pulmonic infundibulum, the connection between the right ventricle and the pulmonary artery. The decrease in the length of the OFT involves apoptosis of the myocardial cells and endocardial cells (Watanabe et al., 1998). The correct placement of this piece of tissue is critical for the proper alignment of the arterial trunks with the ventricular chambers to give rise to a cardiac structure compatible with extrauterine function.

### **Role of neural crest in cardiac development**

In addition to differentiation of various cell types, contributions from an extracardiac source, namely the cardiac neural crest cells, are essential for normal cardiogenesis. These are a population of cells that migrate from the neural fold between the midotic placode to the third somite and infiltrate regions of the heart undergoing active morphogenesis such as the aortopulmonary septum and the semi-lunar valves, as well as the aortic arch arteries. The aortic arches that arise from the aortic sac undergo extensive remodeling during cardiogenesis and contribute to specific regions of the aortic arch and the pulmonary artery (Kirby and Waldo, 1995). An intriguing fact about these neural crest cells is that while in some cases they populate the region they invade, in other cases they undergo apoptosis after having reached their destination. One possible explanation for this is that their arrival gives signals to the neighboring cells to differentiate to form specialized structures. Once they have carried out this function, they are eliminated by programmed cell death. This is seen



during septum formation in the outflow tract where neural crest cell infiltration coincides with muscularization of the septum and also in the bundle of His where the arrival of the neural crest cells results in the differentiation of the surrounding myocytes into conduction tissue (Poelmann and Gittenberger-de Groot, 1999). Neural crest cells are then removed by apoptosis. These observations identify apoptosis as a means to achieve remodeling and temporally regulated differentiation in the heart (Fisher et al., 2000).

### **Congenital heart defects**

In humans, cardiac malformations are the most common birth defect, occurring in approximately 1% of all live births (Hoffman, 1995). The cardiac anomalies observed at birth are typically ones that allow for normal intrauterine function, where the systemic and pulmonary functions are not separated. Some examples of the defects observed are, hypoplasia of specific chambers, malformations of the septae or defects in the vessels that arise from the ventricles. Most often, the defects in the vessels are a result of the misalignment of the vessels with the appropriate ventricular chambers. In many instances this occurs with incomplete septation of the heart, resulting in a double outlet right ventricle (DORV), which is not conducive for survival outside the womb. In addition, there are also several defects that correlated with perturbations in normal neural crest contribution, for example DiGeorge Syndrome, which is characterized by patent truncus arteriosus and interrupted aortic arch (Van Mierop and Kutsche, 1986; Driscoll et al., 1992). Interestingly, the defects observed are not global defects of the heart, but usually result from perturbations of distinct morphogenetic events leading to defects in specific regions of the heart. The

genetic dissection of the cardiovascular development process has led to the identification of several genes required for distinct steps in cardiogenesis. In recent years, several of the same genes have been implicated in cardiovascular defects seen in humans (Garg et al., 2003; Schott et al., 1998; Li et al., 1997; Basson et al., 1997; Srivastava and Olson, 2000). This indicates that understanding molecular mechanisms triggered by specific factors required for cardiac development could lead to better diagnosis and perhaps therapeutic intervention for congenital heart disease.

## References

Basson, C. T., Bachinsky, D. R., Lin, R. C., Levi, T., Elkins, J. A., Soultz, J., Grayzel, D., Kroumpouzou, E., Traill, T. A., Leblanc-Straceski, J., Renault, B., Kucherlapati, R., Seidman, J. G., and Seidman, C. E. (1997). Mutations in human TBX5 [corrected] cause limb and cardiac malformation in Holt-Oram syndrome. *Nat Genet* 15, 30-5.

Brown, N. A., and Wolpert, L. (1990). The development of handedness in left/right asymmetry. *Development* 109, 1-9.

Driscoll, D. A., Budarf, M. L., and Emanuel, B. S. (1992). A genetic etiology for DiGeorge syndrome: consistent deletions and microdeletions of 22q11. *Am J Hum Genet* 50, 924-33.

Fisher, S. A., Langille, B. L., and Srivastava, D. (2000). Apoptosis during cardiovascular development. *Circ Res* 87, 856-64.

Garg, V., Kathiriya, I. S., Barnes, R., Schluterman, M. K., King, I. N., Butler, C. A., Rothrock, C. R., Eapen, R. S., Hirayama-Yamada, K., Joo, K., Matsuoka, R., Cohen, J. C., and Srivastava, D. (2003). GATA4 mutations cause human congenital heart defects and reveal an interaction with TBX5. *Nature* 424, 443-7.

Hoffman, J. I. (1995). Incidence of congenital heart disease: I. Postnatal incidence. *Pediatr Cardiol* 16, 103-13.

Kathiriya, I. S., and Srivastava, D. (2000). Left-right asymmetry and cardiac looping: implications for cardiac development and congenital heart disease. *Am J Med Genet* 97, 271-9.

Kirby, M. L., and Waldo, K. L. (1995). Neural crest and cardiovascular patterning. *Circ Res* 77, 211-5.

Levin, M. (1997). Left-right asymmetry in vertebrate embryogenesis. *Bioessays* 19, 287-96.

Li, Q. Y., Newbury-Ecob, R. A., Terrett, J. A., Wilson, D. I., Curtis, A. R., Yi, C. H., Gebuhr, T., Bullen, P. J., Robson, S. C., Strachan, T., Bonnet, D., Lyonnet, S., Young, I. D., Raeburn, J. A., Buckler, A. J., Law, D. J., and Brook, J. D. (1997). Holt-Oram syndrome is caused by mutations in TBX5, a member of the Brachyury (T) gene family. *Nat Genet* 15, 21-9.

Poelmann, R. E., and Gittenberger-de Groot, A. C. (1999). A subpopulation of apoptosis-prone cardiac neural crest cells targets to the venous pole: multiple functions in heart development? *Dev Biol* 207, 271-86.

Schott, J. J., Benson, D. W., Basson, C. T., Pease, W., Silberbach, G. M., Moak, J. P., Maron, B. J., Seidman, C. E., and Seidman, J. G. (1998). Congenital heart disease caused by mutations in the transcription factor NKX2-5. *Science* 281, 108-11.

Srivastava, D., and Olson, E. N. (2000). A genetic blueprint for cardiac development. *Nature* 407, 221-6.

Van Mierop, L. H., and Kutsche, L. M. (1986). Cardiovascular anomalies in DiGeorge syndrome and importance of neural crest as a possible pathogenetic factor. *Am J Cardiol* 58, 133-7.

Watanabe, M., Choudhry, A., Berlan, M., Singal, A., Siwik, E., Mohr, S., and Fisher, S. A. (1998). Developmental remodeling and shortening of the cardiac outflow tract involves myocyte programmed cell death. *Development* 125, 3809-20.

Yutzey, K. E., and Bader, D. (1995). Diversification of cardiomyogenic cell lineages during early heart development. *Circ Res* 77, 216-9.

## **CHAPTER TWO**

### **Genetic and Comparative Mapping of Genes Dysregulated in Mouse Hearts Lacking the dHAND Transcription Factor**

#### **Background**

Cardiac development is a complex morphogenetic process. Cell proliferation and migration along with alignment of various regions of the developing heart are required to ultimately form a normal functioning heart. Several families of transcription factors have been shown to be expressed in the developing heart. While some are expressed throughout the developing heart, others are restricted to specific regions (Arceci et al., 1993; Cserjesi et al., 1995; Edmondson et. al., 1994; Komuro and Izumo, 1993; Laverriere et al., 1994; Lints et. al., 1993; Srivastava et. al., 1995). One such family of transcription factors is the basic-helix-loop-helix (bHLH) family. Members of this family are involved in differentiation of several cell lineages (Jan and Jan, 1993; Lee et al., 1995; Ma et al., 1996; Olson and Klein, 1994; Shivdasani et al., 1995; Weintraub, 1993; Zhuang et al., 1994). bHLH proteins can dimerize by virtue of their HLH regions which leads to juxtaposition of their basic domains causing formation of a DNA-binding domain which can bind to an E-box consensus site on the target gene.

*dHAND* and *eHAND* are two members of this family that are expressed in the embryonic heart. The *HAND* family of transcription factors is highly conserved across species. In the chick (Srivastava et. al., 1995), *dHAND* and *eHAND* are co-expressed during cardiogenesis; however, in the mouse, *dHAND* is expressed throughout the developing cardiac region but is more abundant in the right ventricle and outflow tract (Srivastava et. al., 1995). *eHAND* is restricted to the left ventricle and the myocardium (Cserjesi et al., 1995; Biben and Harvey 1997; Srivastava et. al., 1997) while *dHAND* is expressed in both the myocardium and the endocardium (Srivastava et. al., 1995). The *HAND* genes in addition to being expressed in the developing cardiac tissue, are also expressed in the aortic sac, the pharyngeal arches and the limb bud (Cserjesi et al., 1995; Srivastava et al., 1995; Thomas et al., 1998; Charite et al., 2000). Normal development of the pharyngeal arches and the arch arteries that traverse through them is required for normal development of the aortic arch and pulmonary artery. Neural crest cells begin populating the pharyngeal arches by E9.0 in the mouse. Detailed analysis of *HAND* gene expression in the mouse has shown that they are also expressed in the pharyngeal arches by E9.0. Both *dHAND* and *eHAND* are expressed in the neural-crest-derived mesenchyme in the distal portion of the arches, with *dHAND* expression being broader than that of *eHAND*. These genes are not expressed in the epithelial layer of the pharyngeal arches or in the migrating neural crest cells (Thomas et al., 1998).

Antisense studies have shown that in chick, the two *HAND* genes have redundant function (Srivastava et al., 1995). Studies in mouse, however, suggest a chamber specific role for the genes, which correlates with their expression pattern. Loss of *dHAND* in the

mouse leads to embryonic lethality at E10.0 with the most obvious defect being the absence of the right ventricle. *dHAND*<sup>-/-</sup> embryos form a normal straight heart tube but the defect is apparent during cardiac looping with the outflow tract connecting directly to the left ventricle. Histologic analysis has also shown that although the left ventricle is present, it has decreased trabeculations in comparison to wild-type embryos. In addition to cardiac defects, *dHAND*<sup>-/-</sup> embryos exhibit dilation of the aortic sac, hypoplasia of the 1<sup>st</sup> and 2<sup>nd</sup> pharyngeal arches, absence of the 3<sup>rd</sup> and 4<sup>th</sup> arches and premature closure of the aortic arch arteries (Srivastava et al., 1997). They also demonstrate severe vascular defects throughout the embryo and the yolk sac, which are characterized by failure of the vascular smooth muscle cells to differentiate (Yamagishi et al., 2000). Analysis of cell proliferation and apoptosis in the *dHAND*<sup>-/-</sup> embryos has revealed that the hypoplasia of the right ventricle and pharyngeal arches is a result of excessive apoptosis (Thomas et al., 1998; Yamagishi et al., 2001).

Congenital heart defects in humans can arise as a result of defects either in the cardiac mesoderm or due to defects in cardiac neural crest cells. The DiGeorge syndrome (DGS) is an example of a congenital defect that is associated with abnormalities of the neural crest cells of the 3<sup>rd</sup> and 4<sup>th</sup> pharyngeal arches (Van Mierop and Kutsche, 1986). DGS is characterized by interrupted aortic arch, persistent truncus arteriosus (PTA), hypoplastic thymus, and craniofacial abnormalities and is linked to a microdeletion in chromosome 22q11 (Driscoll et al., 1992). In addition, deletion of chromosome 10p13-p14 is also associated with certain characteristics of DGS (Daw et al., 1996). In the mouse, loss of endothelin-1 (ET-1) recapitulates defects seen in DiGeorge syndrome in humans (Kurihara et al., 1995a, 1995b). Interestingly, *dHAND*'s expression is downregulated in the pharyngeal

arches of mice lacking ET-1 (Thomas et al., 1998). This, along with cardiac, pharyngeal arch and arch artery defects seen in *dHAND*<sup>-/-</sup> embryos suggests that dHAND might function in a pathway essential for normal cardiovascular development.

In this study we performed a differential display analysis to identify genes dysregulated in the absence of dHAND in the heart. Characterization of such genes could potentially shed light on the molecular mechanisms involved in the defects seen in the absence of dHAND, while also identifying candidate genes required for normal cardiac development. In collaboration with Dr. Reeves (Johns Hopkins University) we determined the map positions in mouse and human of 27 genes whose expression may be altered in hearts of *dHAND*<sup>-/-</sup> mice and compared these positions to mapped phenotypes including arrhythmogenic right ventricular dysplasia, dilated cardiomyopathy, cardiofaciocutaneous syndrome, and DGS. One of these was demonstrated to be the mouse ortholog of nebulin (*NEBL*), an actin-binding protein expressed primarily in the heart. *NEBL* transcripts have been isolated from human embryonic heart and early mouse fetuses. The gene localizes to the DiGeorge syndrome2 (DGS2) region on human chromosome 10p14–p13. Here we refine that localization with respect to the portion of the DGS2 deletion region that is correlated with cardiac defects, as opposed to the region of segmental monosomy in individuals with the hypoparathyroidism, deafness, and renal dysplasia (HDR) spectrum of anomalies. In addition we have also identified, *Bnip3*, a pro-apoptotic molecule that might contribute to the hypoplasia seen in the right ventricle and pharyngeal arches of *dHAND*<sup>-/-</sup> embryos, and a protein similar to a member of a transcriptional co-activator complex that might mediate the functions of nuclear receptors in cardiac development.



## Methods

### Tissue collection and RNA extraction

*dHAND* heterozygous animals were mated and pregnant females sacrificed at E9.5. RNA from E9.5 wild-type, *dHAND*<sup>-/-</sup> hearts, and left ventricles and atria of normal hearts was extracted using Trizol reagent (Invitrogen<sup>TM</sup>, Life Technologies). The RNA was treated with DNaseI to remove any genomic DNA contamination and resuspended in sterile nuclease-free water.

### Differential display analysis

3.4µg of each RNA sample (OD<sub>260/280</sub> ratio ≥ 1.8) were submitted to Genomix corporation (Foster City, CA) for differential display analysis. First-strand cDNA was generated from the RNA using twelve (12) 3' oligo(dT) “anchored” primers which have two non-oligo(dT) nucleotides for selection of different mRNA fractions. These anchored primer reactions are converted into double stranded cDNA fragment using a set of three (3) 5' “arbitrary” primers. This set of 36 reactions was performed in duplicate per sample. Control amplifications were also performed on HeLa cell RNA for quality assurance. The DD-PCR fragments generated from the arbitrary primed amplification were analyzed by gel electrophoresis using the genomixLR<sup>TM</sup> DNA Sequences System and its proprietary HR-1000<sup>TM</sup> gel. Fragments that were up- or down-regulated in the *dHAND*<sup>-/-</sup> heart were excised from the gel and reamplified. These fragments were cloned into TOPO cloning vector and were sequenced to determine gene identity.

## RT-PCR

RNA from E9.25 wild-type or *dHAND*<sup>-/-</sup> heart was extracted using TRIzol (Invitrogen™). 2µg of RNA per sample was treated with Amplification Grade DNaseI (Invitrogen™). One half of each DNaseI treated sample was used to generate first-strand cDNA in the presence of reverse transcriptase (RT) and the other half used without RT. The reaction was performed using SuperScript™ First-Strand Synthesis System for RT-PCR (Catalog# 11904-018, Invitrogen™, Life Technologies) as described in the instruction manual. Transcripts were amplified using the following primers and cycling at 95°C for 30

EST	Forward Primer	Reverse Primer
DDA 5	ACATCGTTATTCCCCACAGC	ACCAACCACCAGAAGAAACG
DDA 7	CCCTCTTCCAAGGAGAGCTT	GCCTCATTGACCAAGACACA
DDA 8	CATACGGGAGGGTGGACTG	TCCAGTGTACACCCATGTC
DDA 9	CTTTCTCCTTCGGAGCCTCT	CAGGAAACAGCAAAGACAGGA
DDA 14	GATTAAGTGCCTTCCCTCCAC	AAGCAGCAAACCTTTCTGGA
DDA 16	TCATGGATTCAAGACCCTGTC	TTCATCACCACAGCCTTCAA
DDA 17	GTATTTACTACCACAAAGCCCG	ACCAGTGGAGGAAGCTGTGT
DDA 21	CTGGCTCCATTGTTCCATGT	GTGTTCTGGGACTTCAAAGGA
DDA 22	TGGTAATGCTTTTCCAGTTTGTG	CAGGGAGAGCCAGAACAAAC
DDA 23	GGAAACATGGAAGCTTACTCAGA	TGGATTCTTTTCCAAAATCAAAA
DDA 24	TCAACAGAACAGGATGTGGC	AGGCTTGAAAGACTGGCTCA
DDA 25	TCCAAGGGATTACCGATTA	AGAGGCAGTGGGCAGATTT
DDA 26	GAATCCTCATCTGCAAAGC	TGCGGGTTATCTGTAAAGGC
DDA 27	CCCACCCAGCTTCTTCAAT	AGGAAAGGGTGGCAAGAAGT
DDA 28	TCAGTTATCGTCACATGGGC	CGGTGGGTTTATGCCATAGT
DDA 29	ACTAGGCGAAGGGACAGAAA	GACATCCGTCTTCACGAGAG
DDA 30	TCCCTCAGCTCCTTCTCTGA	AAGAGGCTCCTTCTTGGAG
DDA 31	CTCCATGGGTAAATGTTTCGG	CAGAGGCAGGAGTTAGGCTG
DDA 33	TGCAAATAGGAAAGGAAGTGG	CAGGAAGCCAAATCATTGCT
DDA 34	CCTAGGCTCCTCCGTCTTTC	ATTTCAAAGCCACGGAGATG
DDA 35	TGGCATCCGATACCTCTCTC	TCGGCGAATCAAAATATCAA
DDA 38	TCTCTAGTCACAGAGGAAGGCA	GCAGAGGTGATGTGGAGTCA
DDA 45	ACACGAAGTTGTGGCCAAGT	TGCTCATTTTCAAGATGTTTTGTG
DDA 46	AACCGCCCAGATGTTAACTG	GTGGGGACATAGTACTGCC
DDA 47	TGGCTACATCCTTCATAACCAA	TTGACCAGGTACCCAGGTTT
DDA 49	CCTTTCCCCCTGCTATTGTA	TTGAAATGCTGTGGAAACCA
DDA 50	AGCCAGGGTCTCTGTTCAAA	CAATATCCCAGCATTACCCC

seconds, 58°C for 30 seconds, and 72°C for 30 seconds. *G3PDH* (forward primer: 5'-accacagtccatgccatcac-3', reverse primer: 5'-tccaccaccctgttgctgta-3') was used as control.

### **Whole mount and radioactive *in situ* hybridization**

Whole mount *in situ* hybridization was performed as previously described (Srivastava et al., 1995) using digoxigenin-labeled antisense riboprobes synthesized from DDA21 and DDA26 cDNA transcribed with T7 and Sp6 polymerase respectively. Briefly, embryos were prehybridized in hybridization buffer without probe at 60°C for 2 hours; digoxigenin-labeled riboprobes were added and incubated at 60°C for 18 hours. After a series of washes, embryos were incubated with AP conjugated anti-digoxigenin antibodies at room temperature for 1 hour. Following another series of washes, color reaction mixture was added (Roche) and embryos were incubated in the dark at room temperature for 12-14 hours. The color reaction was terminated by fixing the embryos in 4% paraformaldehyde, 0.1% glutaraldehyde/PBS solution.

Radioactive *in situ* hybridization was performed on paraffin embedded sections of E9.5 wild-type and *dHAND*<sup>-/-</sup> embryos as described previously (Lu et al., 1998). <sup>35</sup>S-labeled antisense riboprobes were generated from DDA9 cDNA using SP6 RNA polymerase (MAXIscript; Ambion Inc., Austin, TX).

### **Characterization of EST sequences**

Mouse EST sequences obtained by differential display of mRNA from the hearts of wild-type and *dHAND*<sup>-/-</sup> 9.5-dpc embryos were masked for repeat elements

(<http://woody.embl-heidelberg.de/repeatmask/>) and aligned to GenBank's dbest and nonredundant sequence databases (<http://www.ncbi.nlm.nih.gov/BLAST>) and the TIGR EST database (<http://www.tigr.org/tdb/tgi/mgi/>). The EST and its mouse cDNA match in BLAST were considered to be equivalent to each other if they shared  $\geq 98\%$  identity in nucleotide sequence (Table 2). Cognate ESTs were aligned with mouse genomic sequence using the Ensembl ([http://www.ensembl.org/Mus\\_musculus/](http://www.ensembl.org/Mus_musculus/)) or Celera (<http://cds.celera.com/>) database.

## **RACE**

RACE was performed to extend the cDNA sequence of the EST DDA23. Using the TRIzol reagent (Life Technologies), total RNA was collected from 10.5-dpc embryos. 5' RACE-Ready cDNA and 3' RACE-Ready cDNA were synthesized using the SMART RACE cDNA amplification system (Clontech, Inc.). 5' and 3' cDNA products were amplified using the DDA23 radiation hybrid primers with RACE kit universal primers. RACE products were examined on 1% agarose gels. Successful RACE reactions were subcloned using the TOPO TA Cloning Kit (Invitrogen). Restriction digests verified insert sizes. Appropriate clones were sequenced and analyzed as described for other ESTs.

## **RH mapping**

PCR primers were designed using Primer 3 (<http://www.genome.wi.mit.edu/cgi-bin/primer/primer3.cgi>) for the 22 differential display products (ESTs) whose expression was affected in E9.5 *dHAND*<sup>-/-</sup> embryos and that did not match previously mapped genes.

Primers were purchased from Life Technologies (Gaithersburg, MD). Optimal PCR conditions for each EST were established by the successful amplification of the expected product from embryonic stem cell DNA and a different size or no product from A3 hamster DNA. The majority of mouse primers amplified one or more hamster DNA fragments. Primers and optimal PCR conditions used for radiation hybrid mapping of 22 ESTs can be found at (<http://inertia.bs.jhmi.edu/roger.html>). Each primer set was typed at least three times on the entire T31 RH panel (Research Genetics, Huntsville, AL). RH typings were submitted to the Jackson Laboratory Mouse Radiation Hybrid Database (<http://www.jax.org/resources/documents/cmdata/rhmap/RHIntro.html>) for analysis and archiving of results. This service uses Map Manager QTb28 to determine the highest lod scores for each EST mapped and the “best fit” interval where each EST is most likely localized. The markers that identify the boundaries for this interval are indicated in Table 1. RH data are publicly available at the Jackson Laboratory Mouse Radiation Hybrid Database.

### **Comparative mapping**

The best position on the MGI Consensus Linkage Map for each EST mapped on the radiation hybrid panel was determined by comparing the positions of markers common to the RH and MGI maps. Where marker orders disagreed, the most likely marker order was deduced by comparing the RH map, the MGI consensus map ([http://www.informatics.jax.org/searches/linkmap\\_form.shtml](http://www.informatics.jax.org/searches/linkmap_form.shtml)), the MIT F2 Intercross map (<http://www-genome.wi.mit.edu/cgi-bin/mouse/index#genetic>), and the Jackson BSS backcross map (<http://lena.jax.org/resources/documents/cmdata/bkmap/>). The most likely

region of conserved synteny in the human was assigned by comparing map positions of orthologous mouse:human gene pairs from the MGI map. In many cases, this could be confirmed by searching the “complete draft” human genomic sequence from the Human Genome Project and Celera Public databases. Mouse and human phenotypes were obtained from MGI and Online Mendelian Inheritance in Man (OMIM) (<http://www.ncbi.nlm.nih.gov/Omim/searchmap.html>).

### **FISH analysis**

Metaphase spreads were prepared either from peripheral blood lymphocytes or from lymphoblastoid cell lines using standard methodology. Five cell lines and two control samples were used. Three cell lines were purchased from the Coriell mutant cell repository (Camden, NJ). These included GM06936 [46,XX,del(10)(qter3p13)], GM03470 [46,XX,del(10)(pter3p13::p123qter)], and GM10207 [46,XY,t(10;14) (p13;q24.3)]. CH95-199 and CH92-092, two additional cell lines used in this study, have been reported previously (Gottlieb et al., 1998). FISH was performed as previously described (Shaikh et al., 1999). Chromosomes were visualized by counterstaining with DAPI. Probes used for FISH were labeled by nick translation with either biotin-16–dUTP or digoxigenin-11–dUTP as described (Lichter et al., 1988) with minor modifications. The probes were detected by either fluorescein-conjugated avidin or rhodamine-conjugated anti-digoxigenin, respectively. The FISH probes were chromosome10 BACs RP11-45L12 (AC012108) and 56H7 (AL157398) from the RPCI-11 human BAC library (Roswell Park Cancer Institute). These

BACs contain the *nebulette* gene and were identified by searching public databases for sequenced clones using the GenBank entry for the human *nebulette* cDNA (AF047368).

## Results

### Selection of fragments from differential display analysis screen

In an effort to understand the mechanism of dHAND action and to identify genes potentially required for normal cardiovascular development, we performed a differential display analysis, comparing RNA from E9.5 hearts with or without *dHAND*. We picked 40 bands from the differential display gel based on either up- or down-regulation in hearts lacking *dHAND* (Fig 1). We selected bands that were changed in the *dHAND*<sup>-/-</sup> RNA but were unchanged in the LV+A RNA so as to exclude genes that appeared to be dysregulated only due to absence of the right ventricle.

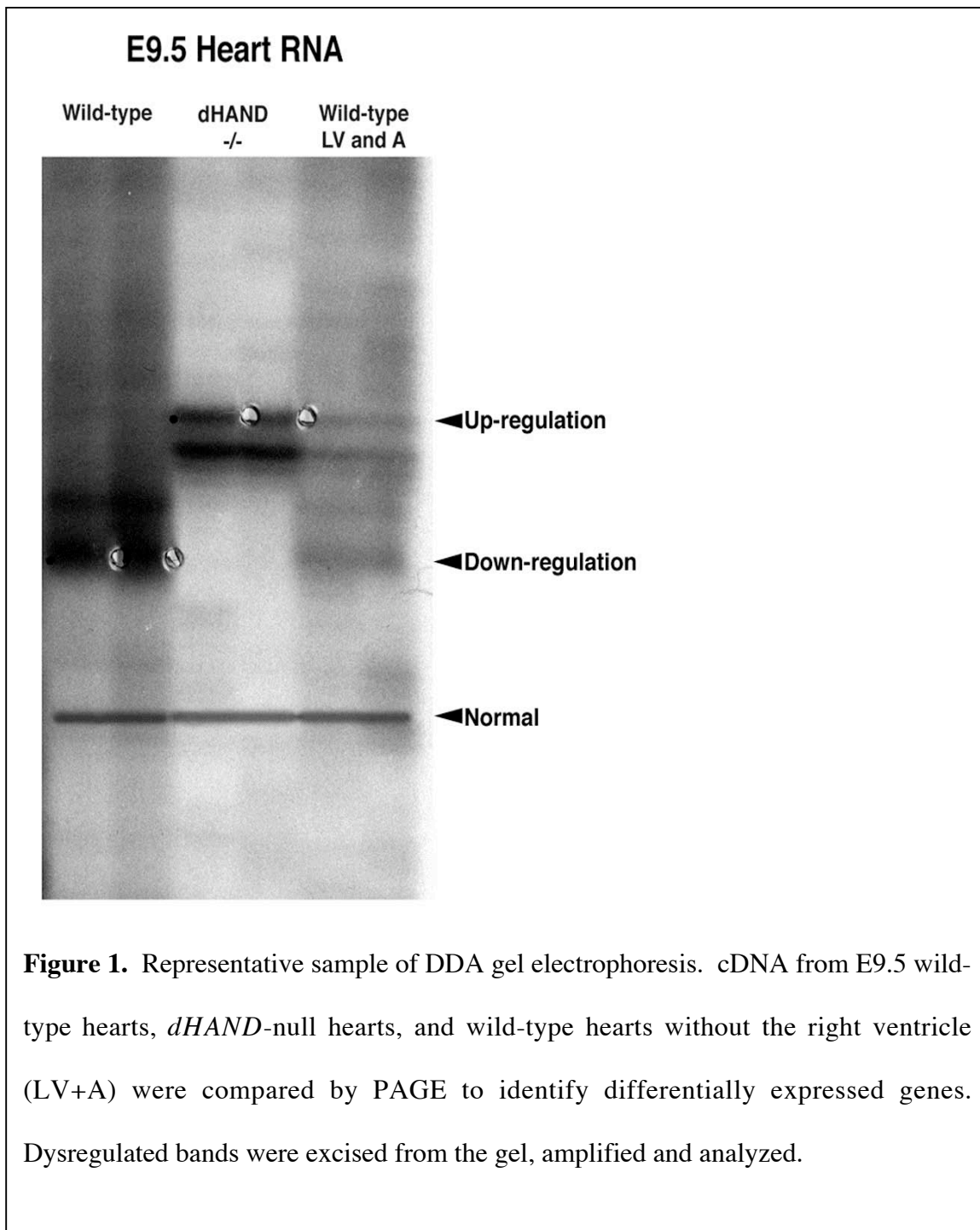




Table 1 shows a list of fragments isolated from the differential display screen.

**Table 1:** List of differentially displayed fragments

DDA 5A	AGGGCTTTTTTTTGCTAATGTAGAGTCTTGCAACAGTAAACTCTTCATCTATCATACCAGTTCCTT CTGGTTGCTTCACATCGTTATTTCCCCACAGCAATTCCTATTTCTGCAAGGTCTTTAATAATGATGC CATCATTTTCAGCTGCTCGTTTCTTCTGGTGGTTGGTCATTTCTACAGCTTCTGAAGCTCAGCATCA ATACTTGCTAAAGTTGCAGATTTTGTATTCAATTCATCACTAAGCAATTCATATTCCTTTGTTTTGT CTTCAACTTCCTGAGACTTCTGA
DDA 7F	ATAGGGCTTTTTTTTGCTTCCACCACAGAAAGGGAGCCTAGGGTCCCTGTAAGCCTGCTTACTAAA GACAGAGAATCCCTTAGTCCCAAGAGCTGTTGATATATTGGAAGGTTAATGAAATTTCTGGTGAGA CCCTCTTCCAAGGAGAGCTTTTCACTGTTCTCGGGATCAATGAGGCCAGACATGATAATCTGGATTCT CAGGAGCACAAGGCCTGTGTCTTGGTCAATGAGGCCCTTTTGCATGGCTCTGAAGATGGGGAATATC TCCACTGTGCCTAGGTCAATCACCCACGCAACTGCTCTGCAACCCCTTTTGTTCGGTCTGCTGAGCCA ACTCGCTTTGGAGCTGCTGGAGTTGGTTTGCAGAACCATCACAAAGGTCATGGTAAGTCTTGTTCAG CACACGCAACTGCTCAGAGATCTGTTCTTCTCTCTTCTGAAAGCTTATGGCCATGCTTGGCTAAG AAGATCTGTGAAGTTTAAATGGCCTCAGAACTTGTCTTCTTGGTTGTCAACTCTTCTGCCAGAA CCTGCTGCTCCAAAATGGCCTTCTCAATGTCTGCAGATGCACTAGTGTGAGATGAGGTAGTTGTCC TTGTGTAT
DDA 8B	CTATNGNCTTAGCTCCTCANTGCTNCATACGGGAGGGTGGACTGGCCAGTTTCATAGAAGAGCAAA TANGCGTCGCTGGNGCNCACCTTGNCTGGAGGACATGGGTGTGACACTGGAATCATTGAAAGNGTGC CATTCGCCTGTAACCGGACTTCGGCAGT
DDA 9B	GCAGACTCTTTATCACTAAAGTAATCTAGAACTTCTGGTTCATCCCAATCTCCATCTGCCCTGCCTT TCTCTGACCCCTTCTCCTTCGGAGCCTCTTTATCCCTGATATTACCCCTATCAAGCAGGAATACTCT AGACTCTTCATCTGTGAACCTTTTTAAAACTTTTCTGTCTTTGTCTGTTTCTGATCTCCTTCAGGA TAAAAGGAGGACCGCCCCCTAGATTCTCTCTTGGAGCATTCTGTGGTGTGATTGTCTTGGCAGGGC TTCTTCGTGATGGGATGTGATGAATCGGACTATTCTGAGAAGGACTATATCGACTCGACCCATTTCC AACAGAGCCAGATCCAGACCTCTCAGGACTGTGCTGAATGGAATGTGAATGCTGAGAAGGGGTATT TTTGGCAGAGTGCACTGTACTAAGCATGGGGCATCTGAGCATGATGAACTCTGACTGGGTGGTGT AGCAATAGGTGAAGGACTATGAGGTGACCTTGGACTATTATCATAAGCTGAAAGGCCAGGCCAAAT ATCACCAGAAGTAGCAGATTTATTAAGCTCATCAATAGATTGAGATGGATCATGTTCAAAAGTATC CTTTGGTTCCTCCTGNGATTTGCTTTTCAAANGACTCTCTTCTGGGGTTCCTCTCAGCTTTT
DDA 14A	NTAATTAATGTCCAAGTTACCATTATGATGCCCTAAAAAATTTGCACTTTCTTTGATATGGGAAA AGAAACTAGAGATGGCACCCTTCCAAATGATTAGACACTGGGAGTGTTATGATAGAATAGAGACA AAAGATTATCAAAATTGCTTTACCAGGCGGTGGCGGCACACCTTTAATCCCAGCTGAAGTGAAT CTTTCAAATGAGAAAGCTTTGNTGCTCTTTAAAAGACCTCTACAAGCTACTCTACCACCAGAATAA GAGCTTTGTGTTTATCTATTAGGTGAAGGCAGATTAAGTGCCTTCCCTCCACCCTTTCTTNAGTTCT CGTGTGGCACCTGCTGGAAGAATGAGAAAAGAAACCAACATTTCCAGAAAAGGTTTGCTGC TTTTCTAAATGTCTGCCTCGTTTAGGGAGAGCTATTCAACTGTAAATCTTCTGATGATCCTATAGG TTAACTATGCTCTCAAT
DDA 16A	TCCNGNTTGGTTGTCTTCACTGNTAAGCAGTAAGTGTGATGGGAGTAATGACCACGCCTTGATTTTT TCCGATATAGCCCCAAGACCTGGCATATCAAGGCTCAGAGGAGTCATGGTTATTAAAAGAGTGATT GAGGAAGTATACTTTATGGTTTACACTAATATTAGCAGCTGTGCAACATGTAGAGAAAGAGGTTT TAATAGAACATGTATGTGAATTACATTTGTATGAAAATTATAAAAAAGGAAACTTGGAAGCCTTT ATTCATGGATTCAAGACCCTGTCCGTGGAAGACACAAGATTTTAAAAGATAAAGATGGACTTTGA AGGCTGTGGTGATGAATCTGTCTGTAAGATGTGGCANAAGAATAATAGATGTTTCAACAGTAACTA GAA
DDA 17B	TCCCAATAGTGCCACTCCCTATGGGCCAAGCATTCAAACACTTGAGTGTGGGGCCATACCTATTCA AATACCACAATAGAATTGAAATTATCATGCTGATTGGTACTTAAAGGGTAAGAGACAGACCTTAT ATTTAAATGGAACACATTCAAATTCATGTGACTGTTTTAAGTACTTCATCCTTTACCTGGTTACTG

	TATAAGGAGTATTTACTACCACAAAGCCCGCCATTTCAATTGTTAGGATGCAGGGTTGAGCAAAG CAGACACAGCTTCTCCTCACTGGTACAACCTCACTCTTTAAGAAACCAAACCTTGA
DDA 21A	GGGGGCACAAAGCAATCCCCTTTAATAAACTTGACAATTAGCTTCACTTAGAACATTTTAAATATG CACATTAAAAAAAAGTATTTGTCTTACAAATTGTTCTGCAATCCAAATATACAACAGCTTGAAAA ACAACATTTAGAAAAACAAAGCCAATGTAAAAAGACAACACTACAACAGTACAGGTTTGATATGGCT CAGATTTTACAGCTTTCTTACTGCGTCATCTATATCAGAGGTCTGTTCCCTCAGCTGGCTCCATTGT TCCATGTATAAAGAAATACCTTTTCTTCTGTTTCATTTACCTTCTGAATCCATCCAATATTCTC TAATATCAATTAGAATTTTCTTTGAAGTCCCGAACACTGACATATCTCATCTTTCCAATCTGGA ACAT
DDA 22B	CATGGTAATGCTTTTCCAGTTTTTGANTATGTTTATAAAATATAAGTGACTTTTTATATACTCATAT TACACTGTGTAACCTGTTGTGGTCTCTTAGTTTGTGTTGCATGCTTCTGCCAATTTTCAATATACAT GTTTCATACCACCTGTAAGTAAAGATAGTTTTACTTCTCCTTTCTTAACATTTTATTTGTTTGTAC ACACATGTATGAGGAGGTGAGAGGGCAACTGTGAAAGTTGGTTCTTTCTTTCCATCATGTGGGTCC CAGGGATCTAACTCGGGTTCTGTGGTAGCGTGGCAGCAAGTGCCTTACCTCTGGAATGTCTTGTT TGTTCTGGCTCTCCCTGGCAAGTCCCATGCTAGCT
DDA 23B	AGGAACAAAGTAATTAANNTACTAAAAAGAAAATGCAGGAGTCACTATATGGCACACAGGGTTTG TATTTTAAACAAGACCAGAGGNTCTAATGGATAATAAGACACAATGATTACACAAACATTTAAATC ACTGNTGCACTTCGTGACCCATGCTTGNAATTTCAACACTCGAGAGGCTGANGCAGGAGGACTGTG AATTGAAGGNCAGACCAGACTACATACTGAGACCTGTCTCAAAACCTNAGGTAAGTAAGGAAAC ATGGAAGCTTACTCAGAGATGAAGGTGTTAGAGTCAATAATGATGACAACAACTGATGTTTTTAA AAATACATTTATAGNTTTTGATTTTGGAAAAGAATCCATCTCATATTACTTCAAAATGGAGCAA TATAAATAGATAAAGGTCTAAAATATACTGAAAAATATAAGATAAATCCTAAGT
DDA 24A	CTATNNGNCCCCAAATCTCAAGTGTCTTACTACAAACACATTTGCCACTCATGTAACAAACATGG CTTTAGGCCAGCTGCTGTGGGCTTTGCTCAGACACCAGGACTACTCCTATTTTCAAGAAATGAGACCTC ACAATANAGGGAAAACAACACANGCCTACTTGCAAACTGCCCATTGACTCTNAAGCTTCTGT CAGATGTGGCACAAGCCCTTGCATGGGCATTGAGAAGTAGAGAATCCAGTAGGGCTCTGANTAGTC CCAGGATCCAAGTTTATACAGTCAACAGAACAGGATGTGGCTTNATGGCTGCAGTCACTTCATGGC ATCCACAGCATCTTAGCTTTCTCCAGGCTGGTGAAGCAACTGAGCCAGTCTTTCAAGCCTTAAGGC CT
DDA 25A	CCATTTAAATATNAACTTTATTTGTAAATACACCATATCAAAACATATGCCACATTTATTCAGAAT GNCATAATCAATGNAAAAATAGAATCTCCTTGNAATGNTAATACTGNGAGCTAGGTACATG ATATTTAGTGAGGGCTTCAGAAATAAATCTTTATAAAACAAATCTATAATTTATACACATTGAAT TTATCGNACAAAATATATACAACAGCATAATTTTGGNGTAGAAAAATGAGATTTGNCAAAATATAA GCAGGNCATTTACACAATATGNATTCTAGNTAACTTTTTCCAAGGGATTCACCGATTAGNCGAATA GCAATACTCTTGNCTTCATCTGTTGGATCACAAGNAAAGCTTCAAATCTGCCACTGCCTCTGGNC TGAAGTGCACCGGATGTGGATATAATGNCGGGCCCTCAAAGTGTA
DDA 26B	AGAGCACATAAGATTTAAATACAAACAAGAGAATTCAGCAGAGTGATAAAGNGCCTGCAACAAA ACTGACCACCCAAGGNAATGGTGACAGCAAGGNGAGAATCCTCATCTGCAAAGCAGGACGAGGG GGAAGTGCAAAGTGGGGTTCGTGGGTAACTTAGCTTCTACTTGCTACTCAGTTCACAAAGTTAGA GGCCTTTACAGATAACCCGCACGCACCTTTAATTTCTGCTATGTAATAGGATTATAAGGNCACA ATATTCCTTTGGGGAAAACCTTTAATGATTTTAAATACACTTACTTGGTCTTTTGAAGTGTAAGN GNCTTAACTGGATTATGATTACAGATCAGTTTTAAATACACCATTGCTACTATATTAATAATTTATTT ATACTATTTATATCTAATATTCAAAGAA
DDA 27B	TATAATCCATACATTAATAAAGTTCCAGGACATCAGACTTTGTCAATCACCTTTTAAAGTTAAA AGTAATCAAATCACTTTAAAAATCCAAACCAGCTAATTGGAGATTTCTTGGGCCACCCAGCTTC TTCAATCATAGCCCATGTGGGTAATCTTTCTTGACAACCTGGTATACTTCACGCTTCTCCAGAGGAA GCTGGACTTCTTGCCACCCTTCTCCTCCATGCTATCTCCTGNGT
DDA 28A	CCNGTTTTTACATTTTATTCATCACAACATTAAGATGCTCGAGAAATGCTGGAGAAAGGCCTTT TAATAACTGATGCGAAGCTGAGCCCTAGGCGTGTGCTTGTCTCCCCCTCCCCCTCAACATGCACT ATCAGTTATCGTCACATGGGCTGGGCTGATCGAGAGTCACAGTTGAGTTTCATGAGTCTCTCCCTGN AACTGAAAACAATTTACCAAGNGCACACAACATATGGCATAAACCCACCGNTCTCAGTGCCAGGC TGGNACATTTACACAATAGCAAACATAAAATCTGAGTCTGTAAAGCATCGTATGTTAAATTACACA AACCAGGATTTGTTTTAACTGGATTTTGAATCTGCTGNTGAGTCCAAGCATGTAGGTACAAAC GACACCTGGATGAAGCTGGATATGGAAGGAAGGCCTTCAGTA
DDA 29A	TNCNACTCACTATANGNNTTGTCTGTTACAATAAAATACATTAGACATTTNAATANNTAACCTTAA AACTAGGCGAAGGGACAGAAACCCAGNCGATTGGATCTGGAGCAATGTTTTCTGCACAAGCGANA

	CAGGCANNCTCTCGTGAAGACGGATGTCNACAGAACCATNNGACCTACAGAAGAAGCCGANCAG GCTGGGGTGGGCTGGGGGTGACANANGCTGANGGTGCANGAAGTGGNCAACNAAAAATACTGACTG AGGTACCANGACTCTGCTCAGTGCAGAAAAATTGGCTTATGAATAAAAAATTAGACTGTGATACCAA ATTTAAATCCACAGAATCATGCNAANGACACAATACATGCTATTTANTTGNNTTATCTTTNNAAACN ACACA
DDA 30A	CCTGATTTTCTNCATTGTNGNNCTCCTCTTTCTCCAGCCGCTCTTGGATTTTGCTTTTCCCTCAGCT CCTTCTCTGAGGAGTGTGTTTGGAGAGCTTTCTGCCGGTGGTGAAGTCCACAGAGTGNCCTGTCTGGT GGCCTGGCTCCAAGGAAGGAGCCTCTTGAGTCTNAGGACTCTCCTGACTCGGAGTTTCTCCATGTC ACTCTCATCACTGNCAGCCAGGGCTTTGGGAAAGCTTCTGCTCTGACTCTTCCCTGAATGTAAGNTC TCCTGAGTGNCTNTGCGCTGTGACGTANGTGGGTTTCTNCGGAGCATCGTCTCTGCCTCANCTN ANAATCGCTGGCTGTAACTTTCTGCTCTTAGGTTTCTTGCTCACAAAAATCTCTCATNAGAA TCTCTTTCACTCAAGGGCTCGAGTGGGTTCAAAGCTGCC
DDA 31B	CCGGCTGGGCACTAATGAGGTAATGAGTTAGATATTCTCTCAGAGCCTGGCTACTCATTATAAA ATGGTTAAGTGAGTCAATGCTGTGTTGTGGGCTGAATCATGTCCCTCCAAGATCCATATGCTATAGC CTACTACAGTTTGGGTTGAAATGTCTCCATGGGTTAATGTTGGGGCTTCTGGAGCTAGAGCCTGGC TGCAGACCTAGGTGCTCAGGAGCAAGCCTTGGAGGTCCCACCCACCTAAGGTTCCAGCCTAACTCT GCCTCTGCTTCTTGGCCTGGACCATGTGAACAGACCTCACCCCATGGTTCCTGACATTGGCTCTG CCCACTGTGCCTTCCACCATGATGAGCT
DDA 33B	CGTCAAGAATAAAATATGNTTTAATTGCAAATAGGAAAGGAACTTGGGTCTCTATAGTAACCAGG AATAGNGTACATTTGCAAACCTCAGTTGTTTAAACATGTCAGTTAATGGTTTATATTTACAAAGTTTG NGCACAAGAAGCAATGATTTGGCTTCTGAATTTATAAATGGAGTTGGAGACAAATGTTTCATTGA CTATAAGAACTGCTTGGAGAACGAGATCCTATGATGCATCTCACTTTCTTTTAAAGAGAAGGCTA GGCGCTTCTCTCCCACTGAGGCCACACAAGGCAGCCAGCTAGAAGAACATAGCCCATTTACAGG CAACAGCTTTTGAATAGCCCTGCTCCAGTTGTTTGGGATCCATATGAAGACCAAGCTGCACATCT GCTTCATATGTGTGGGAGGCTAGGTCCAGCCGTGATGTTCTTTGGATG
DDA 34B	CACACAGGAGCTAGCATGGGAAGGGGAACAGAAAAGGGCCTTAGCAATTGCTTCATTGCGTGCACT AACCGAAGCTCGGAACCTTACAGAATGGGGCTGTGGACCTGGGAGGCTTTTCTCCTCTAACCCCTCT CCCCAGCCCTAGGCTCCTCCGTCTTTCTCCGGCTGCACCAGAGCGCTGCCTCACTCCCTGCGCCATG TCCCACAGTTGCCACCATCTCCGTGGCTTTGAAATGACCACCACCTAAAGTCTGAATCACAGCGC ACCACCCCTTGTCTGAGGACCTTACTCTCTGCTCCATGTGAGAGGACGAAGAGAAACGACTGGAT ATTGGCGATCCTAGGTAGCAGATCAGGGGAGGGCTCAAAAAGCGGCAAGCCACTGAACCTCATGACC AAGTTTGCAGCATTGCTGGTGATGTGGGATCCGTGGGTTTGTGTTTCCCA
DDA 35B	CGTGTAAGTGTGGGAGGNTAATTGATCTGTCCATGGGCTTCCCCGTCCGGCACAGTCATGATGG CATCCGATACCTCTCTCATCCAGATAGAGACAGAGATCCCAAGCTGTGATAGAAAAATCCATTCT CGNGTTGATATTTTGATTCGCCGAACCTCACGGNAGAACATGGAGCTGATGTCAACATCGCCCCAA ATCAACCCAAGTGTGCATGCCAAGACTACATCTTTGTTATAATTCCCTCGGGTCTTCAAGCAGCAC CGTTCACGCTGTGTCTCTG
DDA 38B	CTNCTGANGGAGNGACCCTTCTCTGCACATTCTATGGAGAAATGTTCTTTTGCTACTCTTGATTCTA GGAATGCANAGAGAAAAACAGAACCCTGAGAAATAAGGCCTTCTCTCTAGTCACAGAGGAAGGCA AGNGTCATAGGCATACTGGCANGANGCACATTCTANGCTGGTTGCTGTCCACTGCCAACCCCTCNTA AGACTAGAACATTGACTCCACATGACCTCTGCNAGAATGGGTNCCTCTTTNCTG
DDA 45C	AATAAAGTTTTATTACAACACATATAAGAACATTTTCTTGCAATTCATTCAATTATTGATTTACAT CATAGATCAATTCAATAGATTATAGAAGAGTTTATGTGGTATCTATCACTAAATACTGCATTGTTT GCTAATGAGCTATTCTTAGAAAACTATGCAGGTTTCTCAGGTTAGAATGGTTCTGCTGTTTATTGAC ACGAAGTTGTGGCCAAGTTGCCTTTCCATACTCCAGTTTGCTTAGCCTTGACAAGCAATTCACACAA AACATTCTGAAATGAGCATAGAAGTTAAGCACTCTAATACTACTCCAATAAATTACTCACAG GGAGTATCCTGCTATCAAAGAAAAATCTATATGATCTGGAATTAATGAAATGTGAATACATTGCC CAACAGTTGCTCATTTAGGTTATGTGAGAGAATATGTGGAATGC
DDA 46A	CTAATGTTATCAGGGAAGCAGAGAGCTGTATCTTTTATAAGTCTACTTATAAATTTATGCCACTA ACGCCAACATTGAACAGGCAATTAATAAATAATTTAAAGGCTTGTGCCCA GGCAGCAGAGCTACATGGAAAGTTCCTTTACAGAAGATCCAGCCCCAACCGCCAGATGTTAAC TGTGAAATAAACACCTGTGATGATGGTTTACGAGAATCATGGTGATTTAACTTTTAAACGAAAT ACCTAAAAGGCAGTCACTATGTCCCACTAGACTTAGAAGCTACCCG
DDA 47D	ACAATTACTGCAGTTTTTCCAGAAAACTCACACCAATAAATGTAACAGAACATTCCATTTGTTA ATGGGCATATGTGCATAAGCAGTGTAGAAAATAGGCTCATGTTAGAACTGGCTACATCCTTCATA ACCAAAAGTGTGGTTATATGAATGGACACTGTCAATGTTTATAGCTTAAACCTGGGTACCTGGTCA

	AAATGCTTAGGAAACATTAAAATTGAGCTAAATTGAAAAAAAAAAAAAAAAAAAAAAAAAAAA AAAAAAAAAAAA
DDA 49A	TACAAAAAGACAATATTTATTTTACTTTCTTATAAGTAGTTCAACAGAAAGTCTTCTACTTGAAGA CATTACTGAAAACATTAAACATTATTTTATGCATCCCTTCAGTGCCAGATTGAGAAAAAGGTCATC TGAATGAAGGAAAAGGAATGGTCCTCCTTATGTTGGGTTTACTTATGTAAGTGGGGGAAATCCAT ATACCTTAGTCAAAATAATATGTGAACCTACAAGTTTCCAATAAGCAATGTACTCATATCTTTATG AGTCCCTAAGGCCTGGAGATTACTTTTGTCTGTAAAACAAAGGTACTCTGTACCTGTCCCTTT CCCCTGCTATTGTACTACTGAAAGAGAATTTGAAGCAAAATATGATGTCTTTGTTCCCATGCTGC AAGACTGTCAGCATAGATGGTTTCCACAGCATTTCAAAACAT
DDA 50B	CACACAGGAGCTAGCATAGGGGTGAAGTACAGGAACATAAAAGGTCTCTCACATTCTTCAGTGTG CAGGGTAGTGGGCAGATGTAAATTGGGCTATCAGTAAACAAGTTACTGTGGAGTTCTATGTACCCT TTATCACGTTATTGCTAAGACATTTATTTACTGGAAGTAGTTCAGTAATGTAATGCTGAAGTTGTA TAGTAAATGAATGCAGAACATGGAAGTGGTGTCAATTTTAGAGAGCATTAAAGTTACAAGCC AGGGTCTCTGTTCAAATTGTCTTGGTAAAAGAAAAATGTGTACAAAGTGCTTGTAAATTAGTTTTCA GAACTGACTAGGAGGGGTAATGCTGGGATATTGTTGAGAGACTAGCTTAATAAGGAACTTATAC CATGTGTGCTTTTGATGCTAAGTCACCTAGCATTCAAATTTGAATATACAG

## Mapping of ESTs

Twenty-seven of the ESTs isolated through differential display analysis (DDA sequences) were unique. We developed primers from these, and 20 of them were mapped with high confidence (lod scores ranging from 6.1 to 25.6) on the T31 mouse Radiation Hybrid (RH) panel (Table 2 and <http://www.jax.org/resources/documents/cmdata/rhmap/RHIntro.html>). DDA38, which represents mouse *Kcnql*, was mapped previously to chromosome 7, map position 69.3, by backcross and physical mapping. The human ortholog, *KCNQ1*, has been located on human chromosome 11p15.5. We mapped *Kcnql* to distal mouse chromosome 7, between 71 and 72 map units. Nine additional ESTs corresponded to genes mapped previously in mouse or human (Table 3). Nineteen of the 20 mapped ESTs were localized to mouse chromosomal regions with an interval size <4 map units (Table 2).

We initially used comparison of mouse and human genetic maps to predict the most likely locations in both mouse and human genomes of orthologous genes (Table 2) (see Materials and Methods). Of the 20 ESTs mapped by the RH panel, 16 had an unambiguous

predicted human location and 4 mouse positions did not discriminate between two possible locations in the human genome (Table 2).

**Table 2:** EST RH Mapping Results, Mouse/Human Map Positions, and Phenotypes Associated with Map Positions

Name of EST	Best fit on RII panel (proximal marker-distal marker)	Mouse chromosome (map position)	Predicted human map position	Human genomic sequence matches	Phenotypic associations in mouse and human (M, mouse, and H, human)
DDA5	—	18 (1)	10p11, 8q	10p11.23	
DDA7	—	4 (57.4)	1p35-p34	1p34.2	M: snubnose (98332) H: Schwartz-Jampel syndrome (255800)
DDA8	—	9 (15-30) <sup>a</sup>	11q23.3	11q23.3	M: variable spotting (98939), luxoid (96851) H: Jacobsen syndrome (147791), hydroletharus syndrome (236680)
DDA9	—	10 (7-29) <sup>a</sup>	6q23	6q23.3 and 5q22.1	M: gray-lethal (95725) H: cardiomyopathy (602067)
DDA14	<i>D1Mit415-D1Mit49</i>	1 (52-55)	2q37	—	H: brachydactyly-mental retardation (600430), brachydactyly (113300)
DDA16	<i>D16Mit157-D16Mit169</i>	16 (34-37)	3q28-q29 or 3p11	—	
DDA17	<i>D19Mit57-D19Mit39</i>	19 (24)	10q23-q24 or 9p24	—	H: split hand/foot malformation (600095)
DDA21	—	8 or 14 <sup>a</sup>	8p23.1	8p23.1 <sup>b</sup>	
DDA22	<i>D4Mit91-D4Mit214</i>	4 (15-18)	9p21-p13	—	M: crinkly tail (88573) H: arthrogryposis multiplex congenita (108120), cartilage-hair hypoplasia (250250), acromesomelic dysplasia (602875)
DDA23	<i>D2Mit267-D2Mit464</i>	2 (8-9)	10p11-13	—	M: Danforth's short tail (98265) H: DiGeorge/velocardiofacial syndrome (601362), arrhythmogenic right ventricular dysplasia (604401)
DDA24	<i>D4Mit31-D4Mit146</i>	4 (51-54)	1p33-p32.1	1p32.1-p33	
DDA25	<i>D18Mit183-D18Mit107</i>	18 (37)	18p11.2	18p11.21	
DDA26	—	12 or 14 <sup>a</sup>	14q11.2-q12	14q12 <sup>b</sup>	H: Arrhythmogenic right ventricular dysplasia (602086)
DDA27	<i>D3Mit355-D3Mit154</i>	3 (33)	3q25-q26 or 4q32-q33	3q25.33	H: Cornelia De Lange syndrome (122470)
DDA28	<i>D5Mit336-D5Mit356</i>	5 (41)	4p14-p12	4p11	M: recessive spotting (98188), rump white (98213), patch (97571) H: total anomalous pulmonary venous return (106700)
DDA29	—	5 (B and F)	12q23-q24.1	12q24.11 <sup>b</sup>	H: Darier disease (124200) <sup>e</sup> , brachydactyly (113100), cardiofaciocutaneous syndrome (115150)
DDA30	<i>D9Mit51-D9Mit310</i>	9 (61)	3p24-p21	—	H: cardiomyopathy (601154), arrhythmogenic right ventricular dysplasia (604400)
DDA31	<i>D10Mit60-D10Mit258</i>	10 (30-31)	10q22	—	M: gray-lethal (95725)
DDA33	<i>D19Mit5-D19Mit12</i>	19 (26-34)	10q23-q24	—	M: hemoglobin deficient (96028) H: split hand/foot malformation (600095)
DDA34	<i>D6Mit134-D6Mit255</i>	6 (57-60)	12p13	12p13.31 <sup>b</sup>	H: acrocallosal syndrome (200990)
DDA35	<i>D14Mit134-D14Mit132</i>	14 (1-3)	3p14 or 10q21-q24	—	M: talipes (98479) H: cardiomyopathy (601493), Moebius syndrome (604185), split hand/foot malformation (600095)

**Table 2: Continued**

Name of EST	Best fit on RH panel (proximal marker-distal marker)	Mouse chromosome (map position)	Predicted human map position	Human genomic sequence matches	Phenotypic associations in mouse and human (M, mouse and H, human)
DDA38	<i>D7Mit177-D7Mit15</i>	7 (71-72)	11p15.5	—	M: earlier X zone degeneration (95463) H: Jervell and Lange-Nielsen syndrome (220400), QT syndrome (192500)
DDA45	<i>D16Mit4-D16Mit59</i>	16 (27-28)	3q13-q21	—	H: Moebius syndrome (601471), Charcot-Marie-Tooth neuropathy (600882)
DDA46	<i>D10Mit99-D10Mit71</i>	10 (60-61)	12q21	—	
DDA47	<i>D2Mit245-D2Mit219</i>	2 (43-44)	2q31-q32	2q31.2 and 10q11.21 <sup>b</sup>	H: cardiomyopathy (604145), arrhythmogenic right ventricular dysplasia (602087)
DDA49	<i>DXMit81-DXMit49</i>	X (9-13)	Xq22-q24	—	M: wide-faced (1310006) H: Miles-Carpenter syndrome (309605), Alport syndrome (300195)
DDA50	<i>D3Mit62-D3Mit28</i>	3 (4-6)	8q13-q22	—	

The best fit for each EST mapped on the RH panel was between two MIT markers. ESTs not mapped by the RH panel are indicated by a dash (—) in the second column. Mouse and/or human map positions for these ESTs are based on known map positions or comparative mapping. Map positions in mouse are specified by distance from the mouse centromere in map units on the MGI consensus linkage map. Phenotypic associations in mouse and human are indicated by Mouse Genome Database (MGD) identification numbers and Online Mendelian Inheritance in Man (OMIM) identification numbers, respectively.

<sup>a</sup> Position in mouse predicted based on the chromosomal location of the best human match.

<sup>b</sup> Sequence showed homology to other chromosomal segments with lower but still significant scores.

To resolve some of these ambiguities, we compared the DDA sequences by BLAST to human and mouse genomic sequence. No matches were found to publicly available mouse genomic sequence. However, 13 of them detected one or more significant human matches, and all of these matched the predicted chromosomal location with the highest homology score, refining and confirming predictions from comparative mapping. The 7 sequences that could not be mapped on the RH panel had strong hits in human sequence, such that comparative mapping predicted the mouse genomic location.

### Confirmation of dysregulation

In order to confirm dysregulation of fragments isolated from the differential display analysis, we performed RT-PCR analysis on RNA from E9.25 wild-type and *dHAND*<sup>-/-</sup> hearts

using specific primers (see materials and methods). The following fragments showed downregulation in the *dHAND*<sup>-/-</sup> hearts: DDA5, DDA8, DDA9, DDA14, DDA17, DDA21, DDA23, DDA24, DDA28, DDA29, DDA33, DDA45, DDA50. We also performed whole-mount and radioactive *in situ* hybridization analysis on wild-type and *dHAND*<sup>-/-</sup> embryos at E9.0-9.5 using probes specific for DDA9, DDA21 and DDA26. DDA26 was up-regulated in the *dHAND*<sup>-/-</sup> embryo, while DDA9 and DDA21 were down-regulated.

### **DDA sequence expression and mapped phenotypes**

Twenty-two unique sequences from the differential display analysis could be shown independently to be transcribed sequences based on expression studies or EST matches (Table 3). Twelve of these matched known mouse genes and/or their human orthologs. We identified and mapped a number of these for the first time in mouse or human. Nine DDA sequences matched sequences in “full-length-enriched” Riken cDNA libraries (Kawai et al., 2001). Six were confirmed to occur in heart and/or early embryo.

We identified phenotypes in humans and mice that map near to each EST position in OMIM and MGD (Table 2). Anomalies that involve the heart, vascular system, limb, facies, and neural crest-derived structures might be consistent with the known effects of dHAND. In addition, effects on melanocytes, calcitonin-secreting cells, and the adrenal gland could arise as a result of the loss of dHAND expression affecting neural crest development and migration (Yamagishi et al., 1999). Several DDA sequences mapped to the same chromosomal regions as phenotypes affecting the heart, such as arrhythmogenic right ventricular dysplasia (DDA23, 26, 30, 47), other cardiomyopathies (DDA9, 35, 47), and QT

**Table 3:** Transcript Alignments of DDA Sequences

Mouse EST	Transcript alignments [accession number]	Expect value	Expressed in heart	Expressed in embryo
DDA5	Kinesin family member 5B ( <i>Kif5b</i> ) [NM_008448]	e-147	X	X
DDA7	Microtubule-actin crosslinking factor ( <i>Acip7</i> ) [AF150755]	e-167	X	
DDA8	Ubiquitin-specific protease ( <i>Usp2</i> ) [AF079565]	2e-65		
DDA9	<i>Homo sapiens</i> Bcl 2-associated transcription factor [AF249273]	e-135	X	
DDA14	RIKEN full-length clone 5730526A02 (from 8-day embryo) [AV305124]	e-100		X
DDA17	RIKEN full-length clone A530087E01 (from adult male aorta) [BB224579]	e-131	X	
DDA21	RNA pol II transcriptional coactivator ( <i>Rpo2tcl</i> ) [NM_011294]	0		
DDA23	<i>Homo sapiens</i> Nebulette ( <i>NEBL</i> ) [AF047368]	None <sup>a</sup>	X	X
DDA24	Tetratricopeptide repeat domain 4 ( <i>Ttc4</i> ) [AF177029]	0		
DDA25	Mouse 8.5-dpc whole embryo cDNA [BM249163]	0		X
DDA26	<i>BCL2</i> /adenovirus E1B 19-kDa-interacting protein 3 ( <i>Bnip3</i> ) [NM_009760]	0	X	
DDA27	RIKEN full-length clone 1110032F04 (from 18-day embryo) [AK004029]	e-123		X
DDA28	RIKEN full-length clone 6030432N09 [NM_023429]	e-165		
DDA29	Sarco/endoplasmic reticulum Ca <sup>2+</sup> ATPase ( <i>SERCA2</i> ) [AJ131870]	e-157	X	
DDA30	RIKEN full-length clone, 9.5-day embryo parthenogenote [BB294262]	0		X
DDA34	$\gamma$ -neuronal enolase ( <i>Eno2</i> ) [NM_013509]	e-143		
DDA38	Partial <i>Kcnq1</i> gene for potassium channel protein [AJ271885]	e-113	X	X
DDA45	Mouse EST from 13-day embryo [AV165138]	0		X
DDA46	RIKEN full-length clone A630014C11 [BB228450]	e-106		
DDA47	RIKEN full-length clone 2610209F03; myotubularin related	e-123	X	
DDA49	Multiple mouse ESTs and RIKEN clones [AA408993, BB552273, AV255749]	0		X
DDA50	RIKEN full-length clone 4930431H11 [AK015268]	2e-89		

DDA23 did not share any significant homology with human *NEBL*, and there is no mouse nebulette cDNA sequence in the GenBank database. The extended RACE product of DDA23 shares significant homology with human *NEBL*.

syndrome (DDA38). Two ESTs mapped in human chromosomal regions associated with syndromes that involve both congenital heart defects and craniofacial defects. The human ortholog of DDA29 mapped to HSA 12q24.11, the same region as cardiofaciocutaneous syndrome, while DDA23 mapped to the region responsible for DGS2 on HSA10. We characterized DDA23 further.



### **DDA23 is the mouse ortholog of *nebulette* (*NEBL*)**

Comparative mapping predicted that the human ortholog of DDA23 would be located on 10p14–p13. Haploinsufficiency for this region of HSA 10 results in a clinical presentation of DiGeorge syndrome (Daw et al., 1996; Schuffenhauer et al., 1998). The short DDA23 sequence (448bp) did not match known genes or ESTs. However, extension of the sequence using 5' and 3' rapid amplification of cDNA ends (RACE) identified significant homology to human *NEBL* (Table 3). The open reading frame of human fetal *nebulette* encodes a 115-kDa cardiac actin-binding protein that shares homology with human skeletal muscle nebulin (Moncman and Wang, 1995, 1999).

The current study identifies *nebulette* (as DDA23) from E9.5 mouse heart. *Nebulette* has been identified previously in cDNA libraries of human fetal heart (HSY17673) and embryonic day 13 mouse heart (BB658903). To confirm expression in fetal heart, we performed RT-PCR on mRNA from E9.5 mouse hearts. A *nebulette* product was obtained from both wild-type and *dHAND*<sup>-/-</sup> hearts. Amplification using equal starting amounts of RNA showed a consistent reduction of about four-fold in *nebulette* product from *dHAND*<sup>-/-</sup> hearts after 18, 20, 22, or 24 cycles of PCR.

### **Mapping of human *nebulette* using Fluorescence *in Situ* Hybridization (FISH)**

Previous gene mapping studies indicated that human *nebulette* is mapped to chromosome 10p12 (Millevoi et al., 1998). To identify more precisely the location of *NEBL* in relation to the DGS2 region, we examined cell lines with 10p deletions by FISH using overlapping BACs that contain the gene (Fig. 2). The BACs were absent from two of the

deleted cell lines, CH95-199 and GM03470. CH95-199 was derived from a female with a cardiac defect, immune deficiency, cleft palate, facial dysmorphism, and developmental delay (Gottlieb et al., 1998). GM03470 was derived from a female with microcephaly, microphthalmia, and hypotelorism. The BACs were not deleted from the GM06936 or CH92-092 cell lines, which were derived from patients who had hypocalcemia, immune

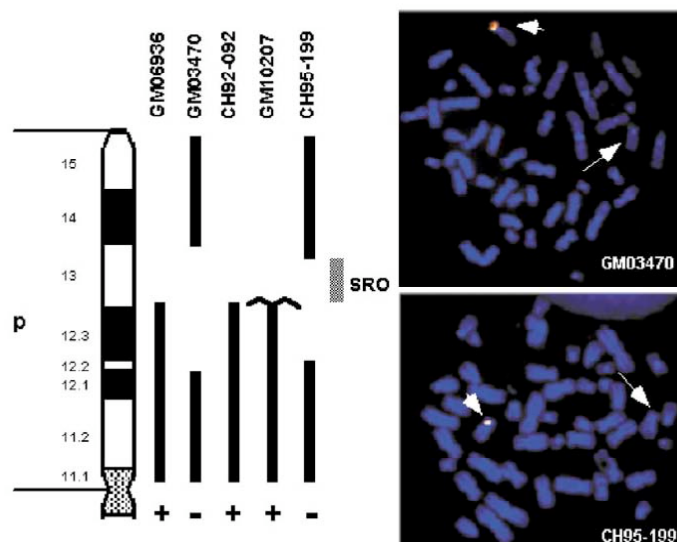


**FIG. 2.** Mapping the *NEBL* gene by FISH. (Left) Chromosomal ideogram with black rectangles alongside indicating the portion of 10p present in the cell lines. In the case of GM10207, only the der(10) is indicated. The presence of a plus sign below the ideogram indicates whether the BACs gave a positive signal on the deleted or der(10) by FISH analysis. A minus sign indicates the BACs were deleted. The SRO in gray indicates the smallest region of deletion overlap for the location of the *NEBL* gene. (Right) Representative FISH images. The shorter arrow indicates the normal chromosome with overlapping signals from the FITC-(BAC 56H7) and rhodamine- (BAC45L12) labeled *nebullette*-containing BACs. The longer arrow indicates the deleted chromosome 10. Chromosome identification was accomplished by converting the DAPI-counterstained image to gray scale.

defect, developmental delay, and renal or genitourinary anomalies (hypoplasia and ureteral reflux, respectively). Neither of these individuals had a cardiac defect. Thus, their features were consistent with the HDR spectrum of DGS2 anomalies. The BAC was present on the der(10) in GM10207, which narrows the gene location to the interval shown in Fig. 2.

## Discussion

dHAND plays an important role during development, and genes expressed downstream of it may be candidates for anomalies of the heart, vascular system, facies, limb, and various neural crest-derived structures. In this study, genes whose expression was affected in hearts of *dHAND*<sup>-/-</sup> mice, as determined by differential display, were mapped to several chromosomal regions linked to phenotypes judged to be consistent with the known effects of dHAND. One gene in particular, human *nebulette*, is expressed in early heart development and maps to the candidate region for heart defects in DiGeorge Syndrome 2 on HSA 10p.

Several of the putative dHAND-dependent genes identified here have vital functions in development. The targeted disruption of *Kif5b* (DDA5) results in embryonic lethality in the mouse, with severe growth retardation at 9.5–11.5 dpc (Tanaka et al., 1998). *Kif5b* is essential for mitochondrial and lysosomal dispersion (Tanaka et al., 1998). *Usp2* (DDA8) is a ubiquitin-specific protease, inhibition of which may result in apoptosis in cells of the developing heart (Yamagishi et al., 1999).

Several genes that show significant sequence similarity to the ESTs obtained by differential display have abundant transcripts in the heart. *Kcnq1*, represented by DDA38, is expressed during mouse development, beginning at embryonic day 9.5, within the atrial and ventricular myocardium (Franco et al., 2001). *Aclp7*, which shares significant sequence similarity with DDA7, is an actin-binding protein that is expressed mainly in the lung, brain, spinal cord, and skeletal and cardiac muscle (Bernier et al., 1996). This gene mapped to the same human chromosomal region as Schwartz–Jampel syndrome (Table 2), which includes facial abnormalities consistent with the *dHAND*<sup>-/-</sup> expression pattern. Many phenotypes mapped to the same regions, as dHAND-dependent ESTs were characterized by anomalies in structures other than heart that have been shown to express dHAND during development, e.g., the limb and facies (Table 2). Finally, dHAND may play a role in neural crest differentiation and migration. The mouse mutant phenotypes *recessive spotting*, *rump white*, and *patch deletion region*, which involve neural crest-derived melanocytes, map on MMU5 near DDA28.

Four ESTs mapped near regions linked to dilated cardiomyopathy (Table 2). Two of these loci (represented by DDA30 and 47) are also linked to arrhythmogenic right ventricular dysplasia (ARVD). DDA47 matches a RIKEN full-length clone (Table 3) that is closely related to myotubularin (*Mtm1*) and myotubularin-related (*Mtmr1*) genes (GenBank Accession No. AF125314, e-103). Mutations in myotubularin have been linked to dilated cardiomyopathy (de Gouyon et al., 1997; Laporte et al., 1997; Tanner et al., 1999). *KCNQ1*, the human ortholog of DDA38, mapped to a chromosomal region linked to syndromes characterized by cardiac arrhythmias, Long QT syndrome (LQTS) and Jervell and

Lange–Nielsen syndrome (JLNS). It has been proposed that mutations in *KCNQ1* provide a molecular basis for the cardiac arrhythmias seen in LQTS and JLNS (Ko et al., 2001; Kubota et al., 2001; Schmitt et al., 2000).

Two ESTs mapped to loci responsible for congenital diseases that demonstrate anomalies of the heart and craniofacial structures. The human ortholog of DDA29, *ATP2A2*, localizes to a chromosomal region characterized by cardiofaciocutaneous syndrome. Patients with this syndrome commonly exhibit pulmonic stenosis, atrial septal defect, and characteristic facial appearance ([http://www.ncbi.nlm.nih.gov/entrez /query.fcgi?db = OMIM](http://www.ncbi.nlm.nih.gov/entrez/query.fcgi?db=OMIM)). The *ATP2A2* gene encodes the sarco(endo)plasmic reticulum  $\text{Ca}^{2+}$ -ATPase2 (SERCA2) isoforms (Ver Heyen et al., 2000). The *ATP2A2a* isoform (SERCA2a) is expressed mainly in the cardiac and skeletal muscle, and its expression and sarcoplasmic  $\text{Ca}^{2+}$  handling are decreased in cardiac hypertrophy and in human heart failure (Arai et al., 1994). Dysregulation of this gene in *dHAND*<sup>-/-</sup> mice could occur secondary to heart failure.

Human *nebullette* maps to HSA 10p14–p13. This chromosomal region is involved in ARVD and is deleted in patients presenting cardiac defects in DGS2. Cardiac defects in DiGeorge patients result primarily from abnormal development of the branchial and aortic arch arteries, a defect that is also observed in *dHAND*<sup>-/-</sup> embryos. Anomalies of embryonic heart development, such as persistent truncus arteriosus and interruption of the aorta, have been detected in DiGeorge patients and are thought to be the result of abnormal development of the third and fourth neural crest-derived branchial arches and their corresponding aortic arch arteries, which are hypoplastic and lack critical growth in *dHAND*<sup>-/-</sup> embryos.

Different features of DiGeorge syndrome map to two regions on HSA 10p (Lichtner et al., 2000). Haploinsufficiency of the more distal region can cause HDR. Deletions that involve only the more proximal region are associated with cardiac defects, cleft palate, and T cell deficiencies (Lichtner et al., 2000). We demonstrated that *nebulette* was deleted in two DGS2 patients with the more proximal deletion who showed cardiac defects, but not in two patients with the more distal deletion, which is associated with HDR.

The genes mapped in this study are linked functionally to dHAND as molecules whose expression is altered in a differential display assay of embryonic hearts with or without this transcription factor. Some may be downstream effectors of dHAND action in heart development. Using RH mapping, comparative sequence analysis, and BLAST searches against genomic databases, we localized 27 of these products and compared their genomic locations to those of mapped phenotypes related to their expression patterns. Several of these sequences are reasonable candidates for the molecular and genetic basis of diseases that affect heart and the derivatives of neural crest, tissues that ultimately lie downstream of dHAND.

Finally, in addition to identifying genes that might be dysregulated in various cardiac diseases, we have identified 2 fragments, DDA26 and DDA9, which represent genes whose characterization might help elucidate the mechanism of dHAND action in the heart and pharyngeal arches. DDA26 represents *BCL2*/adenovirus E1B 19-kDa-interacting protein 3 (*Bnip3*), a pro-apoptotic member of the Bcl-2 family (Chen et al., 1997). DDA26 is one of the few genes isolated from the differential display analysis that was upregulated in the *dHAND*<sup>-/-</sup> heart. Loss of dHAND leads to increased apoptosis in the right ventricle and

pharyngeal arches. Bnip3 might play a role in this increased apoptosis. Further analysis of Bnip3 upregulation and the molecular pathway involved in the programmed cell death seen in *dHAND*<sup>-/-</sup> embryos is described in Chapter 3.

DDA9 is one of four separately cloned fragments that represent the mouse ortholog of human Bcl-2 associated transcription factor (*hbt*) and is specifically downregulated in the *dHAND*<sup>-/-</sup> heart. hBtf is a nuclear localized pro-apoptotic factor with transcription repressor activity. Over expression of Bcl-2 and Bcl-x<sub>L</sub> sequesters Btf in the cytoplasm, abrogating its transcriptional activity (Kasof et al., 1999). This suggests a novel pathway by which the Bcl-2 family of proteins might regulate transcription and control apoptosis. DDA9 also showed similarity in its N- and C-termini to thyroid hormone receptor associated protein 150 (TRAP150). TRAPs are a family of transcription co-activators, which are required for activation of genes downstream of nuclear receptor activation (reviewed in Ito and Roeder, 2001). One such family of ligand dependent nuclear receptors is the retinoid receptor family, which consists of the RAR and RXR subfamilies each with three members- $\alpha$ ,  $\beta$ , and  $\gamma$ . Several of these genes are required for normal cardiac development (Gruber et al., 1996; Kastner et al., 1997; Mendelsohn et al., 1994; Sucov et al., 1994). In addition, TRAP220, another member of the co-activator complex is required for normal cardiac and embryonic development (Ito et al., 2000; Zhu et al., 2000). This suggests that DDA9 might be another member of a co-activator complex with a role in cardiac development. Detailed expression and developmental role of DDA9 is described in Chapter 4.

## References

Arai, M., Matsui, H., and Periasamy, M. (1994). Sarcoplasmic reticulum gene expression in cardiac hypertrophy and heart failure. *Circ Res* 74, 555-64.

Arceci, R. J., King, A. A., Simon, M. C., Orkin, S. H., and Wilson, D. B. (1993). Mouse GATA-4: a retinoic acid-inducible GATA-binding transcription factor expressed in endodermally derived tissues and heart. *Mol Cell Biol* 13, 2235-46.

Bernier, G., Mathieu, M., De Repentigny, Y., Vidal, S. M., and Kothary, R. (1996). Cloning and characterization of mouse ACF7, a novel member of the dystonin subfamily of actin binding proteins. *Genomics* 38, 19-29.

Biben, C., and Harvey, R. P. (1997). Homeodomain factor Nkx2-5 controls left/right asymmetric expression of bHLH gene *eHand* during murine heart development. *Genes Dev* 11, 1357-69.

Charite, J., McFadden, D. G., and Olson, E. N. (2000). The bHLH transcription factor *dHAND* controls Sonic hedgehog expression and establishment of the zone of polarizing activity during limb development. *Development* 127, 2461-70.

Chen, G., Ray, R., Dubik, D., Shi, L., Cizeau, J., Bleackley, R. C., Saxena, S., Gietz, R. D., and Greenberg, A. H. (1997). The E1B 19K/Bcl-2-binding protein Nip3 is a dimeric mitochondrial protein that activates apoptosis. *J Exp Med* 186, 1975-83.

Cserjesi, P., Brown, D., Lyons, G. E., and Olson, E. N. (1995). Expression of the novel basic helix-loop-helix gene *eHAND* in neural crest derivatives and extraembryonic membranes during mouse development. *Dev Biol* 170, 664-78.



Daw, S. C., Taylor, C., Kraman, M., Call, K., Mao, J., Schuffenhauer, S., Meitinger, T., Lipson, T., Goodship, J., and Scambler, P. (1996). A common region of 10p deleted in DiGeorge and velocardiofacial syndromes. *Nat Genet* 13, 458-60.

de Gouyon, B. M., Zhao, W., Laporte, J., Mandel, J. L., Metzenberg, A., and Herman, G. E. (1997). Characterization of mutations in the myotubularin gene in twenty six patients with X-linked myotubular myopathy. *Hum Mol Genet* 6, 1499-504.

Driscoll, D. A., Budarf, M. L., and Emanuel, B. S. (1992). A genetic etiology for DiGeorge syndrome: consistent deletions and microdeletions of 22q11. *Am J Hum Genet* 50, 924-33.

Edmondson, D. G., Lyons, G. E., Martin, J. F., and Olson, E. N. (1994). Mef2 gene expression marks the cardiac and skeletal muscle lineages during mouse embryogenesis. *Development* 120, 1251-63.

Franco, D., Demolombe, S., Kupersmidt, S., Dumaine, R., Dominguez, J. N., Roden, D., Antzelevitch, C., Escande, D., and Moorman, A. F. (2001). Divergent expression of delayed rectifier K(+) channel subunits during mouse heart development. *Cardiovasc Res* 52, 65-75.

Gottlieb, S., Driscoll, D. A., Punnett, H. H., Sellinger, B., Emanuel, B. S., and Budarf, M. L. (1998). Characterization of 10p deletions suggests two nonoverlapping regions contribute to the DiGeorge syndrome phenotype. *Am J Hum Genet* 62, 495-8.

Gruber, P. J., Kubalak, S. W., Pexieder, T., Sucov, H. M., Evans, R. M., and Chien, K. R. (1996). RXR alpha deficiency confers genetic susceptibility for aortic sac, conotruncal, atrioventricular cushion, and ventricular muscle defects in mice. *J Clin Invest* 98, 1332-43.

Ito, M., Yuan, C. X., Okano, H. J., Darnell, R. B., and Roeder, R. G. (2000). Involvement of the TRAP220 component of the TRAP/SMCC coactivator complex in embryonic development and thyroid hormone action. *Mol Cell* 5, 683-93.

Ito, M., and Roeder, R. G. (2001). The TRAP/SMCC/Mediator complex and thyroid hormone receptor function. *Trends Endocrinol Metab* 12, 127-34.

Jan, Y. N., and Jan, L. Y. (1993). HLH proteins, fly neurogenesis, and vertebrate myogenesis. *Cell* 75, 827-30.

Kasof, G. M., Goyal, L., and White, E. (1999). Btf, a novel death-promoting transcriptional repressor that interacts with Bcl-2-related proteins. *Mol Cell Biol* 19, 4390-404.

Kastner, P., Messaddeq, N., Mark, M., Wendling, O., Grondona, J. M., Ward, S., Ghyselinck, N., and Chambon, P. (1997). Vitamin A deficiency and mutations of RXRalpha, RXRbeta and RARalpha lead to early differentiation of embryonic ventricular cardiomyocytes. *Development* 124, 4749-58.

Kawai, J., et al., (2001). Functional annotation of a full-length mouse cDNA collection. *Nature* 409, 685-90.

Ko, Y. L., Tai, D. Y., Chen, S. A., Lee-Chen, G. J., Chu, C. H., and Lin, M. W. (2001). Linkage and mutation analysis in two Taiwanese families with long QT syndrome. *J Formos Med Assoc* 100, 767-71.

Komuro, I., and Izumo, S. (1993). Csx: a murine homeobox-containing gene specifically expressed in the developing heart. *Proc Natl Acad Sci U S A* 90, 8145-9.

Kubota, T., Horie, M., Takano, M., Yoshida, H., Takenaka, K., Watanabe, E., Tsuchiya, T., Otani, H., and Sasayama, S. (2001). Evidence for a single nucleotide polymorphism in the KCNQ1 potassium channel that underlies susceptibility to life-threatening arrhythmias. *J Cardiovasc Electrophysiol* 12, 1223-9.

Kurihara, Y., Kurihara, H., Oda, H., Maemura, K., Nagai, R., Ishikawa, T., and Yazaki, Y. (1995). Aortic arch malformations and ventricular septal defect in mice deficient in endothelin-1. *J Clin Invest* 96, 293-300.

Kurihara, Y., Kurihara, H., Maemura, K., Kuwaki, T., Kumada, M., and Yazaki, Y. (1995). Impaired development of the thyroid and thymus in endothelin-1 knockout mice. *J Cardiovasc Pharmacol* 26 Suppl 3, S13-6.

Laporte, J., Guiraud-Chaumeil, C., Vincent, M. C., Mandel, J. L., Tanner, S. M., Liechti-Gallati, S., Wallgren-Pettersson, C., Dahl, N., Kress, W., Bolhuis, P. A., Fardeau, M., Samson, F., and Bertini, E. (1997). Mutations in the MTM1 gene implicated in X-linked myotubular myopathy. ENMC International Consortium on Myotubular Myopathy. European Neuro-Muscular Center. *Hum Mol Genet* 6, 1505-11.

Laverriere, A. C., MacNeill, C., Mueller, C., Poelmann, R. E., Burch, J. B., and Evans, T. (1994). GATA-4/5/6, a subfamily of three transcription factors transcribed in developing heart and gut. *J Biol Chem* 269, 23177-84.

Lee, J. E., Hollenberg, S. M., Snider, L., Turner, D. L., Lipnick, N., and Weintraub, H. (1995). Conversion of *Xenopus* ectoderm into neurons by NeuroD, a basic helix-loop-helix protein. *Science* 268, 836-44.

Lichter, P., Cremer, T., Borden, J., Manuelidis, L., and Ward, D. C. (1988). Delineation of individual human chromosomes in metaphase and interphase cells by in situ suppression hybridization using recombinant DNA libraries. *Hum Genet* 80, 224-34.

Lichtner, P., Konig, R., Hasegawa, T., Van Esch, H., Meitinger, T., and Schuffenhauer, S. (2000). An HDR (hypoparathyroidism, deafness, renal dysplasia) syndrome locus maps distal to the DiGeorge syndrome region on 10p13/14. *J Med Genet* 37, 33-7.

Lints, T. J., Parsons, L. M., Hartley, L., Lyons, I., and Harvey, R. P. (1993). Nkx-2.5: a novel murine homeobox gene expressed in early heart progenitor cells and their myogenic descendants. *Development* 119, 969.

Ma, Q., Kintner, C., and Anderson, D. J. (1996). Identification of neurogenin, a vertebrate neuronal determination gene. *Cell* 87, 43-52.

Mendelsohn, C., Lohnes, D., Decimo, D., Lufkin, T., LeMeur, M., Chambon, P., and Mark, M. (1994). Function of the retinoic acid receptors (RARs) during development (II). Multiple abnormalities at various stages of organogenesis in RAR double mutants. *Development* 120, 2749-71.

Millevoi, S., Trombitas, K., Kolmerer, B., Kostin, S., Schaper, J., Pelin, K., Granzier, H., and Labeit, S. (1998). Characterization of nebulin and emerging concepts of their roles for vertebrate Z-discs. *J Mol Biol* 282, 111-23.

Moncman, C. L., and Wang, K. (1995). Nebulette: a 107 kD nebulin-like protein in cardiac muscle. *Cell Motil Cytoskeleton* 32, 205-25.

Moncman, C. L., and Wang, K. (1999). Functional dissection of nebulin demonstrates actin binding of nebulin-like repeats and Z-line targeting of SH3 and linker domains. *Cell Motil Cytoskeleton* 44, 1-22.

Olson, E. N., and Klein, W. H. (1994). bHLH factors in muscle development: dead lines and commitments, what to leave in and what to leave out. *Genes Dev* 8, 1-8.

Schmitt, N., Schwarz, M., Peretz, A., Abitbol, I., Attali, B., and Pongs, O. (2000). A recessive C-terminal Jervell and Lange-Nielsen mutation of the KCNQ1 channel impairs subunit assembly. *Embo J* 19, 332-40.

Schuffenhauer, S., Lichtner, P., Peykar-Derakhshandeh, P., Murken, J., Haas, O. A., Back, E., Wolff, G., Zabel, B., Barisic, I., Rauch, A., Borochowitz, Z., Dallapiccola, B., Ross, M., and Meitinger, T. (1998). Deletion mapping on chromosome 10p and definition of a critical region for the second DiGeorge syndrome locus (DGS2). *Eur J Hum Genet* 6, 213-25.

Shaikh, T. H., Budarf, M. L., Celle, L., Zackai, E. H., and Emanuel, B. S. (1999). Clustered 11q23 and 22q11 breakpoints and 3:1 meiotic malsegregation in multiple unrelated t(11;22) families. *Am J Hum Genet* 65, 1595-607.

Shivdasani, R. A., Mayer, E. L., and Orkin, S. H. (1995). Absence of blood formation in mice lacking the T-cell leukaemia oncoprotein tal-1/SCL. *Nature* 373, 432-4.

Srivastava, D., Cserjesi, P., and Olson, E. N. (1995). A subclass of bHLH proteins required for cardiac morphogenesis. *Science* 270, 1995-9.

Srivastava, D., Thomas, T., Lin, Q., Kirby, M. L., Brown, D., and Olson, E. N. (1997). Regulation of cardiac mesodermal and neural crest development by the bHLH transcription factor, dHAND. *Nat Genet* 16, 154-60.

Sucov, H. M., Dyson, E., Gumeringer, C. L., Price, J., Chien, K. R., and Evans, R. M. (1994). RXR alpha mutant mice establish a genetic basis for vitamin A signaling in heart morphogenesis. *Genes Dev* 8, 1007-18.

Tanaka, Y., Kanai, Y., Okada, Y., Nonaka, S., Takeda, S., Harada, A., and Hirokawa, N. (1998). Targeted disruption of mouse conventional kinesin heavy chain, kif5B, results in abnormal perinuclear clustering of mitochondria. *Cell* 93, 1147-58.

Tanner, S. M., Schneider, V., Thomas, N. S., Clarke, A., Lazarou, L., and Liechti-Gallati, S. (1999). Characterization of 34 novel and six known MTM1 gene mutations in 47 unrelated X-linked myotubular myopathy patients. *Neuromuscul Disord* 9, 41-9.

Thomas, T., Kurihara, H., Yamagishi, H., Kurihara, Y., Yazaki, Y., Olson, E. N., and Srivastava, D. (1998). A signaling cascade involving endothelin-1, dHAND and msx1 regulates development of neural-crest-derived branchial arch mesenchyme. *Development* 125, 3005-14.

Van Mierop, L. H., and Kutsche, L. M. (1986). Cardiovascular anomalies in DiGeorge syndrome and importance of neural crest as a possible pathogenetic factor. *Am J Cardiol* 58, 133-7.

Ver Heyen, M., Reed, T. D., Blough, R. I., Baker, D. L., Zilberman, A., Loukianov, E., Van Baelen, K., Raeymaekers, L., Periasamy, M., and Wuytack, F. (2000). Structure and organization of the mouse *Atp2a2* gene encoding the sarco(endo)plasmic reticulum  $\text{Ca}^{2+}$ -ATPase 2 (SERCA2) isoforms. *Mamm Genome* 11, 159-63.

Weintraub, H. (1993). The MyoD family and myogenesis: redundancy, networks, and thresholds. *Cell* 75, 1241-4.

Yamagishi, H., Garg, V., Matsuoka, R., Thomas, T., and Srivastava, D. (1999). A molecular pathway revealing a genetic basis for human cardiac and craniofacial defects. *Science* 283, 1158-61.

Yamagishi, H., Olson, E. N., and Srivastava, D. (2000). The basic helix-loop-helix transcription factor, dHAND, is required for vascular development. *J Clin Invest* 105, 261-70.

Yamagishi, H., Yamagishi, C., Nakagawa, O., Harvey, R. P., Olson, E. N., and Srivastava, D. (2001). The combinatorial activities of *Nkx2.5* and dHAND are essential for cardiac ventricle formation. *Dev Biol* 239, 190-203.

Zhu, Y., Qi, C., Jia, Y., Nye, J. S., Rao, M. S., and Reddy, J. K. (2000). Deletion of PBP/PPARBP, the gene for nuclear receptor coactivator peroxisome proliferator-activated receptor-binding protein, results in embryonic lethality. *J Biol Chem* 275, 14779-82.

Zhuang, Y., Soriano, P., and Weintraub, H. (1994). The helix-loop-helix gene *E2A* is required for B cell formation. *Cell* 79, 875-84.

## **CHAPTER THREE**

### **Loss of Apaf-1 Leads to Partial Rescue of the *dHAND*-null**

#### **Phenotype**

#### **Background**

Cell fate decisions of survival or death play a central role in shaping the developing embryo and its organs. While much is known about the triggers and effectors involved in programmed cell death (apoptosis) (Hengartner, 2000), relatively little is known regarding the transcription factors that influence such decisions. *dHAND* is a basic helix-loop-helix (bHLH) transcription factor that is essential for numerous embryologic events (Srivastava et al., 1997; Thomas et al., 1998; Charite et al., 2000; Fernandez-Te et al., 2000; Howard et al., 2000; Yamagishi et al., 2000; Abe et al., 2002). In mouse, *dHAND* is specifically expressed in the developing heart, pharyngeal arch mesenchyme, and posterior limb buds (Srivastava et al., 1995; Thomas et al., 1998; Charite et al., 2000). Embryos lacking *dHAND* exhibit hypoplasia of the right ventricle, aortic arch arteries, and pharyngeal arches, all of which are associated with apoptosis of *dHAND*-expressing cells (Srivastava et al., 1997; Thomas et al., 1998; Yamagishi et al., 2001). However, the cellular pathways through which *dHAND* promotes cell survival are unknown.

Pathways triggered by both extracellular and intracellular signals can lead to the proteolytic cascade characteristic of cells undergoing programmed cell death (apoptosis) (Li

and Yuan, 1999). The main effectors of apoptosis are cysteine proteases known as caspases, which are highly conserved across species (Budihardjo et al., 1999; Cikala et al., 1999; Earnshaw et al., 1999). Signaling through the cell surface death receptor activates initiator caspase-8, which in turn activates the effector caspases (caspases-3, -7 etc.) that are directly responsible for degrading cellular proteins and causing DNA fragmentation (Li and Yuan, 1999). A similar process is activated when mitochondria are damaged leading to release of cytochrome c (Kluck et al., 1997; Yang et al., 1997), which together with apoptosis protease-activating factor-1 (Apaf-1) activate caspase-9, an initiator caspase that can activate downstream caspases (Liu et al., 1996; Li et al., 1997; Zou et al., 1999).

Targeted deletions of several molecules in the apoptotic cascade have revealed a complex overlap of function and tissue-specific requirement of numerous factors (Ranger et al., 2001). During development, apoptosis can be induced or suppressed by specific pro- or anti-apoptotic stimuli respectively. This complex interplay between the various factors suggests a strict control on their expression and/or activity (Jacobson et al., 1997). This could be at the level of transcription, translation or post-translational modifications in response to specific stimuli. While many mediators of apoptosis have been shown to undergo proteolytic cleavage in response to stimuli (Li and Yuan, 1999), the transcriptional control of the expression of these factors is poorly understood.

Here, we investigated the apoptotic cascades affected by dHAND during mouse embryonic development. By investigating differentially expressed genes, we found that the hypoxia inducible pro-apoptotic Bcl-2 family member, Bnip3 (formerly Nip3), which functions through the mitochondrial damage pathway (Chen et al., 1997; Bruick, 2000; Guo



et al., 2001; Regula et al., 2002), was upregulated in the *dHAND*-null embryo. Bnip3 localizes to the mitochondria (Yasuda et al., 1998) and is implicated in hypoxia-induced apoptosis in cardiomyocytes (Guo et al., 2001; Kubasiak et al., 2002; Regula et al., 2002). Apaf-1, a downstream mediator of mitochondrial-induced apoptosis (Li et al., 1997; Zou et al., 1997), was required for the apoptosis observed in *dHAND*-null pharyngeal and aortic arch mesenchyme, as in vivo loss of Apaf-1 partially rescued mesenchymal apoptosis in *dHAND*-null embryos and delayed embryonic lethality. Despite prolonged survival, the right ventricular hypoplasia was unchanged in the *dHAND*<sup>-/-</sup>*Apaf-1*<sup>-/-</sup> embryos. These results suggest that dHAND, in addition to regulating differentiation and expansion of specific cell types (Yamagishi et al., 2000; Yamagishi et al., 2001), functions by regulating survival of pharyngeal arch mesenchyme through an Apaf-1 mediated pathway. This study also revealed that the early lethality observed in *dHAND*-null embryos is partly due to loss of pharyngeal arch and aortic arch artery integrity rather than hypoplasia of the right ventricle.

## Materials and Methods

### Differential display analysis

Total RNA was extracted from E9.5 wild-type and *dHAND*<sup>-/-</sup> hearts. The samples were submitted to Genomix corporation (Foster City, CA) for differential display analysis. Briefly, first-strand cDNA was generated from the RNA using 3' oligo(dT) "anchored" primers which have two non-oligo(dT) nucleotides for selection of different mRNA fractions. These anchored primer reactions were converted into double stranded cDNA fragment using

a set of 5' “arbitrary” primers. The DD-PCR fragments generated from the arbitrary primed amplification were analyzed by gel electrophoresis. Fragments that were up- or down-regulated in the *dHAND*<sup>-/-</sup> heart were excised from the gel and reamplified. These fragments were cloned into TOPO cloning vector and were sequenced to determine gene identity.

### **Generation of *dHAND*<sup>-/-</sup>*Apaf-1*<sup>-/-</sup> embryos**

Mice heterozygous for the *dHAND* mutation (Srivastava et al., 1997) or *Apaf-1* mutation (Honarpour et al., 2000) were generated and genotyped as described previously on a C57BL/6 or SV129 background respectively. *Apaf-1* mutant animals in a C57BL/6 background were generated by back-crossing with wild-type C57BL/6 mice for seven generations. Mice heterozygous for the *dHAND* mutant allele or the *Apaf-1* mutant allele were intercrossed and their progeny were genotyped to identify double heterozygous (*dHAND*<sup>+/-</sup>*Apaf-1*<sup>+/-</sup>) pups. Pregnancies resulting from intercrosses of *dHAND*<sup>+/-</sup>*Apaf-1*<sup>+/-</sup> animals were terminated at varying points during gestation by cesarean section and embryos were fixed overnight in 4% paraformaldehyde/PBS. Yolk sac DNA was used to genotype the *Apaf-1* mutant allele by PCR and the *dHAND* mutant allele by Southern analysis to identify embryos that were homozygous for both mutations.

### **Histology**

Wild-type, *dHAND*<sup>-/-</sup>, *dHAND*<sup>-/-</sup>*Apaf-1*<sup>+/-</sup> and *dHAND*<sup>-/-</sup>*Apaf-1*<sup>-/-</sup> embryos were embedded in paraffin after fixation. Transverse sections were made through the embedded

tissue at 5µm intervals. Paraffin was cleared with xylene and select sections were counter-stained with hematoxylin and eosin.

### **Whole Mount in situ Hybridization**

Whole mount in situ hybridization was performed as previously described (Srivastava et al., 1995) using digoxigenin-labeled antisense riboprobes synthesized from Bnip3 cDNA linearized with XhoI and transcribed with Sp6 polymerase. Briefly, embryos were prehybridized in hybridization buffer without probe at 60°C for 2 hours; digoxigenin-labeled riboprobes were added and incubated at 60°C for 18 hours. After a series of washes, embryos were incubated with AP conjugated anti-digoxigenin antibodies at room temperature for 1 hour. Following another series of washes, color reaction mixture was added (Roche) and embryos were incubated in the dark at room temperature for 12-14 hours. The color reaction was terminated by fixing the embryos in 4% paraformaldehyde, 0.1% glutaraldehyde/PBS solution.

### **Radioactive Section in situ Hybridization**

Radioactive in situ hybridization was performed on paraffin embedded sections of E9.5 wild-type and *dHAND*<sup>-/-</sup> embryos as described previously (Lu et al., 1998). <sup>35</sup>S-labeled antisense riboprobes were generated from partial cDNAs of Bnip3 using Sp6 RNA polymerase (MAXIscript; Ambion Inc., Austin, TX).

### **TUNEL Assay for Apoptosis**

To visualize apoptotic nuclei in pharyngeal arches and limb buds *in situ*, transverse sections of wild-type, *dHAND*<sup>-/-</sup>, *dHAND*<sup>-/-</sup>*Apaf-1*<sup>+/-</sup> and *dHAND*<sup>-/-</sup>*Apaf-1*<sup>-/-</sup> embryos were subjected to terminal transferase-mediated dUTP-biotin nick end labeling (TUNEL) using the ApopTag kit (Intergen Company). Sections were counter-stained with DAPI.

### **Neonatal rat cardiomyocyte culture**

Hearts were dissected from 2–3-day old Sprague-Dawley rats (Harlan), minced in PBS, and digested with pancreatin (0.1% w/v, Sigma) in PBS. Cells were resuspended in DMEM:M199 (4:1) containing horse serum (10%), fetal bovine serum (FBS) (5%), L-glutamine (2 mM), and penicillin-streptomycin and preplated for 2 h to separate adherent fibroblasts from cardiomyocytes. Cardiomyocytes were plated in media containing serum in 24-well dishes (2x10<sup>5</sup> cells/well) containing laminin-coated glass coverslips. After an overnight incubation the cardiomyocytes were cultured in the absence of serum for 24hrs.

### **Adenovirus treatment and induction of apoptosis**

Cardiomyocytes were infected with adenovirus containing dHAND (Ad-dHAND-IRES-GFP) or control virus (Ad-CMV-IRES-GFP) for 2 hours (mixed every 15 min.) in media with serum. Cells were washed and grown in serum-free medium (for ~40 hours) followed by treatment with staurosporine (1μM) for 24 hours or with ZVAD-fmk (100μM), a caspase inhibitor, for 1 hour prior to staurosporine treatment. Apoptosis was detected using the ApopTag-Red kit (Intergen Company) and nuclei counter-stained using DAPI. In some

cases after 40 hours of infection, cells were fixed in 4% PFA and mounted using Vectashield mounting medium (Vector Labs) to determine infection efficiency.

## Results

### Loss of dHAND activates pro-apoptotic factors

TUNEL analysis of *dHAND*<sup>-/-</sup> hearts and pharyngeal arches previously revealed increased apoptosis compared to wild-type (Thomas et al., 1998; Yamagishi et al., 2001). Furthermore, EM studies on hearts of dHAND mutants showed the presence of disrupted mitochondria (unpublished observations). In an effort to identify downstream targets of dHAND, we performed a differential display analysis using RNA from E9.5 wild-type and *dHAND*<sup>-/-</sup> hearts. Bnip3, a dimeric mitochondrial, pro-apoptotic, 'BH3-domain only' Bcl-2 family member (Chen et al., 1997; Yasuda et al., 1998; Guo et al., 2001; Regula et al., 2002), was up-regulated in *dHAND*<sup>-/-</sup> embryos (data not shown). This led us to hypothesize that upregulation of Bnip3 in the absence of dHAND might mediate mitochondrial damage, leading to apoptosis.

### Loss of Apaf-1 leads to partial rescue of the *dHAND*-null phenotype

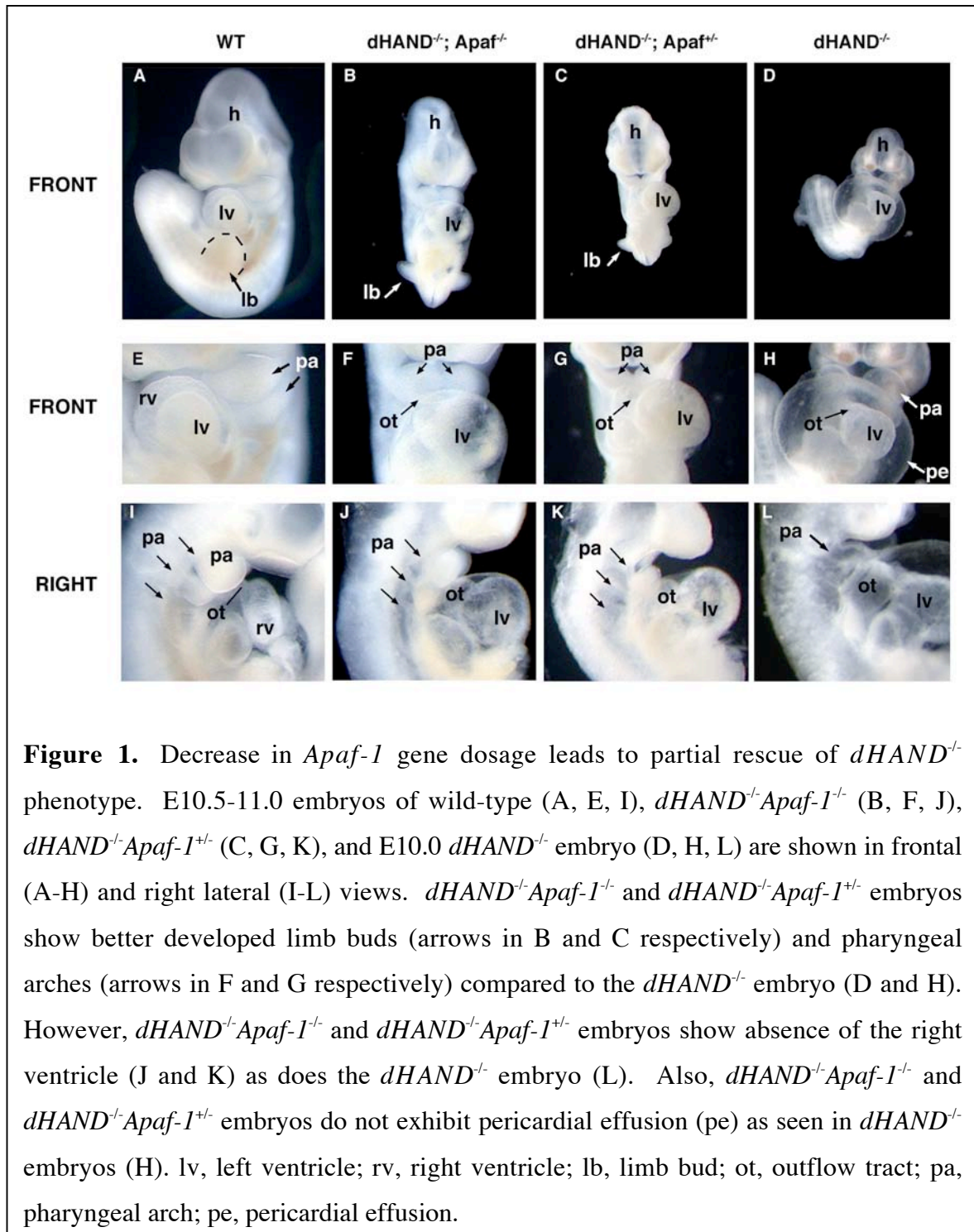
To genetically test the hypothesis that mitochondrial damage and subsequent caspase activation might contribute to the *dHAND* mutant phenotype, we attempted to block mitochondrial-induced apoptotic signals by generating *dHAND*-null mice in the *Apaf-1*-null background. Apaf-1 is a ubiquitously expressed cytosolic protein that interacts with

cytochrome c and dATP and is required for the activation of caspase-9 and subsequent propagation of the apoptotic signal (Liu et al., 1996; Li et al., 1997; Zou et al., 1997). Targeted deletion of *Apaf-1* in mice results in late embryonic or perinatal lethality due to loss of cell death in the nervous system (Cecconi et al., 1998; Yoshida et al., 1998).

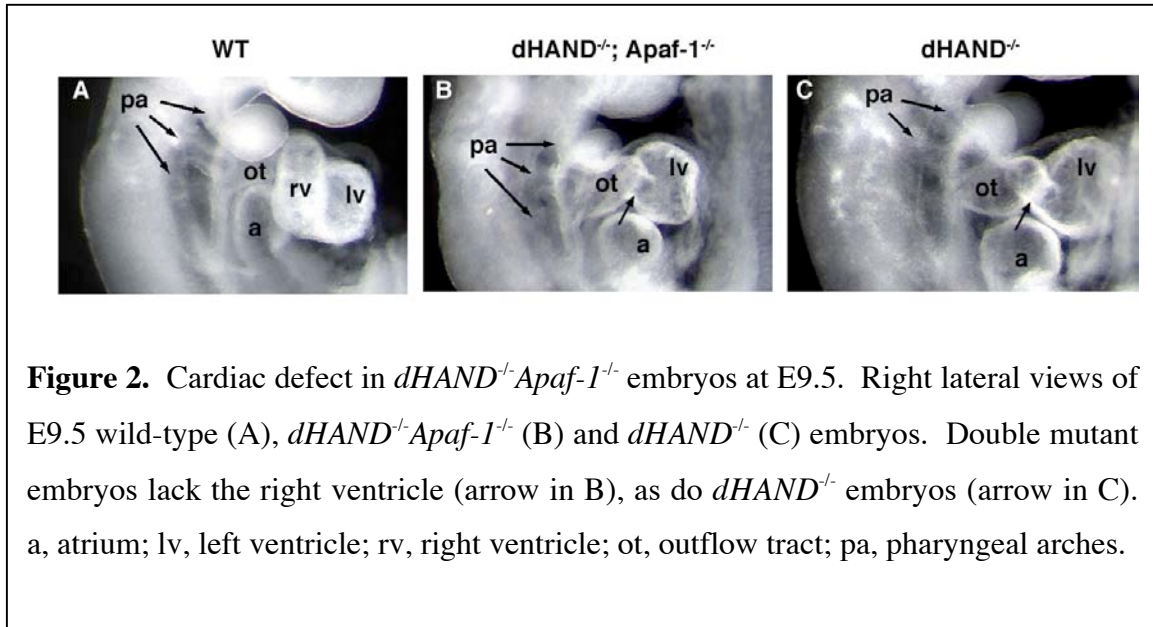
Mice heterozygous for the *dHAND* or *Apaf-1* mutant allele were intercrossed to generate trans-heterozygous mice, all of which appeared normal. *dHAND*<sup>+/-</sup>*Apaf-1*<sup>+/-</sup> mice were intercrossed and resulting offspring were analyzed at E10.5. This stage was chosen for initial analysis because *dHAND*<sup>-/-</sup> embryos at this stage are severely malformed with pericardial effusion, a sign of cardiac failure, and many are already dead with their growth having been arrested at E9.5. As expected, all embryos lacking *dHAND* alone were growth retarded, had extremely small pharyngeal arches and showed severe cardiac failure as evidenced by pericardial effusion (Fig. 1). In contrast, *dHAND*<sup>-/-</sup>*Apaf-1*<sup>-/-</sup> embryos, although growth-retarded in comparison to wild-type litter mates (35 somites), developed 28-32 somites, corresponding to E10.25, had well-preserved pharyngeal arches and limb buds, and showed no pericardial effusion (Fig. 1). *dHAND*<sup>-/-</sup>*Apaf-1*<sup>+/-</sup> embryos showed an intermediate phenotype with respect to preservation of the pharyngeal arches and pericardial effusion (Fig. 1).

Unlike the rescue of the pharyngeal arch and aortic arch artery phenotype, the cardiac phenotype in all three genotypes mentioned above were identical. Hypoplasia of the right ventricle in *dHAND*<sup>-/-</sup> embryos manifests prior to the pharyngeal arch phenotype, and is apparent as early as E8.5. Therefore, in an effort to determine whether loss of Apaf-1 might have rescued the early cardiac phenotype, *dHAND*<sup>-/-</sup> and *dHAND*<sup>-/-</sup>*Apaf-1*<sup>-/-</sup> embryos were

harvested at E9.0-9.5. Even at this early stage, we observed a hypoplastic right ventricle in



*dHAND*<sup>-/-</sup>*Apaf-1*<sup>-/-</sup> embryos (Fig. 2), suggesting that reduction of Apaf-1 dosage did not rescue the myocardial defect in *dHAND* mutants.



Because the initial analyses were done in a C57BL6/SV129 mixed background, we asked whether the partial rescue might be due to genetic modifiers in the SV129 background. To answer this question, the *Apaf-1* mice were back-crossed into the C57BL6 background to achieve greater than 90% pure animals and used to generate *dHAND*<sup>-/-</sup>*Apaf-1*<sup>-/-</sup> embryos. Analyses of *dHAND*<sup>-/-</sup>*Apaf-1*<sup>-/-</sup> in the nearly pure C57BL6 background at E10.5-11.0 showed the same results as those seen in the C57BL6/SV129 mixed background (Table 1). These results indicate that *Apaf-1* function is required to mediate the hypoplasia seen in the pharyngeal arches.

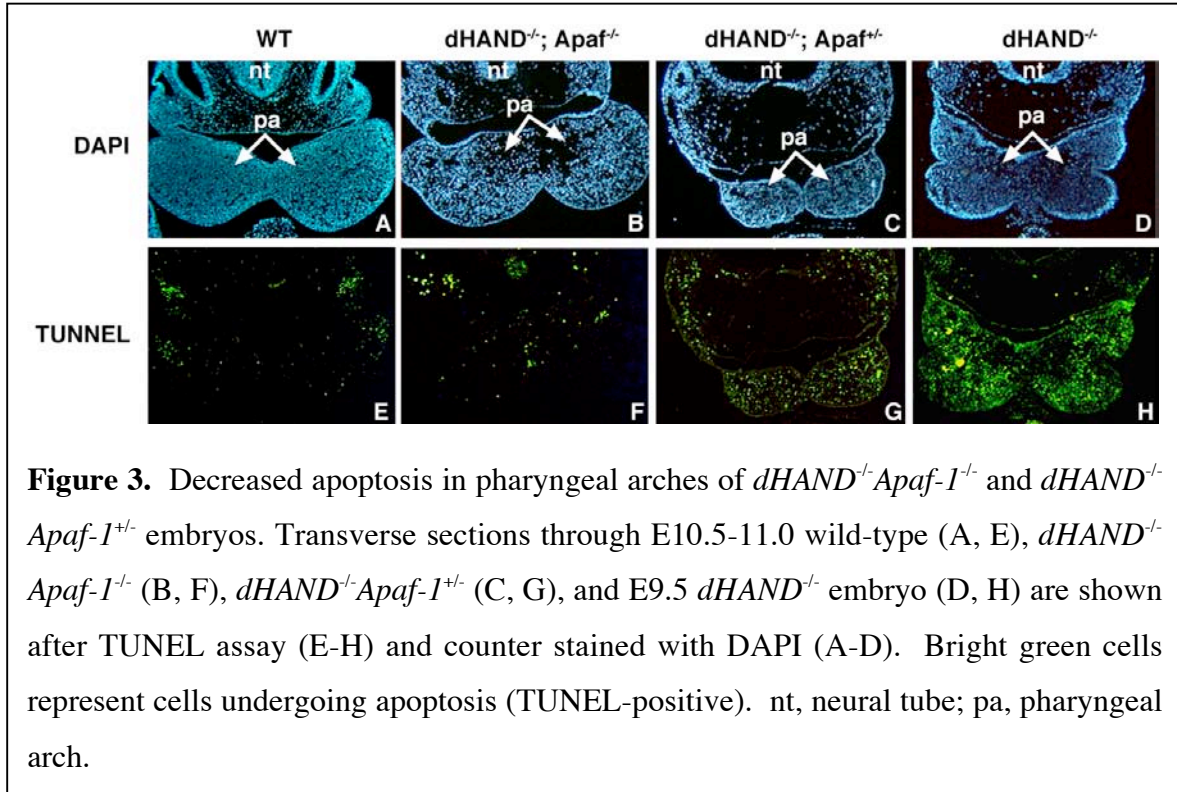


**Table 1**Genotype of embryos from *dHAND*<sup>+/-</sup>*Apaf-1*<sup>+/-</sup> intercrosses

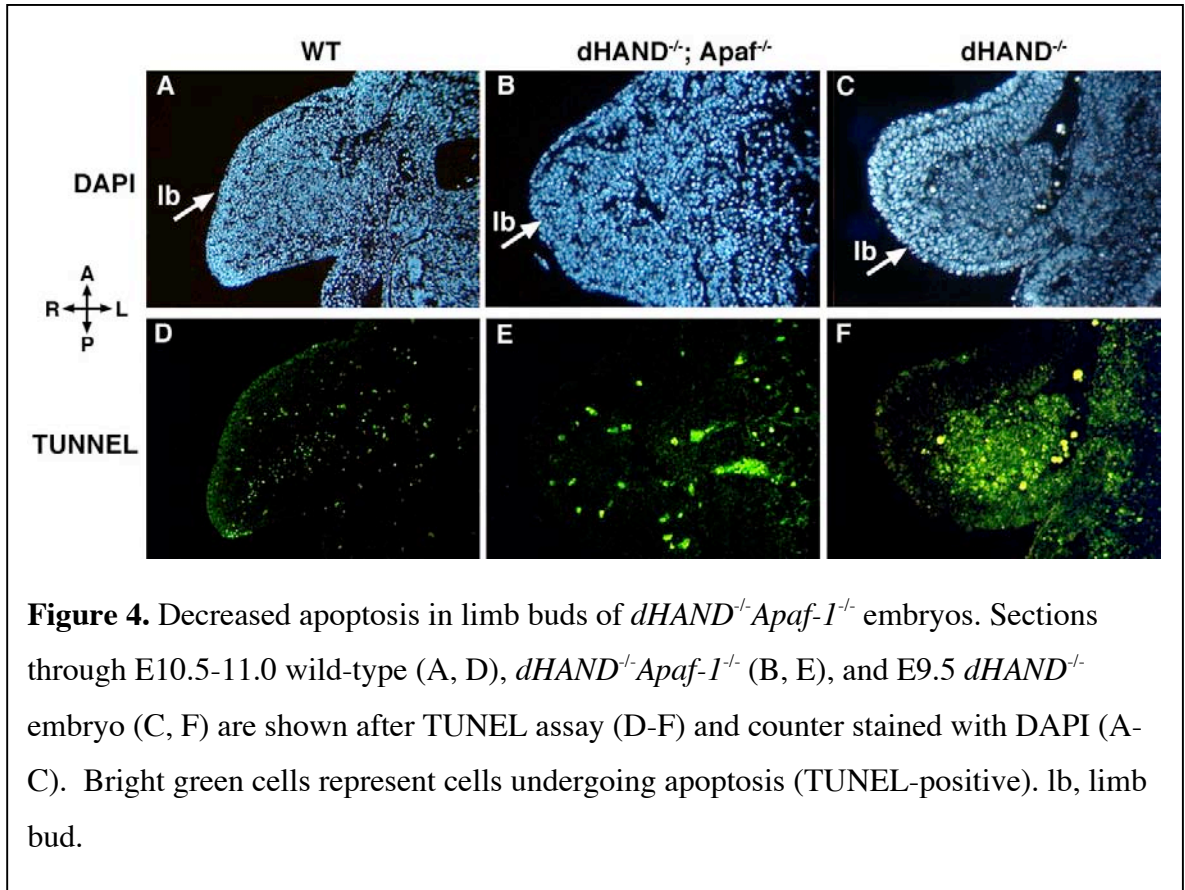
Genotype	dHAND	+/+	+/+	+/+	+/-	+/-	+/-	-/-	-/-	-/-	Total
	Apaf-1	+/+	+/-	-/-	+/+	+/-	-/-	+/+	+/-	-/-	
E9.5	Observed	6	9	5	10	19	8	3	4	3	67
	Expected	4	8	4	8	17	8	4	8	4	
E10.5-11.0	Observed	16	25	13	24	48	22	2	9	8	167
	Expected	11	21	11	21	42	21	11	21	11	
Expected		1/16	1/8	1/16	1/8	1/4	1/8	1/16	1/8	1/16	
Ratio											

To determine the mechanism of the partial rescue, sections through the pharyngeal arches and limb buds of *dHAND*<sup>-/-</sup> and *dHAND*<sup>-/-</sup>*Apaf-1*<sup>-/-</sup> were analyzed using the TUNEL assay to determine the extent of cell death. When embryos were compared at E10.5, the numbers of apoptotic cells were remarkably reduced in the *dHAND*<sup>-/-</sup>*Apaf-1*<sup>-/-</sup> embryos compared to *dHAND*<sup>-/-</sup> embryos (Fig. 3). E9.5 *dHAND*<sup>-/-</sup> embryos were used for comparison with E10.5-11.0 *dHAND*<sup>-/-</sup>*Apaf-1*<sup>-/-</sup> embryos because by E10.5 the pharyngeal arches of *dHAND*<sup>-/-</sup> embryos are severely hypoplastic and the embryo is being reabsorbed. Our results show that the pharyngeal arches of E10.5-11.0 *dHAND*<sup>-/-</sup>*Apaf-1*<sup>-/-</sup> embryos were still healthy and did not demonstrate excessive apoptosis. We also examined apoptosis in limb buds of wild-type, *dHAND*<sup>-/-</sup>, and *dHAND*<sup>-/-</sup>*Apaf-1*<sup>-/-</sup> embryos. As in the pharyngeal arches, we

observed a decrease in apoptosis in *dHAND*<sup>-/-</sup>*Apaf-1*<sup>-/-</sup> embryos in comparison to *dHAND*<sup>-/-</sup> at E9.5 (Fig. 4).



Our previous studies demonstrated that *dHAND*<sup>-/-</sup> embryos have vascular defects with the most prominent being atresia of the pharyngeal arch arteries (Srivastava et al., 1997). The early closure of these vessels that connect the cardiac outflow tract (conotruncus) to the aorta resulted in dilation of the aortic sac (Srivastava et al., 1997; Yamagishi et al., 2000). Because *dHAND* was expressed and had a primary function in right ventricular/myocardial development and pharyngeal arch development, it has remained unclear whether the early lethality was due to the intrinsic myocardial defect or was a result of the pharyngeal arch artery defect. Because the *dHAND*<sup>-/-</sup>*Apaf-1*<sup>-/-</sup> embryos survived longer than *dHAND*<sup>-/-</sup>



embryos in spite of similar right ventricular defects, we carefully examined sections through the pharyngeal arches of *dHAND*<sup>-/-</sup>*Apaf-1*<sup>-/-</sup> embryos to determine the patency of the pharyngeal arch arteries. Mice lacking both genes not only survived longer, but also had well-preserved pharyngeal arch arteries (Fig. 5) that were unobstructed, suggesting that atresia of the arch artery may be a primary cause of death in the *dHAND* mutant embryos. This result also suggests that the right ventricular defect in *dHAND* mutants is not a consequence of obstructed blood flow since right ventricular hypoplasia was still observed in *dHAND*<sup>-/-</sup>*Apaf-1*<sup>-/-</sup> embryos (Fig. 5).

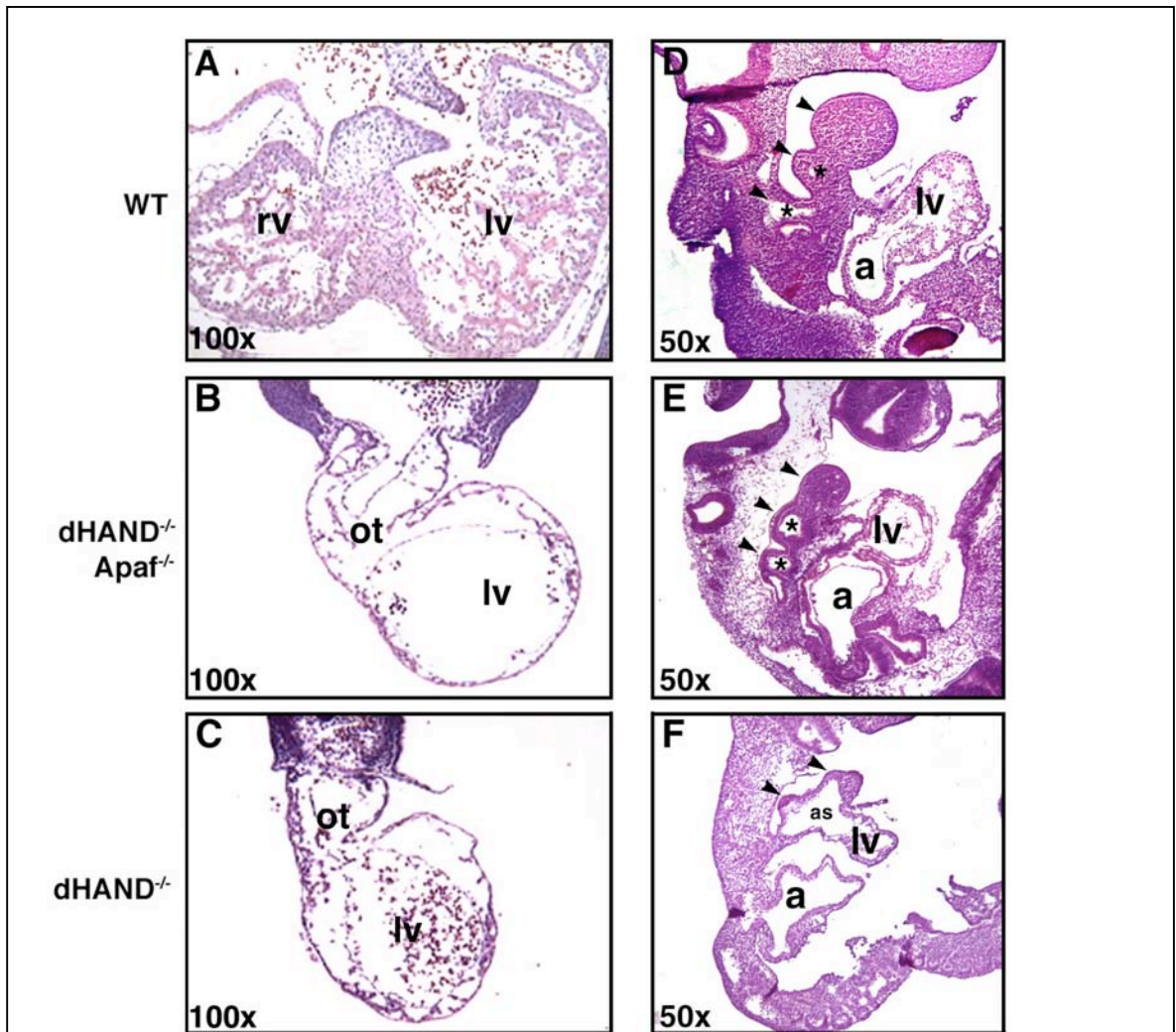


**Figure 5.** Histological analysis of *dHAND*<sup>-/-</sup>*Apaf-1*<sup>-/-</sup> embryos. Transverse (A-C) and sagittal (D-F) sections through E10.5-11.0 wild-type (A, D), *dHAND*<sup>-/-</sup>*Apaf-1*<sup>-/-</sup> (B, E), and E10.0 *dHAND*<sup>-/-</sup> embryo (C, F) are shown. *dHAND*<sup>-/-</sup> animals show absence of the right ventricle irrespective of *Apaf-1* dosage (B,C). *dHAND*<sup>-/-</sup>*Apaf-1*<sup>-/-</sup> embryos however, have better developed pharyngeal arches (arrowheads) with patent arch arteries (asterisk in E) in comparison to *dHAND*<sup>-/-</sup> embryos (F) at E10.0 which show loss of cells in the arch mesenchyme (arrowheads in F) and dilated aortic sac (as). a, atrium; ot, outflow tract; lv, left ventricle; rv, right ventricle; pa, pharyngeal arch; nt, neural tube.

### **dHAND does not prevent apoptosis in differentiated cardiomyocytes in vitro**

In order to determine whether dHAND has anti-apoptotic function, we tested its ability to rescue cell death in primary rat neonatal cardiomyocytes treated with staurosporine, an inducer of apoptosis via the mitochondrial damage and cytochrome C release pathway. Primary rat neonatal cardiomyocytes were infected with either empty or dHAND-expressing adenovirus and treated with staurosporine. ZVAD-fmk, a caspase inhibitor known to block staurosporine induced apoptosis was used as control. TUNEL assay was performed to determine percentage of cells undergoing apoptosis. We did not observe any decrease of staurosporine-induced apoptosis in dHAND-overexpressing cells compared to controls. This result suggests that, at least in differentiated cardiomyocytes, dHAND over-expression alone cannot prevent induced apoptosis, although its role under native conditions in developing cardiac cells remains unknown.

## **Discussion**

In this study, we found that Bnip3, a pro-apoptotic factor that induces mitochondrial damage and subsequent caspase activation, is upregulated in *dHAND* mutant embryos, which exhibit a cell survival defect. *dHAND*<sup>-/-</sup> embryos have hypoplastic ventricles and vascular defects in the embryo as well as the yolk sac. These defects could generate a hypoxic environment in the embryo leading to upregulation of Bnip3. The partial rescue of the *dHAND* mutant phenotype in the *Apaf1*-null background supports the hypothesis that the apoptosis observed in *dHAND*-null embryos occurs in part through non-receptor mediated

activation of a caspase pathway. Our results also suggest that the atresia of pharyngeal arch arteries might be the primary cause of cardiac failure in *dHAND* mutants and that the right ventricular defect is not secondary to obstruction of blood flow from the cardiac outflow tract.

*dHAND*<sup>-/-</sup> embryos exhibit hypoplasia of the right ventricle at E8.5 and pharyngeal arches at E9.5 due to robust apoptosis (Thomas et al., 1998; Yamagishi et al., 2001). Electron microscopy and comparative gene expression analysis suggested a mitochondrial damage induced pathway caused this apoptosis. Consistent with this, loss of Apaf-1 blocked apoptosis in the pharyngeal arches and limb bud of *dHAND*<sup>-/-</sup> embryos. Apaf-1 is a cytosolic protein, which in the presence of ATP and cytochrome C can activate pro-caspase-9, an initiator caspase leading to activation of other caspases (Li et al., 1997; Zou et al., 1997). This causes massive proteolysis and DNA fragmentation in the cell, which is ultimately engulfed by macrophages and cleared. Although most intracellular apoptotic pathways require Apaf-1, other signals transduced by death receptor pathways can also result in apoptosis. Since loss of Apaf-1 only affected pharyngeal arch and limb bud apoptosis, there must be Apaf-1 independent mechanisms that regulate cell death in the right ventricle of *dHAND* mutants. These could be through death receptors or may represent a default pathway secondary to a differentiation defect in the absence of *dHAND*, although we cannot distinguish between these alternatives. It is also possible that cells of the cardiac lineage are more sensitive to the necrosis-like cell death seen in Apaf-1 deficient embryonic fibroblasts (Miyazaki et al., 2001) and in limb buds of Apaf-1 deficient mice (Chautan et. al., 1999).

In the pharyngeal arch of *dHAND* mutants, apoptosis of the arch mesenchyme coupled with loss of VSMC specification causes hypoplasia of the pharyngeal arch artery (Thomas et al., 1998; Yamagishi et al., 2000). Although these studies have been performed in *dHAND*<sup>-/-</sup> embryos at E9.5 prior to presence of cardiac distress, there still exists the possibility that this defect is in some way related to hemodynamic changes caused by the hypoplastic right ventricle and thin walled left ventricle. Therefore, the early lethality of the *dHAND*<sup>-/-</sup> embryo has so far been attributed to cardiac failure observed as a result of right ventricular hypoplasia. However, it is interesting to note that absence of right ventricle alone is not enough to cause lethality in utero, since children can be born without a right ventricle. This suggests that the pharyngeal arch defects might play a causative role in the early lethality of *dHAND*<sup>-/-</sup> embryos.

We have analyzed pharyngeal arches of *dHAND*<sup>-/-</sup> embryos with decreased dosage or absence of Apaf-1 at E10.5-11.0. At this stage *dHAND*<sup>-/-</sup> embryos with normal Apaf-1 dosage are dead, with a complete absence of cells in the pharyngeal arches and severe pericardial effusion caused by cardiac failure. Loss of Apaf-1 function however, maintains the integrity of the pharyngeal arch and the arch artery in *dHAND*<sup>-/-</sup> embryos. The *dHAND*<sup>-/-</sup> *Apaf-1*<sup>-/-</sup> embryos do not exhibit pericardial effusion, suggesting that the maintenance of the arch arteries reduces cardiac stress. These experiments still do not answer the question of whether the pharyngeal arch apoptosis seen in *dHAND*<sup>-/-</sup> embryos is secondary to the cardiac defect. This will require the generation of a cardiac-specific *dHAND* knock-out.

Distinct enhancers control the cardiac and pharyngeal arch expression of *dHAND* (McFadden et al., 2000; Charite et al., 2001). Deletion of an ET-1 and *Dlx6* dependent

pharyngeal arch enhancer causes craniofacial defects in mice harboring the homozygous deletion (Yanagisawa et al., 2003). While levels of apoptosis in the pharyngeal arches were not analyzed in these animals, the defects observed do not support the presence of massive apoptosis. However, these mice continue to express dHAND in the ventral regions of the pharyngeal arches, leading to the hypothesis that these dHAND-expressing cells could produce soluble factors that could promote survival of neighboring cells. These animals also show normal expression of *Msx1*, a gene that is implicated in the proper growth and differentiation of the pharyngeal arches (Satokata and Maas, 1994) and is completely abolished in *dHAND*<sup>-/-</sup> embryos (Thomas et al., 1998). While identification of these sub-domains of pharyngeal arch expression of dHAND help elucidate the fate of specific regions of the arch, a complete loss of dHAND early in pharyngeal arch development will be required to determine its role in cell survival.



## References

- Abe, M., Tamamura, Y., Yamagishi, H., Maeda, T., Kato, J., Tabata, M. J., Srivastava, D., Wakisaka, S., and Kurisu, K. (2002). Tooth-type specific expression of dHAND/Hand2: possible involvement in murine lower incisor morphogenesis. *Cell Tissue Res* 310, 201-12.
- Bruick, R. K. (2000). Expression of the gene encoding the proapoptotic Nip3 protein is induced by hypoxia. *Proc Natl Acad Sci U S A* 97, 9082-7.
- Budihardjo, I., Oliver, H., Lutter, M., Luo, X., and Wang, X. (1999). Biochemical pathways of caspase activation during apoptosis. *Annu Rev Cell Dev Biol* 15, 269-90.
- Cecconi, F., Alvarez-Bolado, G., Meyer, B. I., Roth, K. A., and Gruss, P. (1998). Apaf1 (CED-4 homolog) regulates programmed cell death in mammalian development. *Cell* 94, 727-37.
- Charite, J., McFadden, D. G., Merlo, G., Levi, G., Clouthier, D. E., Yanagisawa, M., Richardson, J. A., and Olson, E. N. (2001). Role of Dlx6 in regulation of an endothelin-1-dependent, dHAND branchial arch enhancer. *Genes Dev* 15, 3039-49.
- Charite, J., McFadden, D. G., and Olson, E. N. (2000). The bHLH transcription factor dHAND controls Sonic hedgehog expression and establishment of the zone of polarizing activity during limb development. *Development* 127, 2461-70.
- Chautan, M., Chazal, G., Cecconi, F., Gruss, P., and Golstein, P. (1999). Interdigital cell death can occur through a necrotic and caspase-independent pathway. *Curr Biol* 9, 967-70.
- Chen, G., Ray, R., Dubik, D., Shi, L., Cizeau, J., Bleackley, R. C., Saxena, S., Gietz, R. D., and Greenberg, A. H. (1997). The E1B 19K/Bcl-2-binding protein Nip3 is a dimeric mitochondrial protein that activates apoptosis. *J Exp Med* 186, 1975-83.

Cikala, M., Wilm, B., Hobmayer, E., Bottger, A., and David, C. N. (1999). Identification of caspases and apoptosis in the simple metazoan *Hydra*. *Curr Biol* 9, 959-62.

Earnshaw, W. C., Martins, L. M., and Kaufmann, S. H. (1999). Mammalian caspases: structure, activation, substrates, and functions during apoptosis. *Annu Rev Biochem* 68, 383-424.

Fernandez-Teran, M., Piedra, M. E., Kathiriya, I. S., Srivastava, D., Rodriguez-Rey, J. C., and Ros, M. A. (2000). Role of dHAND in the anterior-posterior polarization of the limb bud: implications for the Sonic hedgehog pathway. *Development* 127, 2133-42.

Guo, K., Searfoss, G., Krolikowski, D., Pagnoni, M., Franks, C., Clark, K., Yu, K. T., Jaye, M., and Ivashchenko, Y. (2001). Hypoxia induces the expression of the pro-apoptotic gene BNIP3. *Cell Death Differ* 8, 367-76.

Hengartner, M. O. (2000). The biochemistry of apoptosis. *Nature* 407, 770-6.

Honarpour, N., Du, C., Richardson, J. A., Hammer, R. E., Wang, X., and Herz, J. (2000). Adult Apaf-1-deficient mice exhibit male infertility. *Dev Biol* 218, 248-58.

Howard, M. J., Stanke, M., Schneider, C., Wu, X., and Rohrer, H. (2000). The transcription factor dHAND is a downstream effector of BMPs in sympathetic neuron specification. *Development* 127, 4073-81.

Jacobson, M. D., Weil, M., and Raff, M. C. (1997). Programmed cell death in animal development. *Cell* 88, 347-54.

Kluck, R. M., Bossy-Wetzel, E., Green, D. R., and Newmeyer, D. D. (1997). The release of cytochrome c from mitochondria: a primary site for Bcl-2 regulation of apoptosis. *Science* 275, 1132-6.

Kubasiak, L. A., Hernandez, O. M., Bishopric, N. H., and Webster, K. A. (2002). Hypoxia and acidosis activate cardiac myocyte death through the Bcl-2 family protein BNIP3. *Proc Natl Acad Sci U S A* 99, 12825-30.

Li, P., Nijhawan, D., Budihardjo, I., Srinivasula, S. M., Ahmad, M., Alnemri, E. S., and Wang, X. (1997). Cytochrome c and dATP-dependent formation of Apaf-1/caspase-9 complex initiates an apoptotic protease cascade. *Cell* 91, 479-89.

Liu, X., Kim, C. N., Yang, J., Jemmerson, R., and Wang, X. (1996). Induction of apoptotic program in cell-free extracts: requirement for dATP and cytochrome c. *Cell* 86, 147-57.

Lu, J., Richardson, J. A., and Olson, E. N. (1998). Capsulin: a novel bHLH transcription factor expressed in epicardial progenitors and mesenchyme of visceral organs. *Mech Dev* 73, 23-32.

McFadden, D. G., Charite, J., Richardson, J. A., Srivastava, D., Firulli, A. B., and Olson, E. N. (2000). A GATA-dependent right ventricular enhancer controls dHAND transcription in the developing heart. *Development* 127, 5331-41.

Ranger, A. M., Malynn, B. A., and Korsmeyer, S. J. (2001). Mouse models of cell death. *Nat Genet* 28, 113-8.

Ray, R., Chen, G., Vande Velde, C., Cizeau, J., Park, J. H., Reed, J. C., Gietz, R. D., and Greenberg, A. H. (2000). BNIP3 heterodimerizes with Bcl-2/Bcl-X(L) and induces cell death independent of a Bcl-2 homology 3 (BH3) domain at both mitochondrial and nonmitochondrial sites. *J Biol Chem* 275, 1439-48.

Regula, K. M., Ens, K., and Kirshenbaum, L. A. (2002). Inducible expression of BNIP3 provokes mitochondrial defects and hypoxia-mediated cell death of ventricular myocytes. *Circ Res* 91, 226-31.

Satokata, I., and Maas, R. (1994). *Msx1* deficient mice exhibit cleft palate and abnormalities of craniofacial and tooth development. *Nat Genet* 6, 348-56.

Srivastava, D., Cserjesi, P., and Olson, E. N. (1995). A subclass of bHLH proteins required for cardiac morphogenesis. *Science* 270, 1995-9.

Srivastava, D., Thomas, T., Lin, Q., Kirby, M. L., Brown, D., and Olson, E. N. (1997). Regulation of cardiac mesodermal and neural crest development by the bHLH transcription factor, dHAND. *Nat Genet* 16, 154-60.

Thomas, T., Kurihara, H., Yamagishi, H., Kurihara, Y., Yazaki, Y., Olson, E. N., and Srivastava, D. (1998). A signaling cascade involving endothelin-1, dHAND and *msx1* regulates development of neural-crest-derived branchial arch mesenchyme. *Development* 125, 3005-14.

Yamagishi, H., Olson, E. N., and Srivastava, D. (2000). The basic helix-loop-helix transcription factor, dHAND, is required for vascular development. *J Clin Invest* 105, 261-70.

Yamagishi, H., Yamagishi, C., Nakagawa, O., Harvey, R. P., Olson, E. N., and Srivastava, D. (2001). The combinatorial activities of *Nkx2.5* and dHAND are essential for cardiac ventricle formation. *Dev Biol* 239, 190-203.

Yanagisawa, H., Clouthier, D. E., Richardson, J. A., Charite, J., and Olson, E. N. (2003). Targeted deletion of a branchial arch-specific enhancer reveals a role of dHAND in craniofacial development. *Development* 130, 1069-78.

Yang, J., Liu, X., Bhalla, K., Kim, C. N., Ibrado, A. M., Cai, J., Peng, T. I., Jones, D. P., and Wang, X. (1997). Prevention of apoptosis by Bcl-2: release of cytochrome c from mitochondria blocked. *Science* 275, 1129-32.

Yasuda, M., Theodorakis, P., Subramanian, T., and Chinnadurai, G. (1998). Adenovirus E1B-19K/BCL-2 interacting protein BNIP3 contains a BH3 domain and a mitochondrial targeting sequence. *J Biol Chem* 273, 12415-21.

Yoshida, H., Kong, Y. Y., Yoshida, R., Elia, A. J., Hakem, A., Hakem, R., Penninger, J. M., and Mak, T. W. (1998). Apaf1 is required for mitochondrial pathways of apoptosis and brain development. *Cell* 94, 739-50.

Zou, H., Li, Y., Liu, X., and Wang, X. (1999). An APAF-1.cytochrome c multimeric complex is a functional apoptosome that activates procaspase-9. *J Biol Chem* 274, 11549-56.

# **CHAPTER FOUR**

## **BTF: A Transcriptional Regulator Required for Normal Progenitor Cell Development in the Lung**

### **Background**

Nuclear hormone receptors are a class of ligand activated transcription factors that are required for numerous physiological events (reviewed in Mangelsdorf et al., 1995). This superfamily includes, the retinoid receptors (RARs and RXRs), thyroid hormone receptor (TR), vitamin D receptor (VDR), peroxisome proliferator activated receptors (PPAR) and glucocorticoid receptor (GR). While RXR and GR can homodimerize, RAR, TR, VDR and PPAR form heterodimers with RXR and then interact with their respective response elements. In addition, GR can also control transcription by interaction with other factors in a DNA-dependent or independent manner (Drouin et al., 1993; Diamond et al., 1990; Jonat et al., 1990; Schule et al., 1990; Yang et al., 1990). The nuclear receptors assemble various co-activators following ligand binding. One such family of co-activators is the p160 family, which has histone acetylase (HAT) activity and functions in part by acetylating the histones and other proteins to change the chromatin structure (Glass and Rosenfeld, 2000). Another coactivator complex known as the TR associated protein (TRAP) does not possess HAT activity, but has the ability to recruit the RNA polymerase II and general transcription factors (GTFs), leading to transcriptional activation (Fondell et al., 1996). There is also evidence to

suggest that interaction of ligand-bound receptors with HAT-containing co-activators and TRAPs might exist in a balance, with the HAT activity on chromatin facilitating the binding of TRAPs to the receptors and GTFs (Fondell et al., 1999; Yuan et al., 1998).

Further analysis of the TRAP complex showed that one of its subunits, TRAP220, which has ligand-dependent receptor binding activity, could interact with not only TR, but also VDR, RAR $\alpha$ , RXR $\alpha$ , PPAR $\alpha$ , PPAR $\gamma$  and GR (Yuan et al., 1998; Zhu et al., 1997; Hittelman et al., 1999). Interestingly, several such co-activator complexes have been identified in association with other activators, including the VDR-interacting complex (DRIP) (Rachez et al., 1998; Rachez et al., 1999), E1A interacting complex (human Mediator) (Boyer et al., 1999) and mouse mediator (Jiang et al., 1998). While they share many subunits with the TRAP complex, they also have subunits that are unique to each particular complex. The co-activators are related by the presence of subunits homologous to Mediator, a yeast co-activator complex (reviewed in Malik and Roeder, 2000). The evolutionary conservation of nuclear receptors and co-activators suggests an important role in various cellular processes.

It has long been known that hormones are required for normal development. In recent years, targeted deletions of various nuclear hormone receptors and co-activators have been generated in mice and have underscored the importance of nuclear hormone signaling in organogenesis (Gruber et al., 1996; Kastner et al., 1997; Mendelsohn et al., 1994; Sucov et al., 1994; Cole et al., 1995; Ito et al., 2000; Ito et al., 2002). Several nuclear hormone receptors (RXR, RAR, VDR and GR) and co-activators (CBP/p300, p160) are expressed in the embryonic lung (Condon et al., 1998; Masuyama et al., 1995; Nguyen et al., 1990;

Naltner, et al., 2000), suggesting a role in lung development. In mice, lung development (reviewed in Cardoso, 2000) begins at E9.5 in the mouse with the out-pouching of the lung bud from the foregut endoderm. By E10.5 the lung bud forms two main bronchi. Between E10.5-16.5, the pseudoglandular stage, the right bronchus divides to form 4 secondary bronchi, and the branching continues to form an undifferentiated bronchial tree, which consists of terminal bronchioles at the distal end. This branching is an extremely complex process and requires signaling between the epithelium and the surrounding mesenchyme (Hogan et al., 1997; Hogan, 1999). Once the bronchial tree is formed, the cells in the epithelium begin to differentiate (canalicular stage, E16.5-E17.5) and the architecture of the lung begins to change. For example, the terminal bronchioles divide into respiratory bronchioles, which in turn divide into alveolar ducts. Vascularization and epithelial differentiation are also initiated at this stage and continue between E17.5 and postnatal day 5 (P5) (saccular stage).

As the lung branches, it develops in a distinct pattern along the proximal-distal axis. In the distal epithelium, the cells flatten to form two cell types: a) type I pneumocytes that form close associations with the invading capillaries so as to allow for efficient gas exchange and b) type II pneumocytes, the cells that secrete surfactant proteins and lipids that are essential to reduce the surface tension at the alveolar wall to allow adequate inflation of the lung for efficient respiration. However, in the proximal airways, i.e, the bronchi and the bronchioles, epithelial cells differentiate into ciliated cells and the more abundant, non-ciliated Clara cells. The differentiation of these varied cell types is dependent on controlled



temporal and spatial expression of specific genes (reviewed in Warburton et al., 2000; Cardoso, 2000).

Disruption of the signaling by several nuclear hormone receptors leads to abnormal lung development. In case of the *RAR $\alpha$ RAR $\beta$ 2* double knock-out, the defect observed is an early one, leading to absence of the left lung, which has only one lobe, and hypoplasia of the right lung caused by delayed bronchial branching (Mendelsohn et al., 1994). Deletion of GR, on the other hand, leads to a defect late in lung development. *GR*<sup>-/-</sup> lungs show impaired development of type II cells which leads to inefficient fluid removal and abnormal inflation of the lung (Cole et al., 1995). The corticotropin-releasing hormone-deficient mice (*CRH*<sup>-/-</sup>), which are glucocorticoid-insufficient, also show abnormal pulmonary development. The lungs from these animals show delayed development of type II cells (distal epithelium) and Clara cells (proximal airway epithelium) (Muglia et al., 1999).

Clara cells are highly metabolically active cells that are restricted to the epithelium of the proximal airways. Clara cells secrete a variety of proteins, of which Clara cell 10 kDa (CC10) is the most abundant (Hermans and Bernard, 1999). These cells also secrete surfactant proteins and the ability of CC10 to bind surfactant proteins suggests a role in surfactant biology (Singh and Katyal, 1997). One of the primary functions of Clara cells is that of progenitor for replacement of itself as well as ciliated cells in response to lung injury (Brody et al, 1987; Hook et al., 1987). Recent studies have also suggested a role for CC10 and/or Clara cells in lung homeostasis and regulation of inflammatory response in case of injury (Stripp et al., 1999). Although much is known about the potential role of Clara cells, transcriptional control of Clara cell-fate remains a mystery. We have identified the mouse

homolog of human Bcl-2 associated transcription factor (hBtf) (Kasof et al., 1999), mBtf, which shows similarity to TRAP150, a member of the co-activator complex required for optimal functioning of TR down-stream of ligand activation. Btf was expressed in Clara cells, type I, and type II pneumocytes during development, but interestingly, was restricted to Clara cells in the adult. Mice lacking Btf died within the first 24 hours after birth from respiratory failure. In the absence of Btf, the lungs were hyperplastic and contained Clara cells in the distal alveoli. Clara cells in the proximal airway were also abnormal with delayed maturation. These data suggest that *btf* is required for normal Clara cell maturation and proper proximal-distal patterning of the developing lung.

## Materials and Methods

### Identification and cloning of mouse *btf*

We initially identified mouse *btf* from a differential display analysis comparing RNAs from wild-type and *dHAND*<sup>-/-</sup> hearts. We cloned full-length mouse *btf* by RT-PCR from E11.0 mouse embryos. Briefly, RNA was isolated using TRIzol reagent (Invitrogen™) and reverse transcribed using a cDNA Synthesis System (GIBCO, catalog# 18267-013). The following forward: 5'-ctcaaagacatcactgacttctggatcctg-3' and reverse: 5'-aacagggaggcaagttaagagttgtcacag-3' primers were used to amplify full-length mouse *btf* with the Expand™ Long Template PCR System (Boehringer-Roche Catalog # 1681834).

### **Northern blot analysis**

Northern analysis was performed on commercially available adult mouse multiple tissue northern (MTN) blots (Clontech) using  $^{32}\text{P}$ -labeled probes. Mouse *btf* fragment corresponding to amino acid (aa)187- aa385 was used as probe.  $\beta$ -*Actin* was used to normalize data.

### **In situ hybridization**

Radioactive in situ hybridization was performed on paraffin embedded sections (Lu et al., 1998) of wild-type and *btf*<sup>-/-</sup> embryos at E18.5 and post-natal day 0 (P0) pups.  $^{35}\text{S}$ -labeled antisense riboprobes were generated with T3, T7 or SP6 RNA polymerase from partial cDNAs of the following genes: mouse *btf* (SP6), rat *CC10* (SP6), mouse *CEBP- $\alpha$*  (SP6), mouse *Gata6* (T3), mouse *Hfh4* (T7), mouse *Nkx2.1* (SP6), mouse *SP-A* (T7), mouse *SP-B* (T7) and mouse *SP-C* (T7) using the MAXIsript kit (Ambion Inc., Austin, TX). The *Hfh4*, *SP-A*, *SP-B*, and *SP-C* plasmids were obtained from Dr. Whitsett; *CEBP- $\alpha$*  from Dr. Darlington and *CC10* from Dr. Hogan.

### **Gene targeting and genotyping**

We obtained mice harboring a LacZ insertion in the 5'UTR of *btf* from Lexicon Genetics (Houston, TX). Mice heterozygous for the insertion were mated and the resulting pregnancies were terminated at varying time points during gestation and yolk sac DNA used for genotyping. Term deliveries were genotyped at P10. Southern blots of *SacI* (Roche) digested genomic DNA were used for genotyping. A  $^{32}\text{P}$ -labeled 500bp genomic fragment

upstream of the LacZ insertion, obtained by PCR from genomic DNA (forward primer: 5'-ttgagtggctcctgctttgtaag-3' and reverse primer: 5'-tttctgggaagtctcgttgcc-3') was used as probe. The probe recognized a 6kb fragment from the wild-type allele and a 4.5 kb fragment from the mutant allele.

## RT-PCR

RNA from E18.5 or P0 wild-type or *btf*<sup>-/-</sup> lung and liver was extracted using TRIzol (Invitrogen™). 2µg of RNA per sample were treated with Amplification Grade DNaseI (Invitrogen™). One half of each DNaseI treated sample was used to generate first-strand cDNA in the presence of reverse transcriptase (RT) and the other half used without RT. The reaction was performed using SuperScript™ First-Strand Synthesis System for RT-PCR (Catalog# 11904-018, Invitrogen™, Life Technologies) as described in the instruction manual. RT-PCR to amplify *SP-A*, *SP-B*, *SP-C*, *Tlα*, and *PECAM* was performed as described by Roper et al., 2003. The *btf* (forward primer: 5'-gatcggaaattccgacacagaggagacagaggat-3', reverse primer: 5'-cccaagcttgggctaagtgcctttgctggcctg) and *G3PDH* (forward primer: 5'-accacagtccatgccatcac-3', reverse primer: 5'-tccaccacctgttgctgta-3') transcripts were amplified by cycling at 95°C for 45 seconds, 55°C for 45 seconds, and 72°C for one minute.

## Histology

Wild-type and *btf*<sup>-/-</sup> embryos and pups were embedded in paraffin after overnight fixation in 4% paraformaldehyde in PBS at 4°C. Transverse sections were made through

lungs of embedded animals at 5 $\mu$ m intervals. Paraffin was cleared with xylene and select sections were counter-stained with hematoxylin and eosin.

### **Immunohistochemistry**

Lung tissue from E18.5 or newborn lung was fixed and processed as described above. Unstained sections were deparaffinized and hydrated using standard methods. Endogenous peroxidase was quenched with 3% H<sub>2</sub>O<sub>2</sub> in methanol for 15-20 minutes. The following antibodies were used: rabbit anti-human pro-surfactant protein C (Catalog# AB3786, Chemicon International) at a dilution of 1:500 (as described in product information sheet), rabbit anti-mouse CC10 (#R42) was kindly provided by Dr. Jan Ryerse (Ryerse et. al., 2001) and used at dilution 1:100, rabbit anti-human Ki67 (Catalog# NCL-Ki67p, Vector Laboratories) at a dilution of 1:1000, and hamster anti-mouse T1- $\alpha$  (mAb 8.1.1, Developmental Studies Hybridoma Bank, [www.uiowa.edu/~dshbwww/](http://www.uiowa.edu/~dshbwww/)) at a dilution of 1:200.

For Ki67 and T1- $\alpha$ , antigen retrieval was performed by boiling the sections in Antigen Retrieval Citra Solution (Catalog# HK086-9K, BioGenex, CA) for 10 minutes prior to quenching endogenous peroxidase. For Ki67, sections were incubated with primary antibody overnight at room temperature, whereas for all other antibodies incubation was performed at 4°C. After incubating with primary antibody, slides were washed and exposed to appropriate biotinylated-secondary antibodies (1:200 dilution) for 30 minutes followed by incubation with streptavidin-horseradish peroxidase (1:500 dilution) for 30 minutes. Antibody binding was detected using diaminobenzidine (Catalog# S3000, DAB Chromogen

tablets, DAKO Corporation, CA). Sections were then either counter-stained with nuclear fast red (Sigma) or directly dehydrated and mounted using Permount (Fisher Scientific).

### **LacZ staining**

Lungs from wild-type, *btf<sup>ex/-</sup>*, or *btf<sup>fl/-</sup>* P0 pups and wild-type or *btf<sup>ex/-</sup>* adult mice were dissected and fixed in 2% paraformaldehyde, 0.2% glutaraldehyde/PBS on ice for 60-90 min. The samples were then washed in PBS and incubated in staining solution (5mM ferrocyanide, 5mM ferricyanide, 2mM MgCl<sub>2</sub>, 1mg/ml X-gal dissolved in N’N’-dimethyl formamide/ PBS) in the dark on a shaker at room temperature for 20 hours. The tissues were washed in PBS, fixed in 4% paraformaldehyde overnight at 4°C and embedded in paraffin and sectioned. The sections were counter-stained with nuclear fast red (Sigma), dehydrated and mounted using Permount (Fisher Scientific).

### **Electron microscopy**

1-2 mm portions of lung were fixed in 2% glutaraldehyde and routinely processed for electron microscopy. In brief, tissue was dehydrated in graded alcohols, embedded in resin, sectioned and stained with lead citrate and uranyl acetate. Ninety nanometer tissue sections were viewed on a Hitachi 7500 transmission electron microscope (Tokyo, Japan) fitted with a Advanced Microscopy Techniques digital camera (Danvers, MA). Measurements of distance between the apical surface of the type I pneumocyte to the capillary lumen were performed using Advanced Microscopy Techniques Advantage software (Danvers, MA).

### **Lung morphometry**

Newborn lungs were inflated with 4% paraformaldehyde under constant pressure via a tracheal cannula with a 25-gauge luer. After inflation the trachea was clamped and the animals fixed in 4% paraformaldehyde overnight at 4°C and embedded in paraffin. Sections were cut at 5µm intervals. Paraffin was cleared with xylene and select sections were counter-stained with hematoxylin and eosin. Images of the distal epithelium were captured using a Zeiss camera Axiocam mounted on a Leica microscope.

### **Measurment of body weight and blood glucose**

Newborn animals were weighed prior to feeding. Blood glucose of newborn animals was measured using the OneTouch® FastTake® compact blood glucose monitoring system (Lifescan, Johnson&Johnson). Blood was obtained from tails of animals prior to feeding.

### **Quantification of proliferation**

To quantify proliferation, sections from wild-type (n=3) or *btf*<sup>+/−</sup> (n=4) animals were immunostained with Ki67, a marker of proliferation. We counted approximately 3000 cells in the distal epithelium per animal from several regions of the lung and approximately 400 cells in the proximal airways per animal. The proliferating cells are represented as a percentage of total number of cells counted.

## TUNEL assay

To visualize apoptotic nuclei, sections through *btf*, *btf<sup>+/+</sup>* and *btf<sup>-/-</sup>* lung were subjected to terminal transferase-mediated dUTP-biotin nick end labeling (TUNEL) using the ApopTag kit (Intergen Company). Sections were counter-stained with DAPI.

## Results

### Mouse Btf shows similarity to TRAP150

We identified a gene that was down regulated in the *dHAND<sup>-/-</sup>* heart and subsequent cloning of the full-length gene from an E11.5 whole embryo cDNA library revealed identity to *hbtf* (human Bcl-2 associated transcription factor). We identified a long form (mBtf<sub>L</sub>) and a short form (mBtf<sub>S</sub>) of the gene. Btf<sub>S</sub> was missing 49 amino acids in its C-terminus between residues 796 and 845 similar to hBtf (Kasof et al., 1999). Sequence alignment revealed that the gene was highly conserved between mouse and humans, showing 96% identity at the protein level. Also, Btf showed 81% similarity (62% identity) between residue 1-162, and 71% similarity (56% identity) between residue 562-917, to TRAP150 (Fig. 1). TRAP150 is a member of a complex of factors required for efficient functioning of nuclear hormone receptors activated by ligands (Ito et al., 1999).



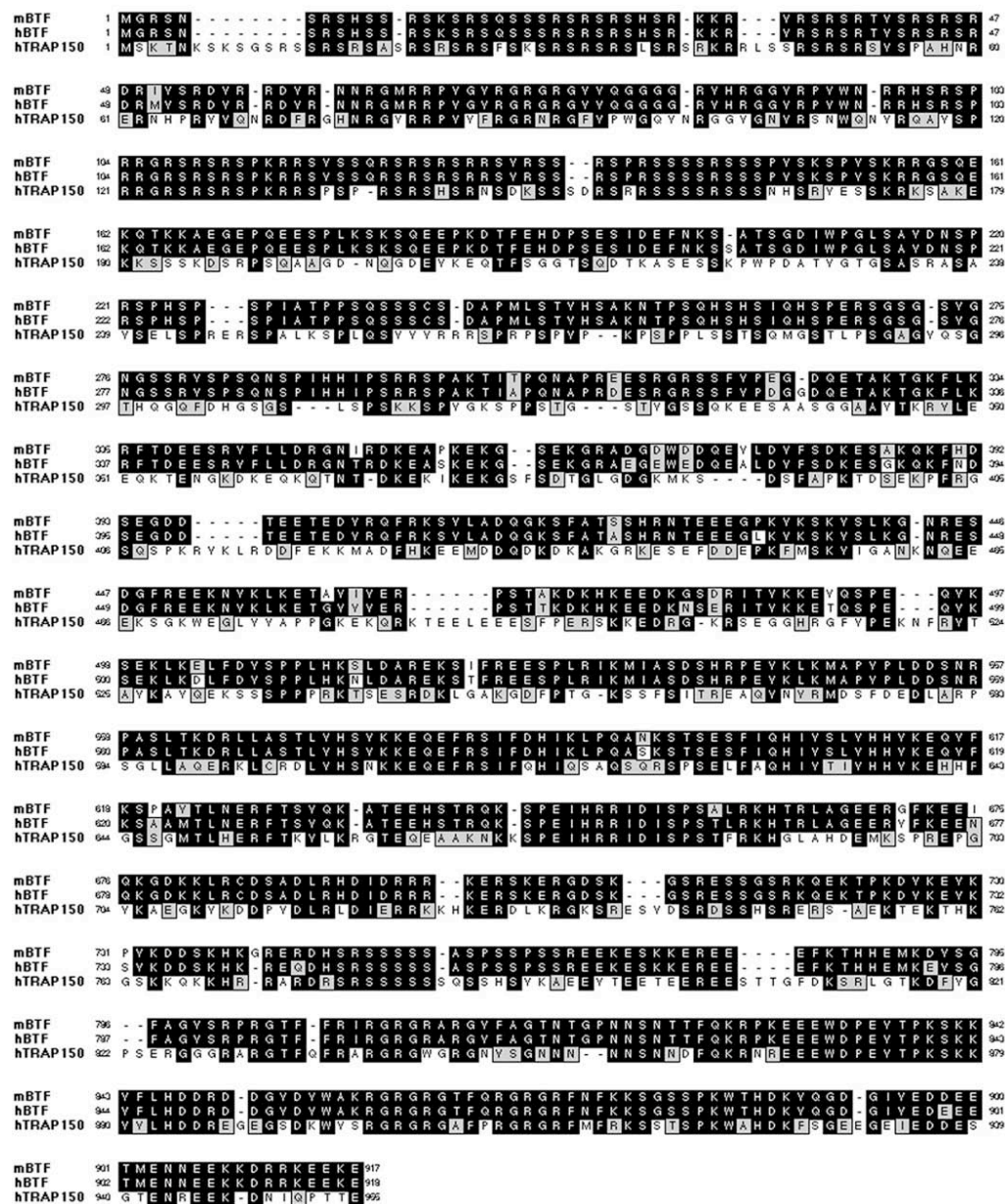
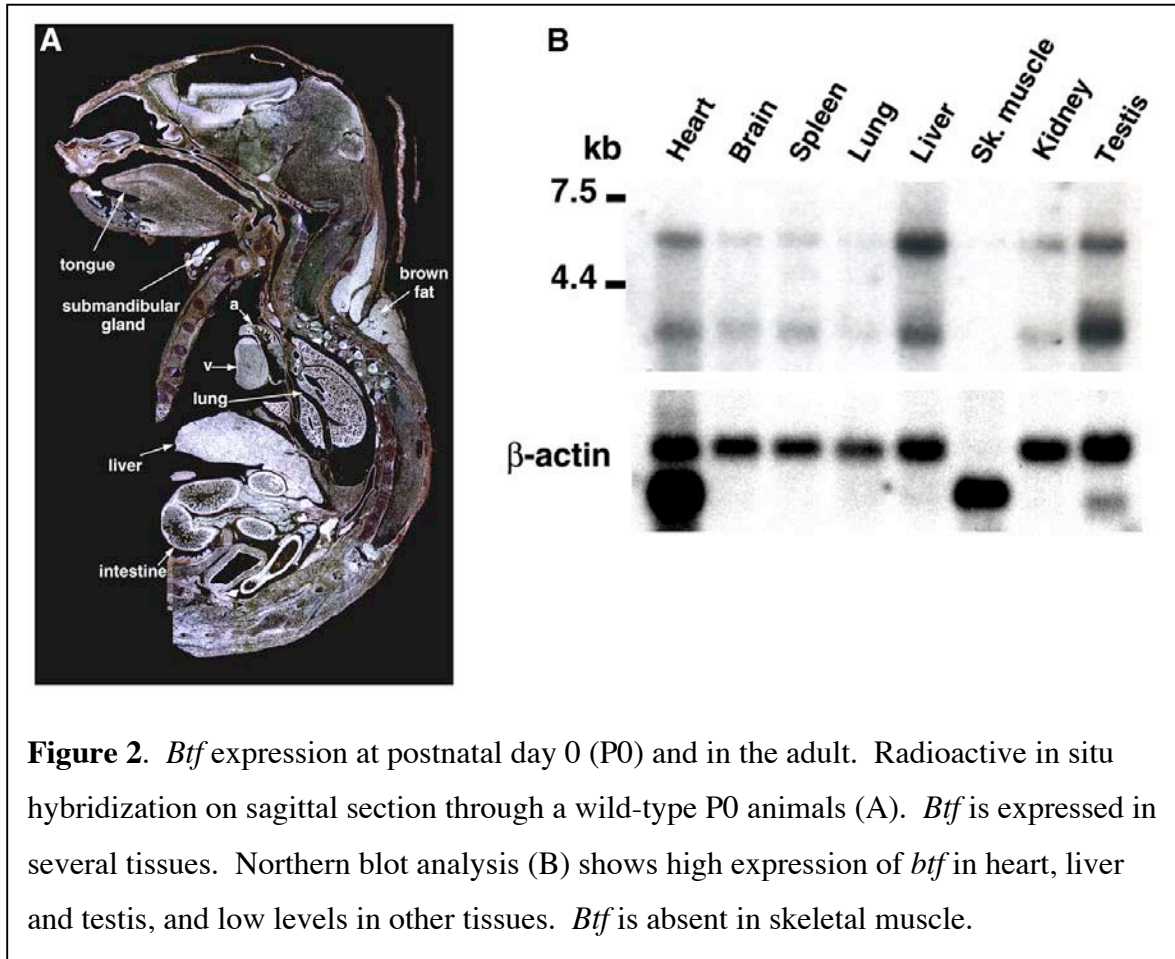


**Figure 1.** Sequence alignment of mBtf with hBtf and hTRAP150. mBtf and hBtf show 96% identity. Btf and hTRAP150 show 60% identity between residues 1-162 and residues 562-917.

Radioactive in situ hybridization analysis showed that *btf* was expressed ubiquitously during development (data not shown), but became restricted to specific tissues by birth (Fig.

2A). Northern blot analysis on tissues from adult mice revealed the strongest expression in the heart, liver and testis, with low levels observed in other tissues (Fig. 2B). Interestingly, no transcript was observed in the skeletal muscle.



Since *btf* was isolated in a screen to identify factors dysregulated in *dHAND*<sup>-/-</sup> hearts, we performed radioactive in situ hybridization to confirm the dysregulation. As shown in figure 3, *btf* was down regulated in the heart of *dHAND*<sup>-/-</sup> embryo, while *Nkx2.5* expression

was unaffected in a serial section of the same embryo at E9.5, suggesting that the down regulation of *btf* in *dHAND*<sup>-/-</sup> hearts was not due to poor RNA preservation.

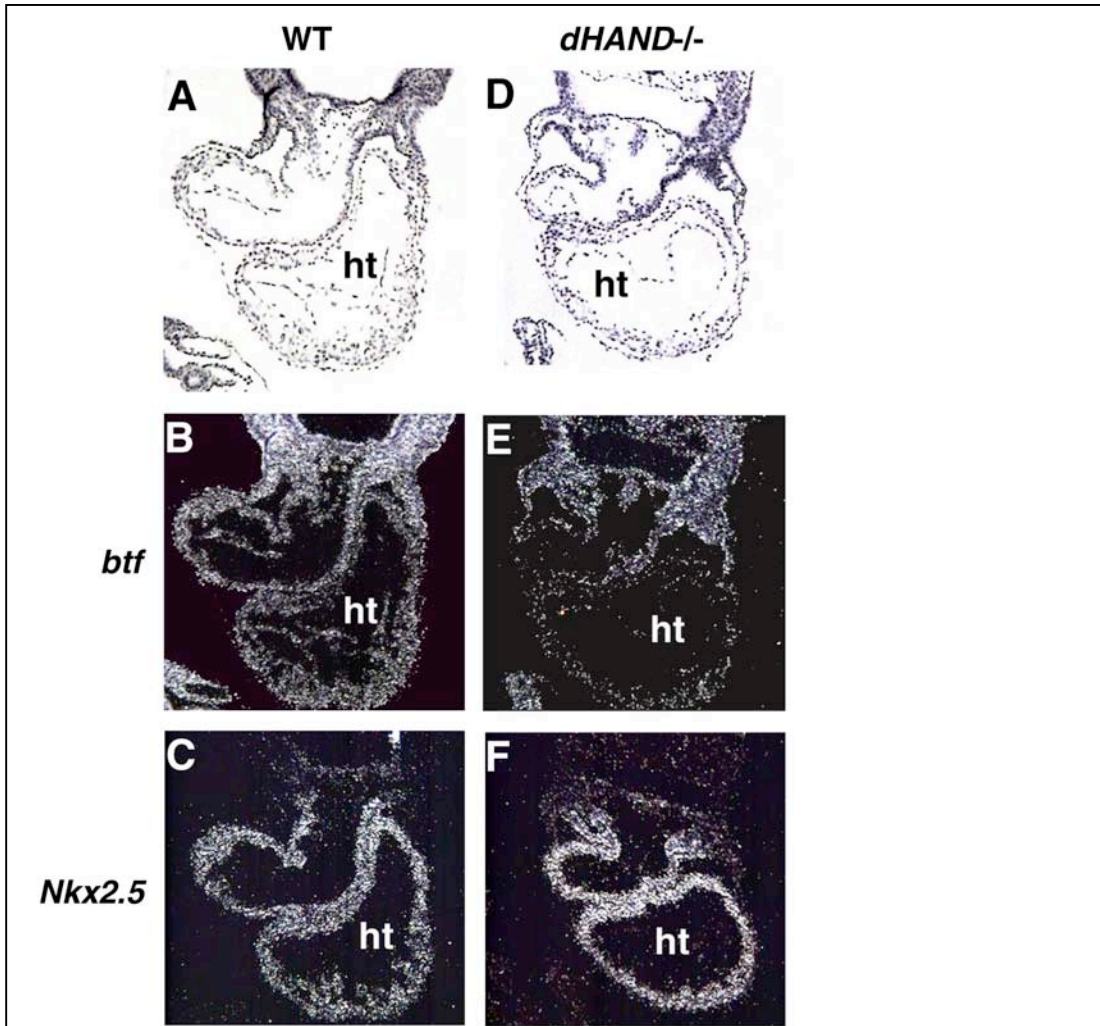
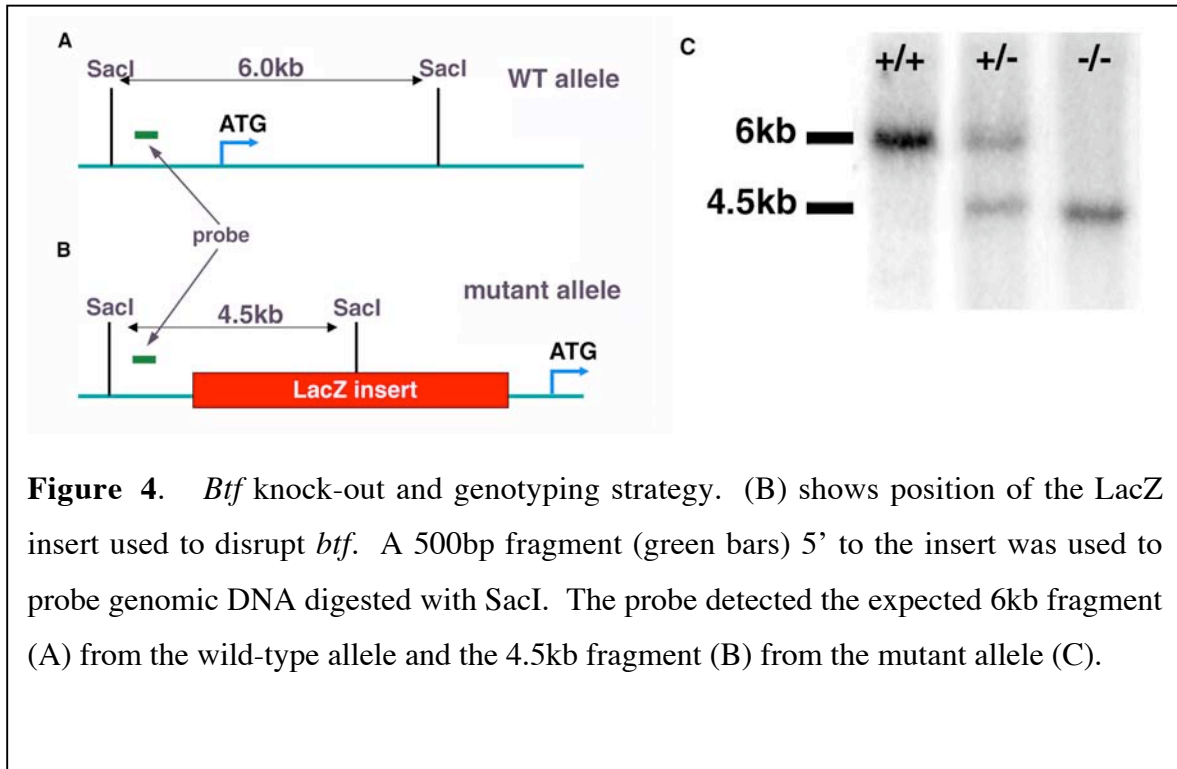


**Figure 3.** *Btf* is specifically downregulated in the *dHAND*<sup>-/-</sup> heart. Serial transverse sections of E9.25 wild-type (WT) (A-C) and *dHAND*<sup>-/-</sup> (D-F) embryos were examined for expression of *btf* (B, E) and *Nkx2.5* (C, F) by 35S radioactive *in situ* hybridization. Bright field images of the sections are shown in (A) and (D). *Btf* expression was decreased in *dHAND*<sup>-/-</sup> heart (B) in comparison to WT (E). *Nkx2.5* expression was unchanged (compare C and F).

### Loss of *Btf* in mice leads to perinatal lethality

The high level of conservation between mouse and human Btf, which is thought to be a transcription repressor (Kasof et al., 1999), and their similarity to hTRAP150 suggested that Btf might function in concert with nuclear hormone receptors in embryonic development. Mice heterozygous for a LacZ insertion in the 5'UTR of *btf* (fig. 4B) were phenotypically normal. The heterozygous mice were mated, and their offspring genotyped at postnatal day 10 (P10) (Fig. 4C).



No *btf*<sup>-/-</sup> pups were recovered at P10 (Table 1). Analysis of embryos at embryonic day (E) 18.5 (data not shown) revealed mendelian ratios of all genotypes, suggesting early postnatal lethality.



**Table1**Genotype of pups at postnatal day 10 (P10) from *btf*<sup>+/−</sup> intercrosses

Genotype	<i>btf</i>	+/+	+/-	-/-	Total
P10	Expected	23	47	23	94
	Observed	32	61	1*	

\*pup died by P14

No *btf* mRNA transcripts were detectable in *btf*<sup>−/−</sup> animals suggesting that they were null mutants (Fig. 5). This was confirmed by radioactive in situ hybridizations performed on

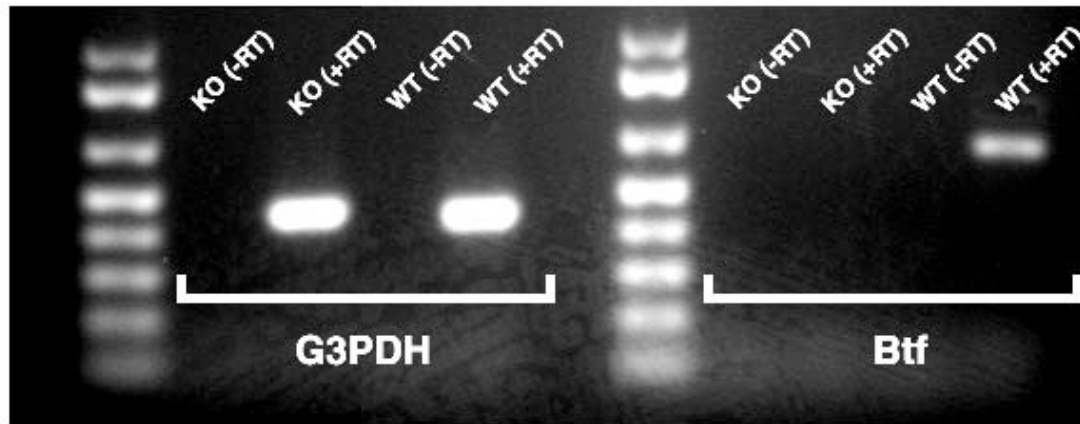
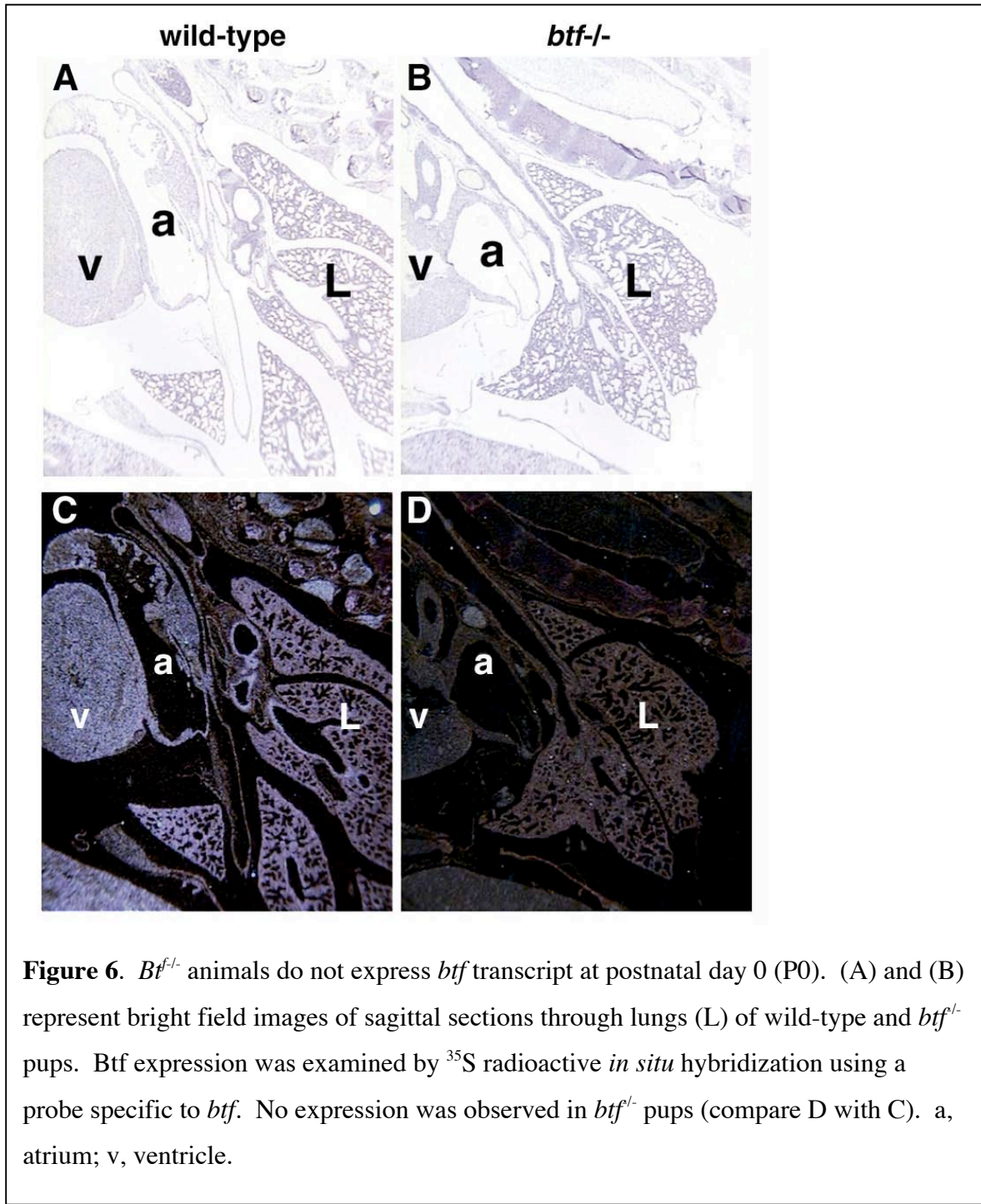


**Figure 5.** Animals homozygous for the mutant allele lack *btf* transcript. RT-PCR on wild-type (WT) and mutant RNA using primers specific for *btf* revealed absence of *btf* transcript in *btf*<sup>−/−</sup> animals (KO+RT). G3PDH expression showed no change. Samples transcribed without reverse transcriptase (−RT) samples were used to confirm absence of genomic contamination.

sagittal sections through wild-type and *btf*<sup>−/−</sup> animals (Fig. 6). Examination of newborn animals revealed that *btf*<sup>−/−</sup> pups were born but do not survive more than 24 hours. Further analysis showed that 60% of *btf*<sup>−/−</sup> pups were smaller than their wild-type littermates

( $1.2 \pm 0.02$  vs  $1.5 \pm 0.1$ ), 40% did not feed and 25% were cyanotic, showed evidence of respiratory distress and died within the first 10 hours after birth.



### Abnormal lung morphology in *btf*<sup>-/-</sup> animals

In order to determine the cause of lethality, we performed a detailed histological analysis of *btf*<sup>-/-</sup> animals. While we observed no histological defects in the heart, brain, liver or kidneys of these animals, the lungs of *btf*<sup>-/-</sup> animals showed evidence of hyper-cellularity

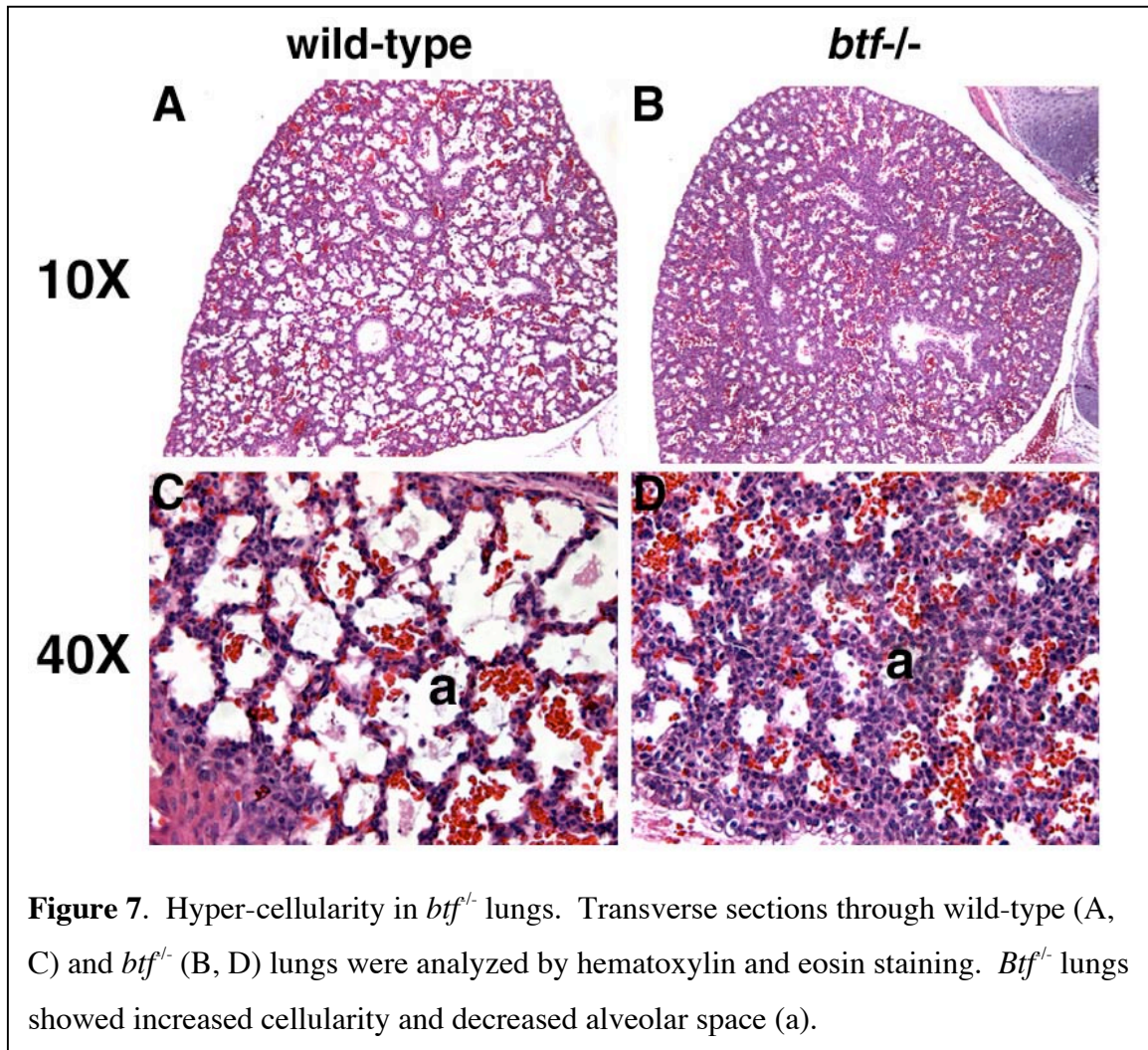
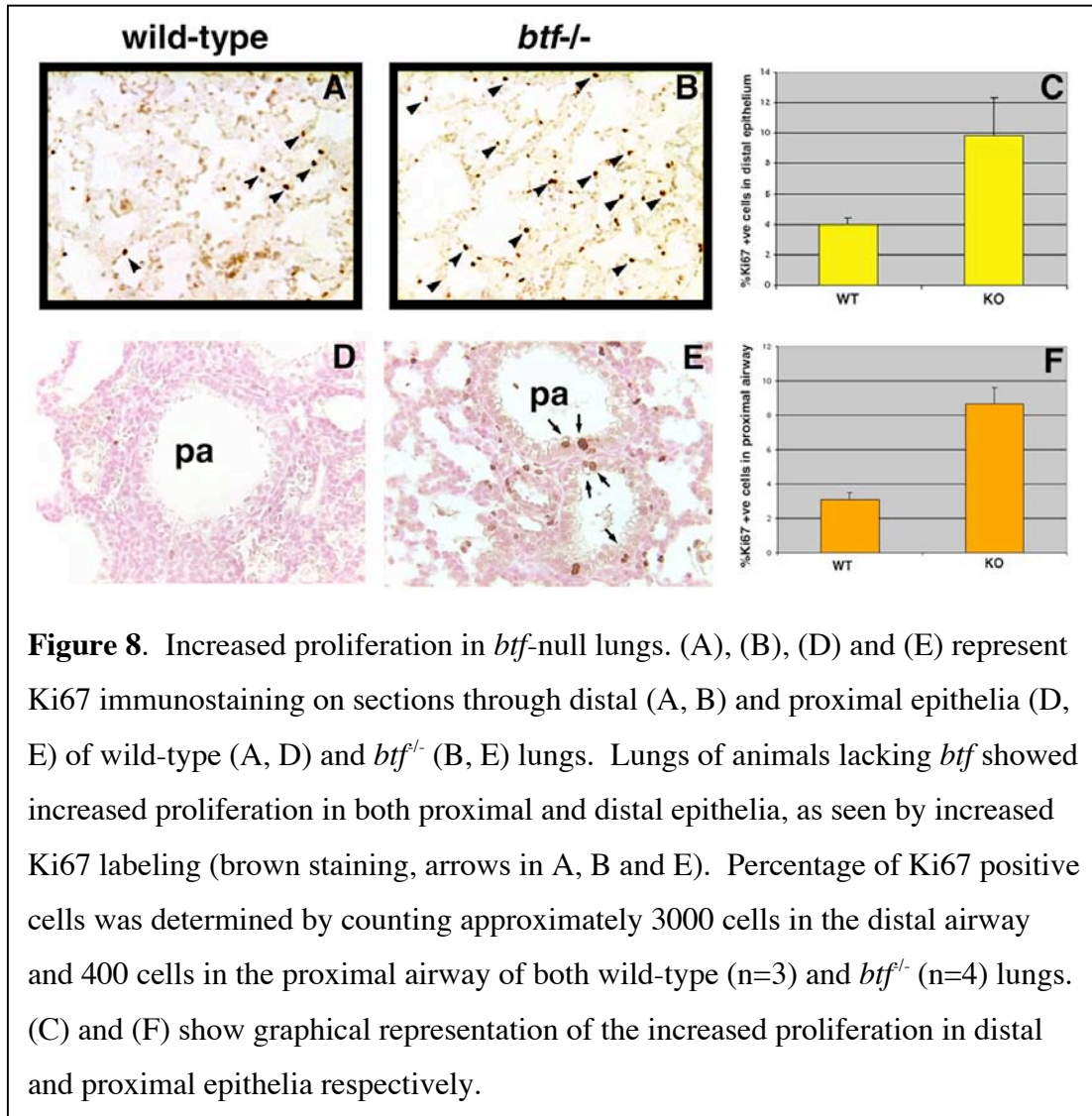


(Fig. 7). In order to determine the cause of hyper-cellularity, we performed TUNEL assay or Ki67 immunostaining to determine changes in cell death or cell proliferation, respectively. While we did not observe any changes in cell death between wild-type and *btf*<sup>-/-</sup> lungs, cell proliferation was increased 2-fold in the distal epithelium of *btf*<sup>-/-</sup> lungs compared with wild-



type animals. A similar analysis on the proximal airways revealed an almost 3-fold increase in proliferation in the *btf*<sup>-/-</sup> lungs over wild-type (Fig. 8).

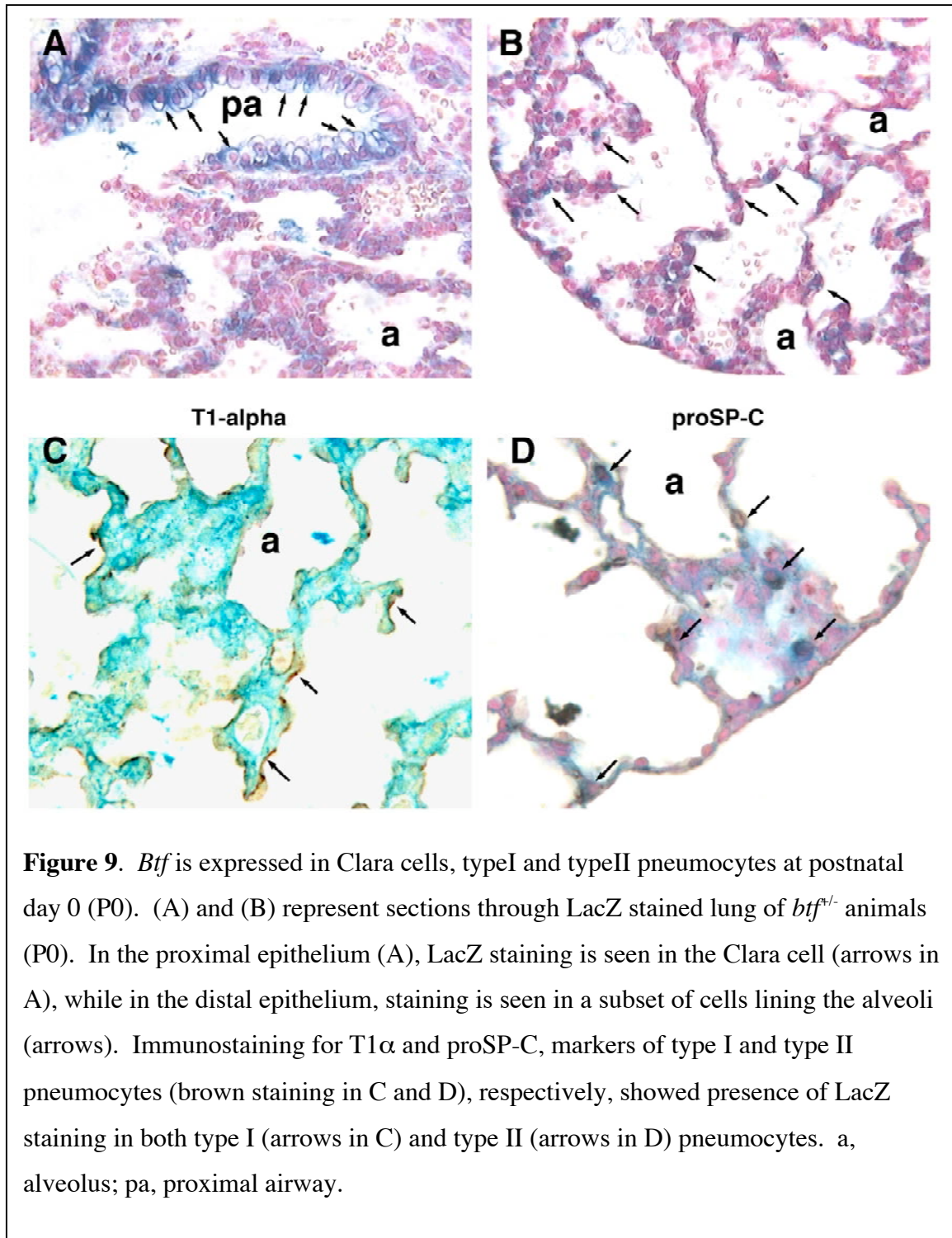


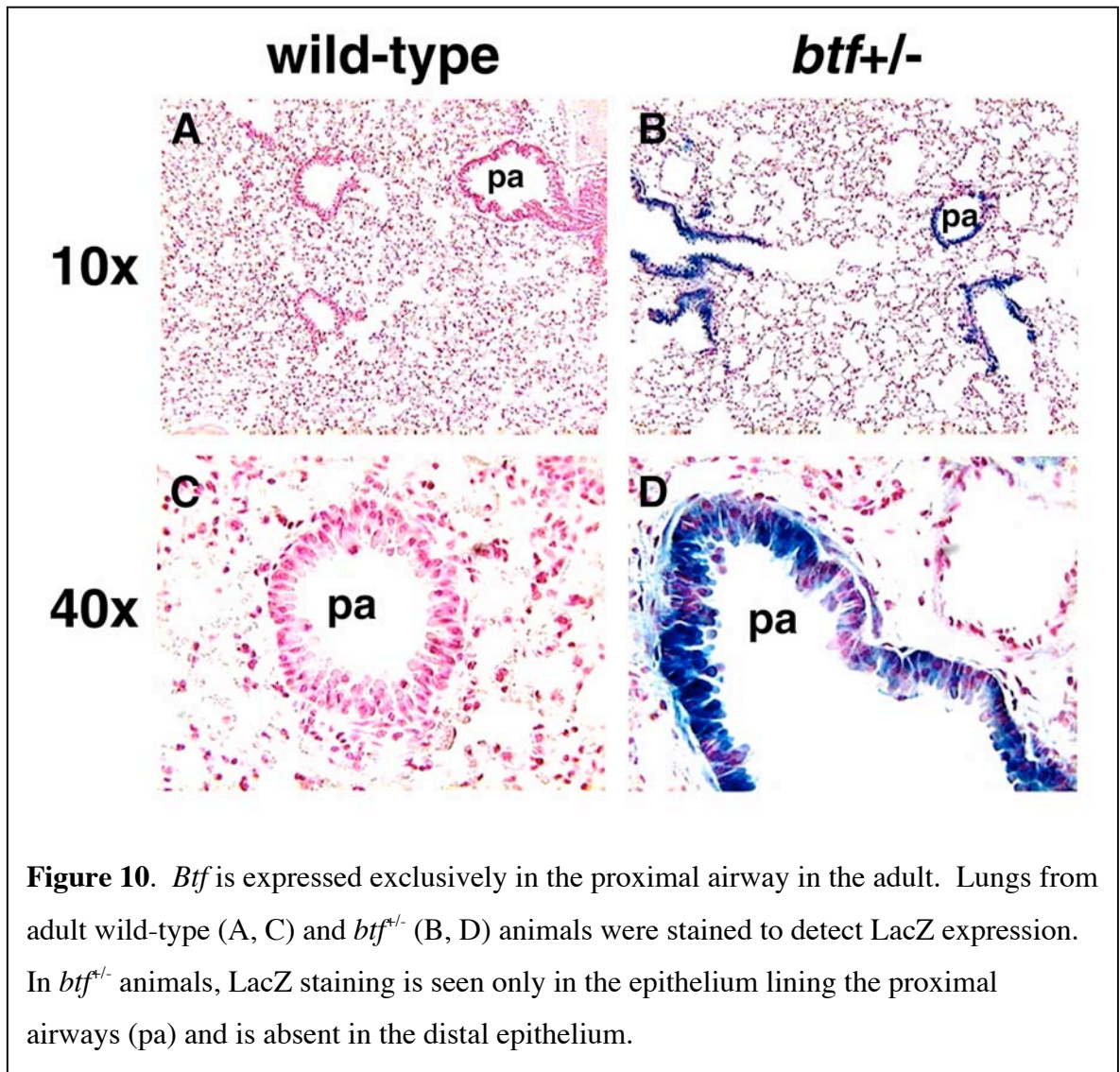
We also analyzed blood glucose levels in wild-type and *btf*<sup>-/-</sup> animals to determine whether hypoglycemia contributed to the observed lethality. Mutant animals did not show any change in blood glucose levels at birth or 12 hours after birth, suggesting normal glucose metabolism in the mutants.



***Btf* is expressed in various cell types in the newborn lung but is restricted to Clara cells of the proximal airways in the adult**

In order to better understand the defects observed in the *btf*<sup>-/-</sup> lung, we used *btf*<sup>+/-</sup> pups to study the expression pattern of *btf* in the lung in greater detail. The LacZ insertion in the *btf* gene recapitulated the expression pattern observed by radioactive in situ hybridization. Our analysis revealed that at P0, *btf* was expressed in both the proximal airways and the distal epithelium. In the proximal airways, expression was seen in the non-ciliated Clara cells (Fig. 9A), which were identified based on morphology (cells with clear cytoplasm), while in the distal epithelium, expression was seen in a subset of cells lining the alveoli (fig. 9B). In order to determine the identity of the LacZ expressing cells in the distal epithelium, we performed immunohistochemistry on LacZ stained sections using antibody against T1- $\alpha$  (fig. 9C), a marker of type I pneumocytes and pro-surfactant protein-C (proSP-C), a marker of typeII pneumocytes (Fig. 9D). This analysis revealed that *btf* was expressed in both typeI and typeII pneumocytes. Interestingly, in the adult lung, *btf* expression, as assessed by LacZ staining, was restricted to the Clara cells in the proximal airways only (Fig. 10).





### Normal surfactant protein expression and type I and type II pneumocyte morphology in *btfa/-* lungs

Cell specific expression of *btf* in distal lung epithelium combined with the respiratory distress observed in *btfa/-* pups suggested a defect in lung epithelium in *btfa/-* animals. We analyzed expression of surfactant proteins A, B and C by RT-PCR in lungs of E18.5 and P0



wild-type and *btf*<sup>-/-</sup> animals. G3PDH was used as control. We observed no change in surfactant protein expression between wild-type and mutant lung (data not shown). Ultrastructure analysis of *btf*<sup>-/-</sup> lungs at P0 and E18.5 by electron microscopy revealed the

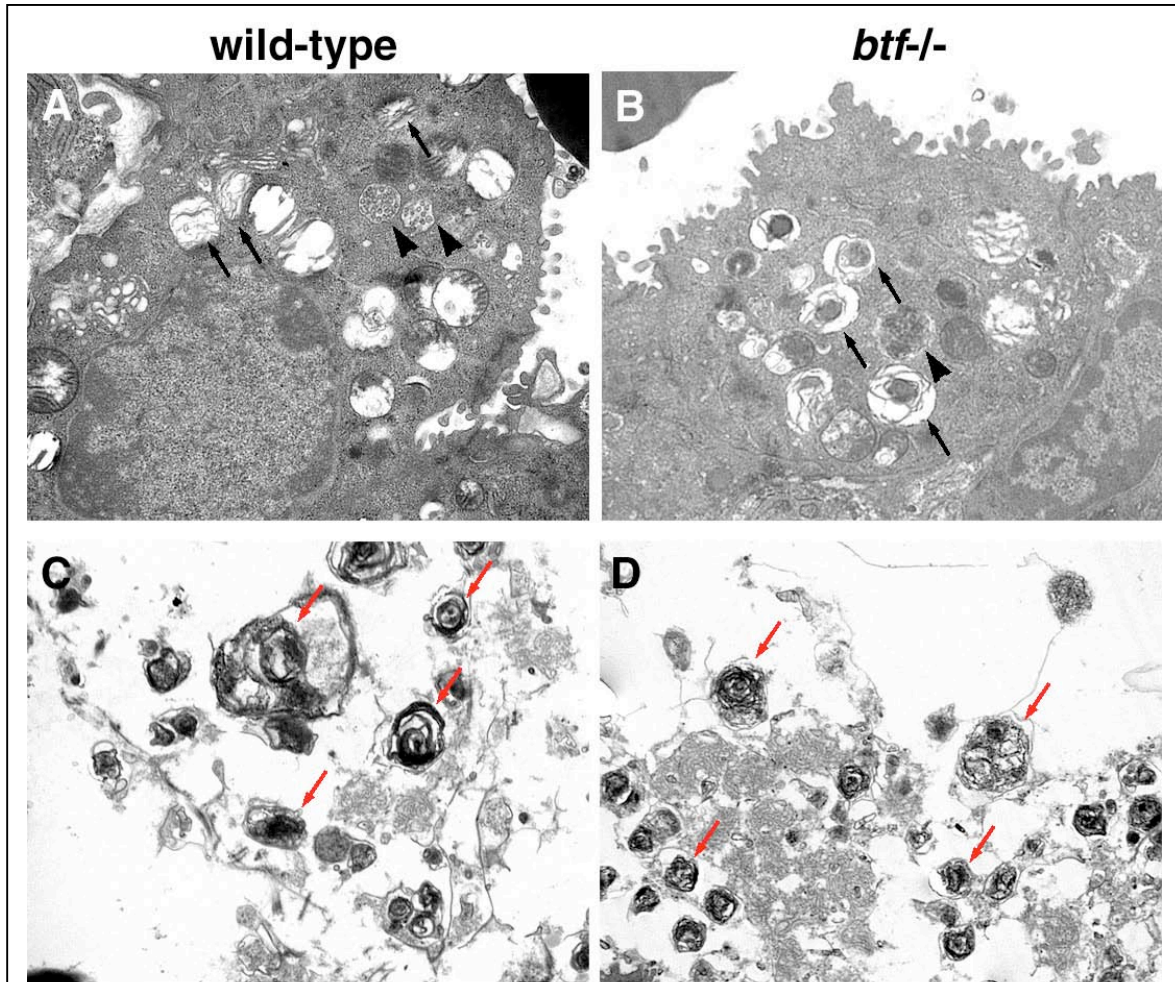
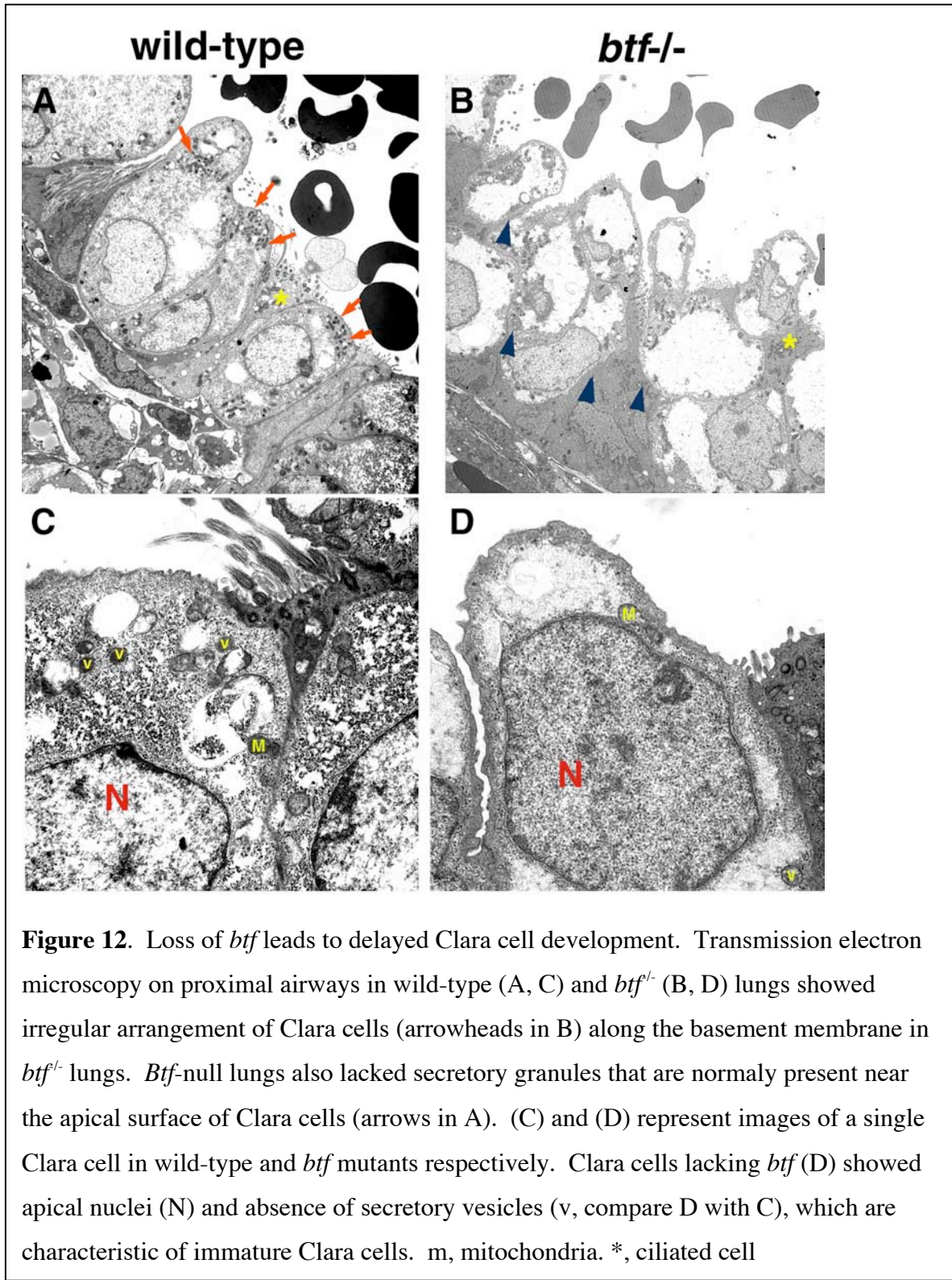


**Figure 11.** Normal lamellar body ultrastructure in *btf*-null lungs. Wild-type and *btf*<sup>-/-</sup> lungs were analyzed by transmission electron microscopy. *Btf*-null animals showed presence of lamellar bodies (arrows in A and B) and multivesicular bodies (arrowheads in A and B) in type II pneumocytes similar to wild-type. Analysis of secretions in the alveoli revealed normal secretion of lamellar bodies (red arrows) in *btf*<sup>-/-</sup> lungs (compare D with C).

presence of type II pneumocytes with lamellar bodies. We also observed lamellar bodies in the alveolar space suggesting normal secretion of surfactant proteins into the alveolar space (Fig. 11). The expression of *Tl $\alpha$* , a marker of type I cells, was unchanged in the mutant lung. In addition, analysis of type I pneumocytes showed similar numbers in wild-type and *btf<sup>-/-</sup>* lungs. Measurement of the distance between the apical surface of the type I cell to the lumen of the underlying capillary did not reveal any differences between wild-type and *btf<sup>-/-</sup>* animals. Together, these results suggested that type I, and type II cell differentiation were not affected in the absence of Btf. Finally, we also tested *PECAM* expression by RT-PCR to determine any change in vascularization. Again, our results revealed no difference between wild-type and mutants (data not shown).

### **Abnormal Clara cell morphology in *btf<sup>-/-</sup>* pups**

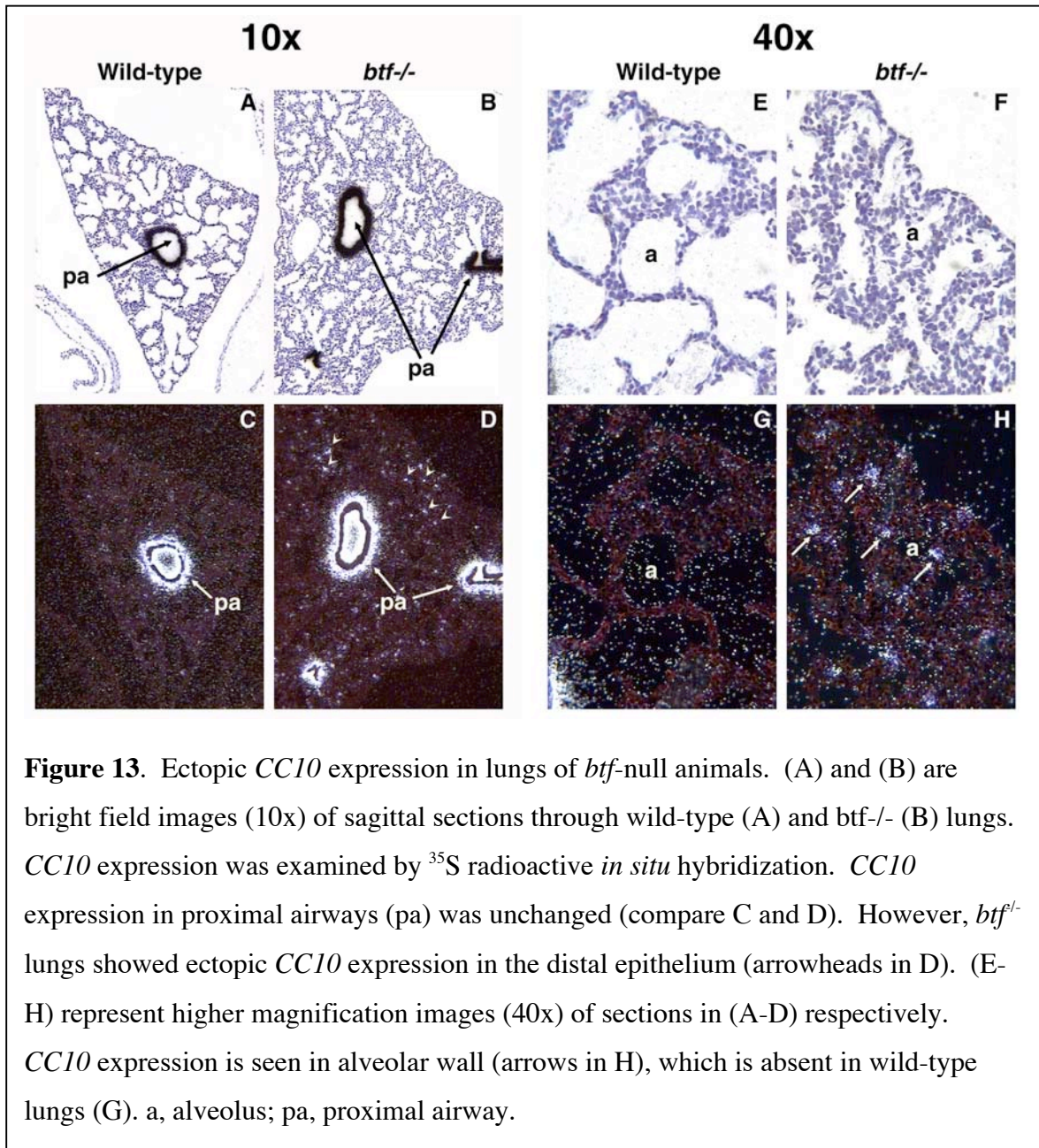
Restricted expression of *btf* in Clara cells of the adult lung suggested a role for it in development of this cell type. We therefore studied the ultrastructure of Clara cells in the proximal airways of wild-type and *btf<sup>-/-</sup>* pups by transmission electron microscopy. We observed that Clara cells in *btf<sup>-/-</sup>* animals had an irregular and disorganized arrangement along the basal membrane in contrast to the uniform monolayer in the wild-type (Fig. 12A, B). Also, in the *btf<sup>-/-</sup>* lung a large number of Clara cells had apical nuclei and showed a decrease in the number of vesicles, which was characteristic of primitive Clara cells (Fig 12C, D).



### **Ectopic CC-10 expression in *btf*<sup>-/-</sup> lungs and presence of Clara-like cells in the alveolar walls**

Clara cells are normally restricted to the proximal airway epithelium. Because Clara cells retain some progenitor cell characteristics, and the hyper-proliferative activity of *btf*<sup>-/-</sup> epithelial cells, we used a Clara cell marker, CC10, to determine if there might be a defect in patterning of Clara cells in the absence of *btf*. While we did not observe any change in the level of CC10 expression in the proximal airways of *btf*<sup>-/-</sup> lungs, we found ectopic expression of CC10 mRNA in the distal epithelium of the mutant lung (Fig. 13). This was confirmed by immunohistochemistry on P0 wild-type and *btf*<sup>-/-</sup> lung sections using an antibody against CC10 (Dr. Ryerse, St. Louis Univ.)(Fig. 14). Detailed ultrastructural analysis on distal epithelia revealed the presence of excessive glycogen containing cells. While some of these cells contained lamellar bodies characteristic of type II pneumocytes, other lacked lamellar bodies, showed absence of processes that are characteristic of type II cells and morphologic similarity to Clara cells (asterisk in Fig. 14D). The presence of Clara cells in the distal epithelium has never been reported and was not observed in any of our wild-type lungs. This suggested that loss of *btf* in the distal epithelium leads to abnormal specification of Clara cells in the distal epithelium.







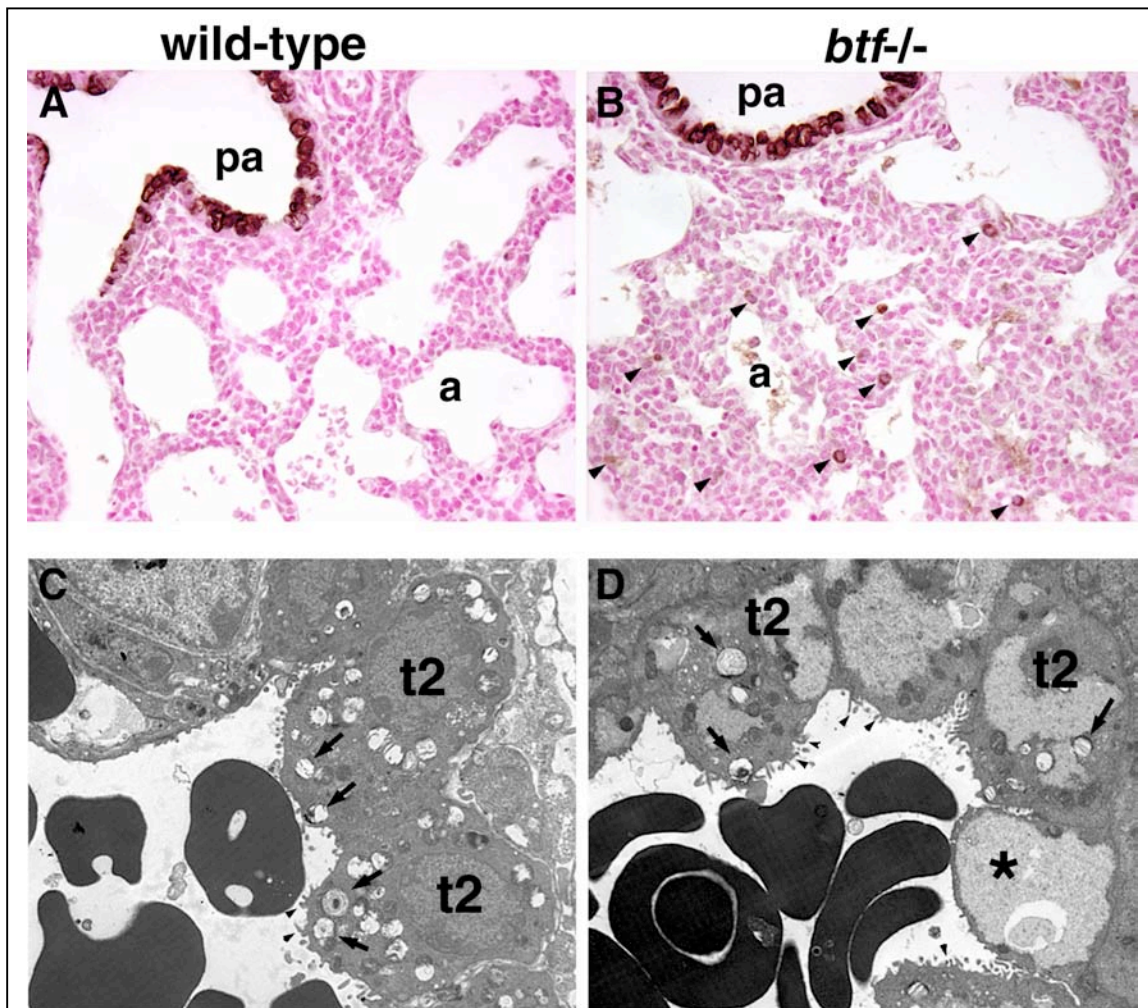


**Figure 14.** *Btfl*-null lungs have Clara-like cells in the distal epithelium. (A) and (B) represent sections through wild-type and *btfl*<sup>-/-</sup> lungs stained for CC10 expression (brown staining). Loss of *btfl* resulted in ectopic presence of CC10 expressing cells (arrowheads in B) in the distal epithelium. Transmission electron microscopy showed increased glycogen containing cells in *btfl*<sup>-/-</sup> lungs (D). Some of these cells were identified as typeII cell (t2) due to presence of lamellar bodies (arrows in D), however, some glycogenated cells lacked lamellar bodies and processes (arrowheads in C and D) at the apical surface characteristic of typeII cells, showing similarity to Clara cells (asterisk in D).

## Discussion

We have found that in vivo deletion of mBtf, an evolutionary conserved molecule similar to hTRAP150, causes early neonatal lethality. Loss of *btf* retards Clara cell development, and disrupts the tightly controlled proximal-distal epithelial cell patterning. Mice lacking *btf* show ectopic expression of CC-10 in the cells of the alveoli. Lungs of *btf*<sup>-/-</sup> mice are hyper-cellular due to increased proliferation in the proximal and distal epithelium, possibly due to defects in maturation and patterning of the progenitor pool of Clara cells. Also, the immaturity of the Clara cells in the proximal epithelium and ectopic presence of Clara cells in the distal epithelium may affect the composition of the fluid lining the airways. The increased cellularity coupled with the altered fluid composition could potentially result in inefficient respiration leading to respiratory distress and eventually death of the animals.

Clara cells are secretory cells, which function as progenitors with ability for self-renewal as well as differentiation into ciliated cells, and are exclusively present in the epithelial lining of the bronchi and bronchioles, i.e the proximal airways (Singh and Katyal, 1997). Clara cell differentiation begins at the end of the pseudoglandular stage (E16.5) and one of the first markers of Clara cell differentiation is CC10 (also known as CCSP or uteroglobin). Initially Clara cells are heavily glycogenated and do not contain any secretory granules, however by E17.5 these granules can be observed in the apical region of the cell (Ten Have-Opbroek and De Vries, 1993). CC10 is a secretory protein, which comprises the majority of protein secreted by Clara cells and is required for normal development of the secretory apparatus in these cells as shown by deletion of CC10 in mice (Stripp et al., 2000). Mice lacking CC10 survive to adulthood and show a complete absence of secretory granules

in the Clara cells. CC10 deficiency also changes the composition of the airway lining fluid, and increases the susceptibility of the animal to pollutants and microorganisms (Stripp et al., 2000, 2002).

While the regulation of Clara cells is poorly understood, there is some evidence that it might involve glucocorticoid signaling (GR). Corticotropin-releasing hormone (CRH) knock-out animals, which are glucocorticoid insufficient, die at birth due to respiratory failure, which is caused by undifferentiated distal epithelia. Analysis of the proximal airway revealed that Clara cells were undifferentiated, indicated by lack of CC10 expression (Muglia et al., 1999). The phenotype in the *btf*<sup>-/-</sup> mutant differs from the *CRH*<sup>-/-</sup> animal in that the Clara cells present an immature morphology irrespective of maintenance of CC10 expression, suggesting that CC10 expression alone is not indicative of normal Clara cell differentiation. However, it is possible that the *CRH*<sup>-/-</sup> lungs also have Clara-like cells in the alveolar walls, which cannot be detected by immunohistochemical methods due to its role in controlling CC10 expression. We believe that we have identified a transcriptional regulator that is involved in Clara cell maturation and analysis of genes downstream of *btf* could shed light on the secretory function of Clara cells, leading to perhaps a better understanding of Clara cell function in maintaining efficient lung function.

The strict control of proximal-distal patterning is an important aspect of lung development. The epithelial cells in the proximal and distal airways have very different functions and are therefore morphologically distinct. This distinction is brought about by restricted expression of differentiation-inducing genes in specific regions of the lung (reviewed in Cardoso, 2000). For example HFH4, a forkhead transcription factor, is

expressed in the cells that will ultimately form the ciliated cells in the distal epithelium. Both, misexpression and targeted deletion of *HFH4* support a role for it in specification, differentiation or maintenance of the ciliated cell type (Blatt et al., 1999; Tichelaar et al., 1999). Similarly, targeted deletion of *T1 $\alpha$* , a gene specifically expressed in the type I pneumocyte (Dobbs et al., 1988), leads to absence of type I cells (Ramirez et al., 2003). However, it is interesting to note that while loss of cell specific factors leads to absence of that cell type, it usually does not lead to a switch in cell fate. The *btf* mutant is interesting in this respect, because its absence in the distal epithelium leads to ectopic presence of CC10 expressing cells. Detailed ultrastructural analysis has shown that animals lacking *btf* have Clara-like cells in the distal epithelium, suggesting a role for *btf* in normally suppressing proximal cell fates in the distal epithelia of the lung. Furthermore, Clara cells are thought to be the progenitor cells in the epithelium of the proximal airway. The increased proliferation in the distal epithelium of the *btf<sup>fl/-</sup>* lungs might therefore be a result of misplacement of Clara cells in the distal epithelium.

Our studies have identified a transcriptional regulator with a dual role in lung development. While on one hand, Btf is required for maturation of Clara cells in the proximal airway, it also plays a role in controlling the proximal-distal patterning of the lung epithelium.

## References

- Blatt, E. N., Yan, X. H., Wuerffel, M. K., Hamilos, D. L., and Brody, S. L. (1999). Forkhead transcription factor HFH-4 expression is temporally related to ciliogenesis. *Am J Respir Cell Mol Biol* 21, 168-76.
- Boyer, T. G., Martin, M. E., Lees, E., Ricciardi, R. P., and Berk, A. J. (1999). Mammalian Srb/Mediator complex is targeted by adenovirus E1A protein. *Nature* 399, 276-9.
- Brody, A. R., Hook, G. E., Cameron, G. S., Jetten, A. M., Butterick, C. J., and Nettesheim, P. (1987). The differentiation capacity of Clara cells isolated from the lungs of rabbits. *Lab Invest* 57, 219-29.
- Cardoso, W. V. (2000). Lung morphogenesis revisited: old facts, current ideas. *Dev Dyn* 219, 121-30.
- Cole, T. J., Blendy, J. A., Monaghan, A. P., Krieglstein, K., Schmid, W., Aguzzi, A., Fantuzzi, G., Hummler, E., Unsicker, K., and Schutz, G. (1995). Targeted disruption of the glucocorticoid receptor gene blocks adrenergic chromaffin cell development and severely retards lung maturation. *Genes Dev* 9, 1608-21.
- Condon, J., Gosden, C., Gardener, D., Nickson, P., Hewison, M., Howie, A. J., and Stewart, P. M. (1998). Expression of type 2 11beta-hydroxysteroid dehydrogenase and corticosteroid hormone receptors in early human fetal life. *J Clin Endocrinol Metab* 83, 4490-7.
- Diamond, M. I., Miner, J. N., Yoshinaga, S. K., and Yamamoto, K. R. (1990). Transcription factor interactions: selectors of positive or negative regulation from a single DNA element. *Science* 249, 1266-72.

Dobbs, L. G., Williams, M. C., and Gonzalez, R. (1988). Monoclonal antibodies specific to apical surfaces of rat alveolar type I cells bind to surfaces of cultured, but not freshly isolated, type II cells. *Biochim Biophys Acta* 970, 146-56.

Drouin, J., Sun, Y. L., Chamberland, M., Gauthier, Y., De Lean, A., Nemer, M., and Schmidt, T. J. (1993). Novel glucocorticoid receptor complex with DNA element of the hormone-repressed POMC gene. *Embo J* 12, 145-56.

Fondell, J. D., Ge, H., and Roeder, R. G. (1996). Ligand induction of a transcriptionally active thyroid hormone receptor coactivator complex. *Proc Natl Acad Sci U S A* 93, 8329-33.

Fondell, J. D., Guermah, M., Malik, S., and Roeder, R. G. (1999). Thyroid hormone receptor-associated proteins and general positive cofactors mediate thyroid hormone receptor function in the absence of the TATA box-binding protein-associated factors of TFIID. *Proc Natl Acad Sci U S A* 96, 1959-64.

Glass, C. K., and Rosenfeld, M. G. (2000). The coregulator exchange in transcriptional functions of nuclear receptors. *Genes Dev* 14, 121-41.

Gruber, P. J., Kubalak, S. W., Pexieder, T., Sucov, H. M., Evans, R. M., and Chien, K. R. (1996). RXR alpha deficiency confers genetic susceptibility for aortic sac, conotruncal, atrioventricular cushion, and ventricular muscle defects in mice. *J Clin Invest* 98, 1332-43.

Hermans, C., and Bernard, A. (1999). Lung epithelium-specific proteins: characteristics and potential applications as markers. *Am J Respir Crit Care Med* 159, 646-78.

Hittelman, A. B., Burakov, D., Iniguez-Lluhi, J. A., Freedman, L. P., and Garabedian, M. J. (1999). Differential regulation of glucocorticoid receptor transcriptional activation via AF-1-associated proteins. *Embo J* 18, 5380-8.

Hogan, B. L., Grindley, J., Bellusci, S., Dunn, N. R., Emoto, H., and Itoh, N. (1997). Branching morphogenesis of the lung: new models for a classical problem. *Cold Spring Harb Symp Quant Biol* 62, 249-56.

Hogan, B. L. (1999). Morphogenesis. *Cell* 96, 225-33.

Hook, G. E., Brody, A. R., Cameron, G. S., Jetten, A. M., Gilmore, L. B., and Nettesheim, P. (1987). Repopulation of denuded tracheas by Clara cells isolated from the lungs of rabbits. *Exp Lung Res* 12, 311-29.

Ito, M., Yuan, C. X., Malik, S., Gu, W., Fondell, J. D., Yamamura, S., Fu, Z. Y., Zhang, X., Qin, J., and Roeder, R. G. (1999). Identity between TRAP and SMCC complexes indicates novel pathways for the function of nuclear receptors and diverse mammalian activators. *Mol Cell* 3, 361-70.

Ito, M., Yuan, C. X., Okano, H. J., Darnell, R. B., and Roeder, R. G. (2000). Involvement of the TRAP220 component of the TRAP/SMCC coactivator complex in embryonic development and thyroid hormone action. *Mol Cell* 5, 683-93.

Ito, M., Okano, H. J., Darnell, R. B., and Roeder, R. G. (2002). The TRAP100 component of the TRAP/Mediator complex is essential in broad transcriptional events and development. *Embo J* 21, 3464-75.

Jiang, Y. W., Veschambre, P., Erdjument-Bromage, H., Tempst, P., Conaway, J. W., Conaway, R. C., and Kornberg, R. D. (1998). Mammalian mediator of transcriptional regulation and its possible role as an end-point of signal transduction pathways. *Proc Natl Acad Sci U S A* 95, 8538-43.

Jonat, C., Rahmsdorf, H. J., Park, K. K., Cato, A. C., Gebel, S., Ponta, H., and Herrlich, P. (1990). Antitumor promotion and antiinflammation: down-modulation of AP-1 (Fos/Jun) activity by glucocorticoid hormone. *Cell* 62, 1189-204.

Kasof, G. M., Goyal, L., and White, E. (1999). Btf, a novel death-promoting transcriptional repressor that interacts with Bcl-2-related proteins. *Mol Cell Biol* 19, 4390-404.

Kastner, P., Messaddeq, N., Mark, M., Wendling, O., Grondona, J. M., Ward, S., Ghyselinck, N., and Chambon, P. (1997). Vitamin A deficiency and mutations of RXRalpha, RXRbeta and RARalpha lead to early differentiation of embryonic ventricular cardiomyocytes. *Development* 124, 4749-58.

Lu, J., Richardson, J. A., and Olson, E. N. (1998). Capsulin: a novel bHLH transcription factor expressed in epicardial progenitors and mesenchyme of visceral organs. *Mech Dev* 73, 23-32.

Malik, S., and Roeder, R. G. (2000). Transcriptional regulation through Mediator-like coactivators in yeast and metazoan cells. *Trends Biochem Sci* 25, 277-83.

Mangelsdorf, D. J., Thummel, C., Beato, M., Herrlich, P., Schutz, G., Umesono, K., Blumberg, B., Kastner, P., Mark, M., Chambon, P., and et al. (1995). The nuclear receptor superfamily: the second decade. *Cell* 83, 835-9.

Masuyama, H., Hiramatsu, Y., and Kudo, T. (1995). Effect of retinoids on fetal lung development in the rat. *Biol Neonate* 67, 264-73.

Mendelsohn, C., Lohnes, D., Decimo, D., Lufkin, T., LeMeur, M., Chambon, P., and Mark, M. (1994). Function of the retinoic acid receptors (RARs) during development (II). Multiple abnormalities at various stages of organogenesis in RAR double mutants. *Development* 120, 2749-71.

Muglia, L. J., Bae, D. S., Brown, T. T., Vogt, S. K., Alvarez, J. G., Sunday, M. E., and Majzoub, J. A. (1999). Proliferation and differentiation defects during lung development in corticotropin-releasing hormone-deficient mice. *Am J Respir Cell Mol Biol* 20, 181-8.



Naltner, A., Wert, S., Whitsett, J. A., and Yan, C. (2000). Temporal/spatial expression of nuclear receptor coactivators in the mouse lung. *Am J Physiol Lung Cell Mol Physiol* 279, L1066-74.

Nguyen, T. M., Guillozo, H., Marin, L., Dufour, M. E., Tordet, C., Pike, J. W., and Garabedian, M. (1990). 1,25-dihydroxyvitamin D3 receptors in rat lung during the perinatal period: regulation and immunohistochemical localization. *Endocrinology* 127, 1755-62.

Rachez, C., Suldan, Z., Ward, J., Chang, C. P., Burakov, D., Erdjument-Bromage, H., Tempst, P., and Freedman, L. P. (1998). A novel protein complex that interacts with the vitamin D3 receptor in a ligand-dependent manner and enhances VDR transactivation in a cell-free system. *Genes Dev* 12, 1787-800.

Rachez, C., Lemon, B. D., Suldan, Z., Bromleigh, V., Gamble, M., Naar, A. M., Erdjument-Bromage, H., Tempst, P., and Freedman, L. P. (1999). Ligand-dependent transcription activation by nuclear receptors requires the DRIP complex. *Nature* 398, 824-8.

Ramirez, M. I., Millien, G., Hinds, A., Cao, Y., Seldin, D. C., and Williams, M. C. (2003). T1alpha, a lung type I cell differentiation gene, is required for normal lung cell proliferation and alveolus formation at birth. *Dev Biol* 256, 61-72.

Ryerse, J. S., Hoffmann, J. W., Mahmoud, S., Nagel, B. A., and deMello, D. E. (2001). Immunolocalization of CC10 in Clara cells in mouse and human lung. *Histochem Cell Biol* 115, 325-32.

Schule, R., Rangarajan, P., Kliwer, S., Ransone, L. J., Bolado, J., Yang, N., Verma, I. M., and Evans, R. M. (1990). Functional antagonism between oncoprotein c-Jun and the glucocorticoid receptor. *Cell* 62, 1217-26.

Singh, G., and Katyal, S. L. (1997). Clara cells and Clara cell 10 kD protein (CC10). *Am J Respir Cell Mol Biol* 17, 141-3.

Stripp, B. R., Reynolds, S. D., Plopper, C. G., Boe, I. M., and Lund, J. (2000). Pulmonary phenotype of CCSP/UG deficient mice: a consequence of CCSP deficiency or altered Clara cell function? *Ann N Y Acad Sci* 923, 202-9.

Stripp, B. R., Reynolds, S. D., Boe, I. M., Lund, J., Power, J. H., Coppens, J. T., Wong, V., Reynolds, P. R., and Plopper, C. G. (2002). Clara cell secretory protein deficiency alters clara cell secretory apparatus and the protein composition of airway lining fluid. *Am J Respir Cell Mol Biol* 27, 170-8.

Sucov, H. M., Dyson, E., Gumeringer, C. L., Price, J., Chien, K. R., and Evans, R. M. (1994). RXR alpha mutant mice establish a genetic basis for vitamin A signaling in heart morphogenesis. *Genes Dev* 8, 1007-18.

Ten Have-Opbroek, A. A., and De Vries, E. C. (1993). Clara cell differentiation in the mouse: ultrastructural morphology and cytochemistry for surfactant protein A and Clara cell 10 kD protein. *Microsc Res Tech* 26, 400-11.

Tichelaar, J. W., Lim, L., Costa, R. H., and Whitsett, J. A. (1999). HNF-3/forkhead homologue-4 influences lung morphogenesis and respiratory epithelial cell differentiation in vivo. *Dev Biol* 213, 405-17.

Warburton, D., Schwarz, M., Tefft, D., Flores-Delgado, G., Anderson, K. D., and Cardoso, W. V. (2000). The molecular basis of lung morphogenesis. *Mech Dev* 92, 55-81.

Warburton, D., Schwarz, M., Tefft, D., Flores-Delgado, G., Anderson, K. D., and Cardoso, W. V. (2000). The molecular basis of lung morphogenesis. *Mech Dev* 92, 55-81.

Yang-Yen, H. F., Chambard, J. C., Sun, Y. L., Smeal, T., Schmidt, T. J., Drouin, J., and Karin, M. (1990). Transcriptional interference between c-Jun and the glucocorticoid receptor: mutual inhibition of DNA binding due to direct protein-protein interaction. *Cell* 62, 1205-15.

Yuan, C. X., Ito, M., Fondell, J. D., Fu, Z. Y., and Roeder, R. G. (1998). The TRAP220 component of a thyroid hormone receptor- associated protein (TRAP) coactivator complex interacts directly with nuclear receptors in a ligand-dependent fashion. *Proc Natl Acad Sci U S A* 95, 7939-44.

Zhu, Y., Qi, C., Jain, S., Rao, M. S., and Reddy, J. K. (1997). Isolation and characterization of PBP, a protein that interacts with peroxisome proliferator-activated receptor. *J Biol Chem* 272, 25500-6.

## **CHAPTER 5**

### **CONCLUSIONS**

dHAND is a basic helix-loop-helix transcription factor that is required for various developmental processes in the embryo. Loss of dHAND leads to hypoplasia of the right ventricle, the pharyngeal arches and embryonic lethality at E10.0. The hypoplasia observed is a result of increased apoptosis. We performed a differential display analysis on RNA from hearts of E9.5 wild-type and *dHAND*<sup>-/-</sup> embryos in an effort to identify genes that were dysregulated in the *dHAND*<sup>-/-</sup> embryos. This thesis represents work on two of the genes identified through the screen.

#### **Mechanism of apoptosis in *dHAND*<sup>-/-</sup> embryos**

Bnip3, a hypoxia inducible, pro-apoptotic molecule that can induce mitochondrial damage, was upregulated in *dHAND*<sup>-/-</sup> hearts. This suggested that hypoxia resulting from poor cardiac function in *dHAND* mutants might lead to mitochondrial damage mediated by Bnip3 leading to increased apoptosis. In order to test this hypothesis, we chose to determine whether loss of Apaf-1 a key mediator of mitochondrial-induced apoptosis had any effect on the apoptosis observed. Loss of Apaf-1 led to a partial rescue of the *dHAND*<sup>-/-</sup> phenotype. *dHAND*<sup>-/-</sup>*Apaf-1*<sup>-/-</sup> animals showed decreased apoptosis in the pharyngeal arches and limb buds and had well-developed pharyngeal arches and arch arteries. However, the cardiac phenotype was unchanged in *dHAND*<sup>-/-</sup>*Apaf-1*<sup>-/-</sup> animals suggesting an Apaf-1 independent mechanism in the cardiac apoptosis or perhaps an

increased sensitivity of cardiac tissue to necrosis-like cell death in the absence of Apaf-1. These data showed that hypoplasia of the pharyngeal arches and arch arteries contribute to the early lethality observed in the *dHAND*<sup>-/-</sup> embryos. However, our results do not answer the question whether the pharyngeal arch phenotype is a primary defect resulting from the loss of dHAND or is secondary to the cardiac defect.

Mice lacking the pharyngeal arch enhancer of dHAND have been generated and show craniofacial defects, which is not consistent with massive apoptosis. However, dHAND expression is not completely abolished in these animals suggesting that the cells expressing dHAND could secrete factors to promote survival of the neighboring cells. Analysis of pharyngeal arch-specific and cardiac-specific *dHAND* knock-out will help us better understand the relation between the observed cardiac and pharyngeal arch phenotypes.

### **Role of *btf* in embryonic and postnatal development**

The mouse ortholog of human Btf (Bcl2 associated transcription factor) represented 10% of the clones isolated from the differential display analysis. hBtf is a nuclear localized pro-apoptotic factor with transcription repressor activity. Btf showed similarity in its N- and C-termini to thyroid hormone receptor associated protein 150 (TRAP150). TRAPs are a family of transcription co-activators, which are required for activation of genes downstream of nuclear receptor activation. One such family of ligand dependent nuclear receptors is the retinoid receptor family, which consists of the RAR and RXR subfamilies each with three members- $\alpha$ ,  $\beta$ , and  $\gamma$ . Several of these genes are required for normal cardiac development. In addition, TRAP220, another member of the

co-activator complex is required for normal cardiac and embryonic development. This suggested that Btf might be another member of a co-activator complex with a role in cardiac and embryonic development. Btf was expressed ubiquitously during development, but was restricted to specific tissues at birth.

Mice lacking *btf* died within 24 hours after birth and showed signs of respiratory failure. We concentrated our efforts on determining the cause of lethality, and performed a histological analysis of *btf<sup>el/-</sup>* pups at postnatal day 0 (P0). The brain, heart, liver and kidneys showed normal histology, however, the lungs of *btf<sup>el/-</sup>* animals were abnormal. The lungs of *btf<sup>el/-</sup>* animals were hyper-cellular and hyper-proliferative. In addition, Clara cells, highly metabolic, secretory cells in the bronchioles of the lung, were poorly developed with decreased secretory granules. We also saw ectopic presence of Clara cells in the alveolar walls suggesting a disruption of proximal-distal patterning in the lung. We hypothesize that the hyper-cellularity combined with abnormal airway lining fluid due to abnormal development and specification of Clara cells could lead to the respiratory distress and eventually death of the animals. Analysis of the composition of broncho-alveolar lavage obtained from wild-type and *btf<sup>el/-</sup>* lungs will be required to confirm this hypothesis.

During lung development, the epithelia of the bronchioles (proximal airway) and the alveolar walls (distal epithelium) undergo distinct differentiation programs. Bmp4 has been implicated in controlling this process, and studies blocking Bmp4 signaling have shown that decreased Bmp4 signaling leads to the formation of bronchioles in the distal epithelium of the lung. The bronchioles are lined by predominantly two cell types the ciliated cells, and the non-ciliated Clara cells, and blocking Bmp4 expression in the

distal airway causes ectopic presence of both these cell types. Our results show that *btf* has a role in specifically suppressing Clara cells in the distal epithelium. It would therefore be interesting to determine whether Bmp4 signaling can control *btf* expression and the effect of misregulation of Bmp4 on *btf* expression.

Loss of *btf* leads to ectopic CC10 expression and Clara-like cells in the alveolar walls. Btf could function by either directly controlling CC10 expression or might be involved in determining Clara cell-fate, with the ectopic CC10 expression being a result of this mis-specification. Our ultrastructure analysis and absence of any change in CC10 expression in the proximal airways supports the latter hypothesis, but it is possible that this function of *btf* requires other factors that are present only in cells of the distal epithelium. This can be addressed by determining the effect of overexpression of *btf* in the proximal epithelium, also by *in vitro* studies on the effect of btf on CC10 expression in lung epithelial cells. Since *btf* is expressed in both type I and type II cells in the distal airways, this ectopic presence of Clara-like cells could be due to trans-differentiation of either cell type. Analysis of loss of *btf* in transgenic lines that specifically express GFP under the control of either a type I or type II cell specific gene would help determine the origin of these Clara-like cells.

Our analysis of lung markers was limited to proteins that are expressed in specific cell types. However, lipids are an important component of surfactant and we did not test for changes in lipid content in *btf<sup>el</sup>* lungs. The normal architecture of lamellar bodies in type II cells and in the alveolar spaces argues against there being any dramatic change in lipid content. However, our analyses have shown that *btf*-null animals have several lung

defects and it is possible that several subtle changes can contribute to the observed lethality.

In addition to the lung defects, we observed that 40% of *btf<sup>el/-</sup>* animals did not feed. It is possible that the decreased feeding is a result of the lung abnormality since it is conceivable that inefficient respiration can affect normal feeding behavior. However, *btf* is expressed in the cerebellum and therefore it is also possible that loss of *btf* affects coordination, which might affect feeding.

A majority of *btf<sup>el/-</sup>* animals are smaller than their wild-type littermates, but this phenotype cannot be explained by decreased feeding since this decreased size is also evident *in utero*. In addition to being expressed in the cerebellum, *btf* is also expressed in the pituitary gland. Given the role of the pituitary in hormone regulation, it is possible that loss of *btf* in the pituitary affects secretion of growth hormone, which could lead to the observed decrease in size. Interestingly, we observed variability in all the phenotypes observed, including survival of *btf<sup>el/-</sup>* animals. All *btf* mutant animals died, however we found one animal that had survived to postnatal day 10 (P10). Our analyses concentrate on lung defects seen within the first 24 hours after birth, however it would be interesting to determine the number of animals that survive longer than one day. Identification of defects leading to lethality in these animals would lead to a better understanding of the role of *btf* in early postnatal development.



## VITAE

Aparna Aiyer was born in Bombay (Mumbai), India on August 29<sup>th</sup>, 1975, the only child of Saroj and Raju Aiyer. After graduating from high school, in 1992, she entered St. Xavier's College, Bombay, and received the degree of Bachelor of Science with a double major in Microbiology and Biochemistry, in May 1995. In August 1995 she entered the Tata Institute of Fundamental Research to pursue her Masters degree. Her research on the development of the chemosensory system of *Drosophila melanogaster* was under the guidance of Veronica Rodriguez, Ph.D. She received the degree of Master of Science in Molecular Biology in February 1998. She entered the Graduate School of Biomedical Sciences at the University of Texas Southwestern Medical Center at Dallas, Texas in August 1997 and joined the laboratory of Deepak Srivastava, M.D. in the summer of 1998.

Permanent Address: 8/304, Sri Nalini C.H.S. Ltd.

Sion Trombay Road,

Chembur, Mumbai-400071

India.